A Thesis for the Degree of Ph.D in Engineering

Coupling of Motion Components and Environmental Adaptation for Multi-Degree-of-Freedom Motion Reproduction

August 2017

Graduate School of Science and Technology
Keio University

TSUNASHIMA, Noboru

Acknowledgements

I have been a member of Katsura laboratory since I was an undergraduate student. This thesis is the result of several years of my work. During these years, I have been accompanied and supported by many people. I would like to express my gratitude to all those who gave me the possibility to complete this thesis here.

The first person I would like to express my deep and sincere gratitude to is my supervisor Associate Professor Dr. Seiichiro Katsura. His detailed and constructive comments and his important support throughout this work are a great help to me. I greatly appreciate his warm advice and guidance. Furthermore, he gave me the best research environment. It was a good experience for me to attend some conferences and to join in some projects.

I would like to offer my special thanks to the members of my Ph.D. dissertation committee, Professor Dr. Hiromitsu Ohmori, Professor Dr. Toshiyuki Murakami, Associate Professor Dr. Maki Sugimoto.

I am deeply grateful to Professor Dr. Kouhei Ohnishi, Professor Dr. Hiroaki Nishi, Associate Professor Dr. Takahiro Yakoh, Associate Profesor Dr. Ryogo Kubo, and Assistant Professor Dr. Takahiro Nozaki for giving me a lot of helpful advices in SUM meeting when I was master's course student. Their kind support and guidance have been of great value in this study.

I wish to thank Dr. Yuki Yokokura, Dr. Wataru Yamanouchi, Mr. Takeshi Okura, Mr. Kazuki Nagase, Mr. Shutaro Yorozu, and Mr. Tatsuhito Watanabe who were the member of the laboratory when I was master's course student They gave me many good advices, and we learn many thing about research, presentation, and so on. We had great experiences about our lives in the laboratory.

I would like to express my gratitude to Dr. Yuki Nagatsu, Dr. Kazumasa Miura, and Mr. Satoshi Nishimura who supported the research when I am doctor's course student. They set up the experimental system, ave me insightful comments and suggestions.

I would like to express my gratitude to everyone who collaborated with me. Everything I had experienced in the laboratory is wonderful.

I am warmly grateful to my family who have brought me up and supported me. I am happy to have grown up with my family.

August, 2017

Noboru Tsunashima

Table of Contents

List of Figures

List of Tables

Chapter 1

Introduction

1.1 Background

Currently, decrease of population is becoming a serious problem in many countries. In particular in Japan, working-age population ratio is decreasing because of the falling birth rate and the aging population. Under such background, it is required to achieve higher productivity by fewer people. The technology of automation or replacement of human task is attracted attention, and robotics is major technology of them. For example in the industrial field, the aging of expert operators and the decrease in the number of successors are serious problems. If expert skills can be recorded and reproduced by robots, production efficiency is improved because many robots can carry out skilled motion at the same time [1, 2]. Moreover, recorded skills can be applied training systems to enable successors to learn the skills [3]. The key point that robot works like as human is how to teach human motion to robots [4, 5].

In order to record and reproduce human motion, many researches have been carried out. The researches about this field are categorized by two perspectives; (i) the motion is dealt with by which information; (ii) the motion is reproduced in virtual world or real world.

First, some methods using several kinds of information are described. Ogawa $et\ al.$ proposed a method to teach a robot about manipulation tasks by generating task model from motion capture [6]. This method is one of the methods which focus only position information [6–11]. On the other hand, Skubic $et\ al.$ realized to reproduce a force-based assembly skill from human demonstration [12]. This method is one of the methods which can treat only trajectory or applied force of human motion. However, they are insufficient to represent human motion because both trajectory and strength are important. The designer needs to choose between the trajectory and the strength to deal with the human motion. Kormushev *et al.* proposed a method to learn and reproduce robot force interactions in a human-robot interaction setting. In the research, position profile and force profile are acquired separately, and the two profiles are encoded as a mixture of dynamical systems [13]. However, the reproduced motion is not human own motion, because the force information and the position information are not acquired from one motion. To acquire both position and force information at the same time is important for recording and reproduction of the human motion.

Then, the methods to treat haptic information in virtual world are introduced. Generally, haptic information is constructed by position and force information and the research field is known as haptics [14–16]. There are some researches to acquire skills of motion and teach a trainee to them based on virtual reality. Yokokohji *et al.* proposed a visual/haptic display system to develop a training system [17], and Hennmi *et al.* proposed the concept of virtual lesson [18–20]. Saga *et al.* proposed "Haptic Video" which is a system that records an expert's operations and reproduces them [21]. In these methods, the position and force information are acquired by a haptic device at the same time. Then, a trainee can learn the stored motion by operating a virtual object. These methods are effective for training system, but an ability to reproduce skilled motion is not focused mainly. In particular, a motion which acts an object in the real world is not reproduced, because these systems are constructed on the basis of virtual reality.

In order to store and reproduce human motion in real world applications, it is necessary to deal with not only trajectory but also applied force at the same time. Motion reproduction based on bilateral control is known as one of the efficient methods to achieve recording and reproducing human motion targeting an real object. The bilateral control is one of the achievements of real-world haptics. The real-world haptics is a study field that acquires, transmits, and reproduces haptic information from real objects. A fundamental research of the real-world haptics is a teleoperation system with force feedback, and this kind of study field has been researched since the 20th century. One of major aims of a bilateral control is to achieve transparency which is defined as a correspondence of impedance which are perceived by an operator and an environment [22, 23]. In order to attain high transparency, many methods have been proposed [24–32]. In particular, bilateral control based on acceleration control is constructed for the teleoperation system with high transparency [33, 34]. The key technology of this system is a disturbance observer (DOB) [35–38] and a reaction force observer (RFOB) [39, 40]. The robust acceleration control is attained by the DOB [41], and the high bandwidth force control is achieved by the vivid force information which is acquired by the RFOB [42–45]. Many researches are derived from this fundamental method as real-world haptics. For example, Natori *et al* researched bilateral control system under communication time delay [46–48]; Shimono *et al* researched micro-macro bilateral control system to operate finer object [49–51]; Ohnishi *et al* applied the bilateral control to medical surgery field [52, 53]; Yamanouchi *et al* implement the bilateral control to teleoperation system of vehicle [54, 55]. Katsura *et al* proposed multilateral control which targets haptic broadcasting [56–58]; Mitsantisuk *et al* realized power assist system from acquired information [59,60]; and Yamanouchi *et al* proposed training systems by haptic information [61, 62];. Because the position and force information of device can be acquired by bilateral control system, the information of a target environment or an operator's motion can be recorded. Yokokura *et al* proposed methods to estimate and represent a target environment [63, 64]. In addition, Yokokura *et al* proposed a motion-copying system [65, 66].

The motion-copying system [65, 66] is the technology for preservation and reproduction of a human motion on the basis of position and force information in real world. As described previously, most of conventional approaches deal with only position information or force information. On the other hand, the motion-copying system deals with not only the trajectory but also the strength of a human motion. Because both position information and force information are important in most of human motions, the introduced system is more useful method to acquire, record, and reproduce a human motion. In this thesis, advanced methods of motion-copying system are researched.

By the motion-copying system, the haptic information is recorded and reproduced like as audio and visual recording. Therefore, the technology of recording haptic information is called "haptic recording." The haptic recording can potentially be utilized in our daily lives for tasks such as audio recording and visual recording. In order to use haptic recording for more applications, some research have been studied [67–70]. The recorded motion is reproduced in variable speed by Yokokura *et al* [71]. The recorded motion is processed like equalizer by Kobayashi *et al* [72, 73]. The motion-copying system is implemented in multilateral control by Yokokura *et al* [74,75]. Tanaka *et al* researched data compression and decompression method of motion copying system [76–78]. Yokokura *et al* proposed construction of the motion database [79, 80].

1.2 Motivation

The purpose of this research is to expand the adaptability of the motion-copying system. In other words, we want to apply the motion-copying system to more application in future. By using the motion-copying system, human motion will be able to be recorded and reproduced at any time anywhere. However, the motion-copying system has several problems which need to be solved. In this thesis, following three points are focused and researched based on them;

- motion recording and reproduction in multi-DOF system;
- integrated reproduction of motion components;
- adaptation for difference of environment condition.

1.2.1 Motion Recording and Reproduction in Multi-DOF System

For the future applications of the motion-copying system, it is important to deal with human motions as multi-DOF motions. In order to apply the motion-copying system to multi-DOF system, the motion data should be dealt with in common coordinate. In particular, the information acquired by actuators mounted on the haptic device need to be transformed into the information of common coordinate. The concept of motion recording and reproduction in a multi-DOF system is shown in Fig. 1-1. By dealing with the motion information on the common coordinate, the recorded motion can be reproduced even if the structures of the devices are different.

In this thesis, three types of coordinates are discussed based on the view point of abstraction and specialization. First, work space is selected as common coordinate to abstract motion data not to depend on structure of hardware [81]. By this transformation, the motion data can be reproduced even if the structures of the haptic devices are different. Then, human modal space and motion modal space are introduced to specialize motion data for applications. The human modal space is introduced to treat human motion on the basis of the human model [82]. It is assumed that an exoskeleton haptic device is used in motion recording and an endoskeleton haptic device is used in motion reproduction. On the other hand, the motion modal space is introduced to separate motion elements from human motion. By this transformation, the proper control methods can be implemented in each motion element.

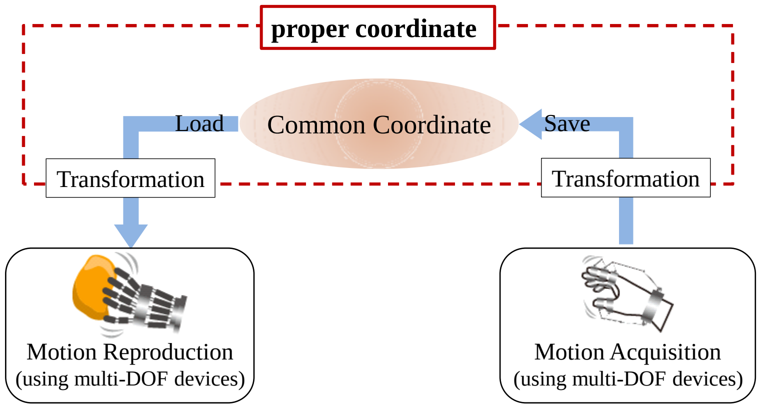

Fig. 1-1: Concept of motion recording and reproduction in multi-DOF system.

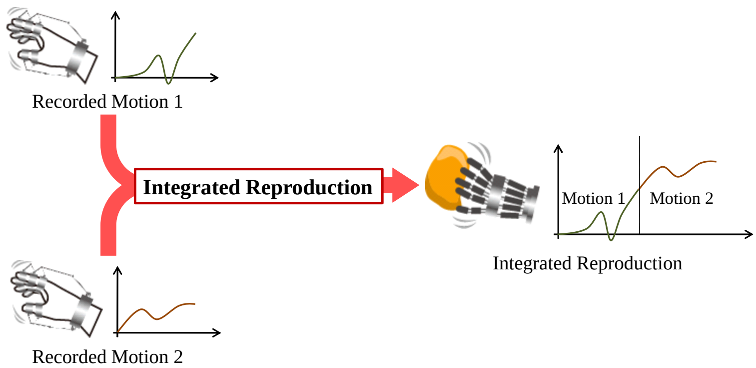

Fig. 1-2: Concept of integrated reproduction of motion components.

1.2.2 Integrated Reproduction of Motion Components

For the future applications of the motion-copying system, it is important to reproduce many motions from fewer recorded motions. In this thesis, methods to connect two recorded motions in time series and reproduce in a single motion are proposed. The concept of integrated reproduction is shown in Fig. 1-2. By the integrated reproduction, the motions in separated process are recorded independently, and whole task is realized by connect any motion components of each process.

In this thesis, two coupling methods are proposed. One of the methods assumes that human motions are dealt with position and force information [83–85]. The other method assumes that human motions are dealt with acceleration information [86]. These methods depend on the format of motion data. We can choose motion data format according to the aim or the environmental condition of motion reproduction. These proposed methods can apply to the basic motion-copying system [65] and the motion-copying

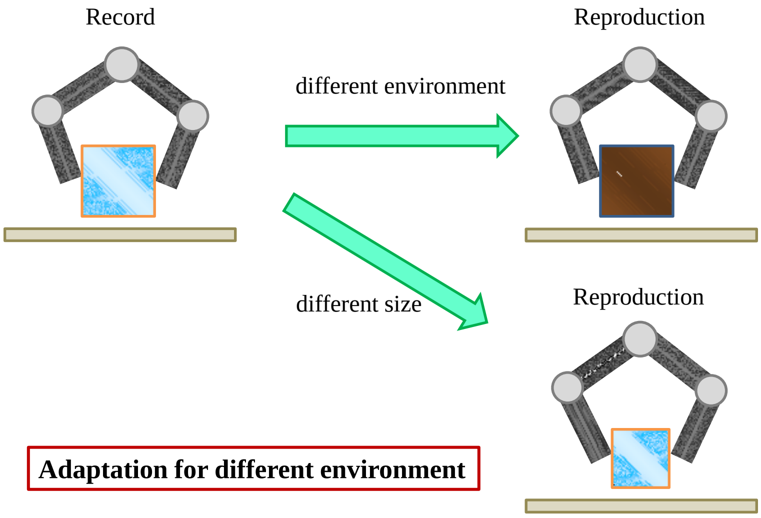

Fig. 1-3: Concept of adaptation for difference of environment.

system based on acceleration information [91].

1.2.3 Adaptation for Difference of Environment

The motion-copying system is hybrid control of the position and force. It is known that motion-copying system needs the exactly same environment between motion recording phase and motion reproducing phase [87–90]. When the environmental condition is greatly different, both position and force of the reproduced motion do not correspond with the recorded ones. For the future applications of the motion-copying system, it is important to reproduce recorded motions even if the environmental condition is different. The concept of adaptation for difference of environment is shown in Fig. 1-3.

In this thesis, two types of difference of the environmental condition are discussed. First, motion reproduction method when target environmental size is different is proposed [91–94]. Both position and force cannot be reproduced at the same time when environmental location is different. Here, the motion reproduction which does not depend on the base of the position is achieved [95]. Then, motion reproduction method when target environmental material is different is proposed. We assume that the motion-copying system is applied to the application of "peg-in-hole." In the proposal, the applied force to the external environment can be separated to the force on the basis of the difference of a target object and the common force which does not depend on it.

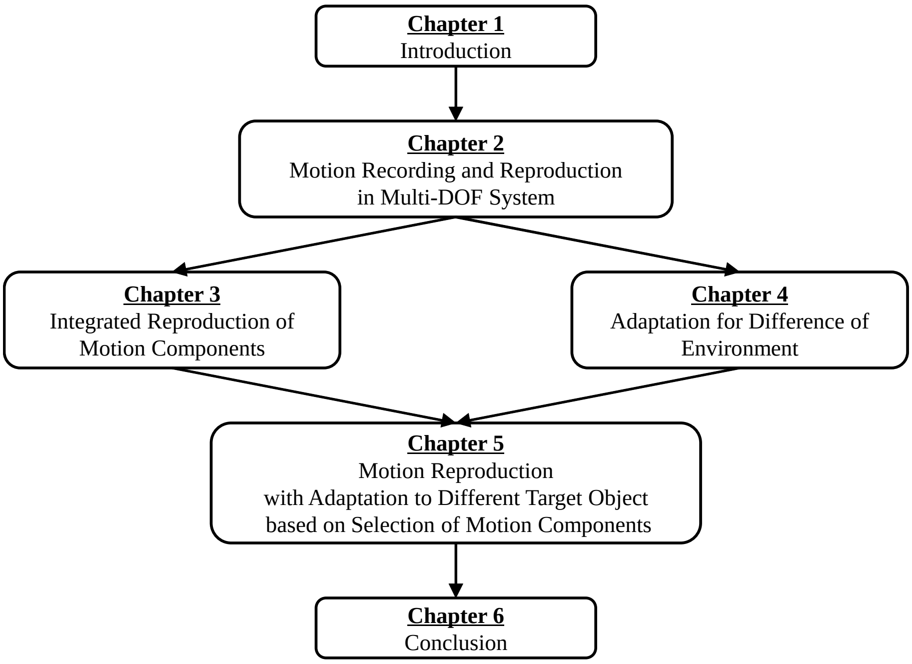

Fig. 1-4: Chapter organization.

1.3 Chapter Organization

This thesis is organized as Fig. 1-4. The following chapter shows the motion-copying system in the multi-DOF system. In this chapter, three coordinates described subsection 1.2.1 are introduced. The researches described after chapter 3 are based on any three coordinates. In chapter 3, the methods for integrated reproduction of motion components are shown. Then, the motion-copying system with adaptation for difference of environmental condition is shown in chapter 4. Finally, the proposed methods described in chapters 2–4 are combined. In the chapter 5, motion reproduction with the different target object under the application of "peg-in-hole" is achieved by coupling the motion elements. In each chapter, the validities of the proposed methods are confirmed by experimental results. This thesis is concluded in the last chapter.

Chapter 2

Motion Recording and Reproduction in Multi-DOF System

2.1 Background and Overview of This Chapter

For the future applications of the motion-copying system, it is important to deal with human motions as multi-DOF motions. Human can carry out various motions because human body is multi-DOF system. Hence, if the motion-copying system can be applied the multi-DOF system, it can be achieved to deal with human's complicated motions. The major theme to actuate multi-DOF system is in which coordinates the information is dealt with. For example, humanoid robot can be controlled by the information of joint space which is acquired by motion capture system [6–9]. In addition, humanoid robot can be controlled in the work space under the application to access the object in the open space [96, 97]. In the most of the researches to achieve the motions by humanoid robots, the first assumption is to use the specific robot. On the other hand, the purpose of motion-copying is to deal with motion data like as audio data or visual data. Hence, in this research, the motion data is assumed as contents and the robots are the just devices to reproduce recorded contents. In this chapter, coordinates to deal with human motion acquired by the motion-copying system is discussed from the view point to deal with the human motion as a contents. Here, two concepts of abstraction and specialization are introduced.

Fig. 2-1 shows the concept of abstraction of motion data. In the motion-copying system, human motions are acquired by the actuator mounted on the haptic devices. Hence, the "raw" motion data depend on the structure of haptic devices, and recorded motion can be reproduced by only the same device between motion recording and motion reproduction. By dealing with the motion data as the

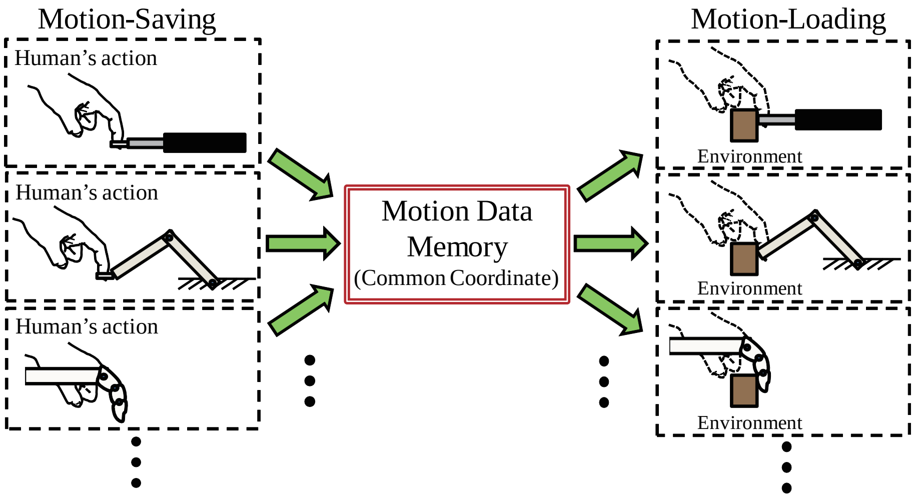

Fig. 2-1: Concept of coordinate transformation for adaptation.

information which depends on the structures of the devices, the motion data cannot be reproduced other devices. Therefore, the motion data cannot be used generally. In order to use recorded motion by various devices, it is required to deal with the motion data in the common coordinate. In particular, the information acquired by actuators mounted on the haptic device need to be transformed into the information of common coordinate. By transforming the motion data to the common coordinate, the motion data are abstracted. By the abstraction, we can use motion data without depending on the structure of the devices. As a result, human motions which are recorded by any devices are reproduced by arbitrary devices.

Fig. 2-2 shows the concept of specialization of motion data. In order to achieve more complicated application, specialized coordinate is more suitable than generalized coordinate. The information acquired by actuators is transformed into the information of the specialized-coordinate which is designed depending on the application.

In this chapter, three types of coordinates are discussed. First in section 2.2, work space is chosen as common coordinate to abstract motion data which depend on structures of devices [81]. By this transformation, motion data can be reproduced even if the structures of haptic devices are different. Then, the human modal space and motion modal space are introduced to specialize motion data for applications in section 2.3 and section 2.4, respectively. The human modal space is introduced to treat human motion on the basis of human model [82]. It is assumed that an exoskeleton haptic device is used in motion recording and an endoskeleton haptic device is used in motion reproduction. The human

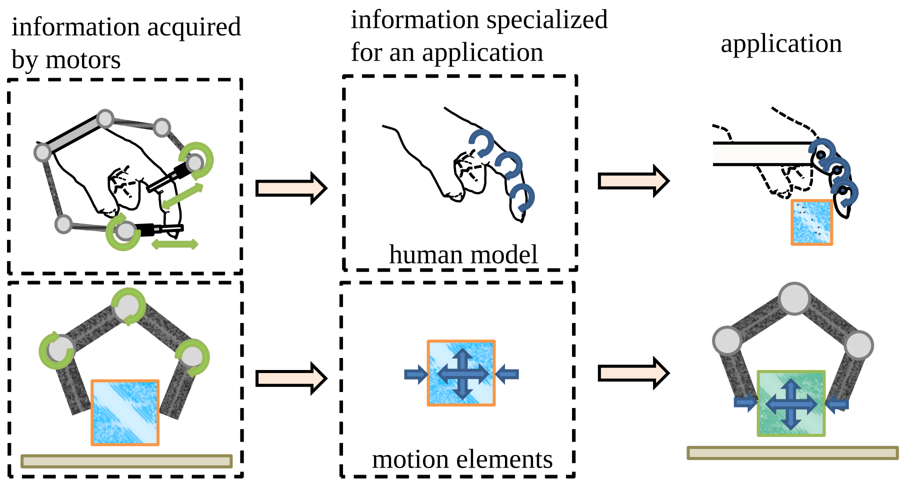

Fig. 2-2: Concept of coordinate transformation for specialization.

motion is acquired by the exoskeleton haptic device. However, the acquired motion is a device's motion which is not a human own motion. When the recorded motion is reproduced by the human like robots, the motion needs to be transformed with the human own motion. Therefore, the motion data are dealt with the information of the coordinates of human model. On the other hand, the motion modal space is introduced to separate motion elements from human motion. The human motion is separated into the elements of the motion, and the appropriate control methods can be implemented in each motion element. By implementing the appropriate controller in each axis according to the features of the motion elements, the recorded motion can be reproduced more flexible.

The relation of each transformation is shown in Fig. 2-3. In this research, the motor space information is transformed into work space information for abstraction. Then, the workspace information is transformed into the modal space information to deal with the human motion depending on its application. In each section, experimental results show the validity of the proposed methods.

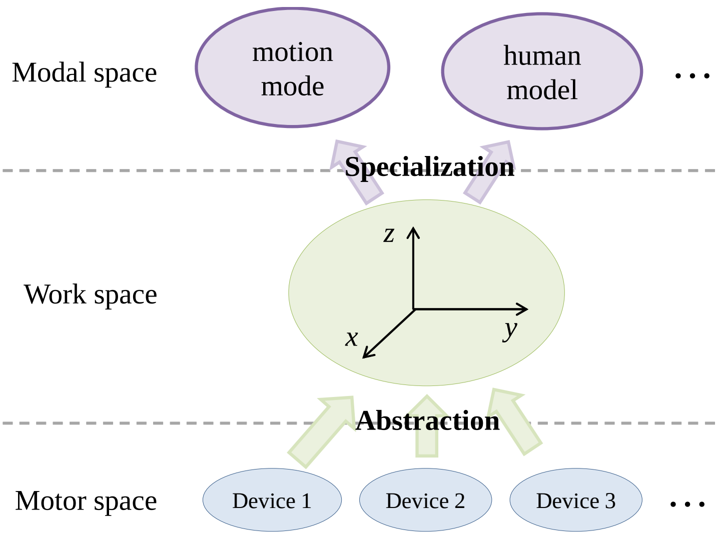

Fig. 2-3: Concept of coordinate transformation.

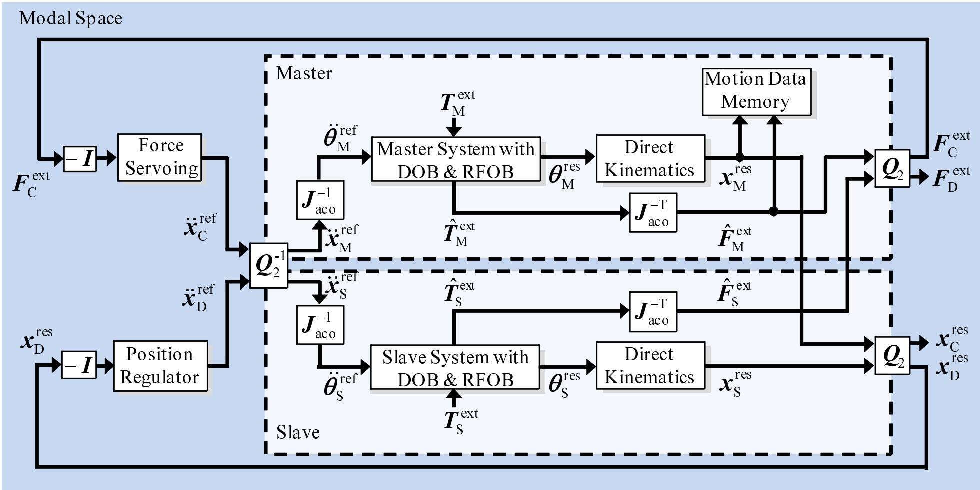

Fig. 2-4: Control structure of motion-saving system based on work space information.

2.2 Abstraction of Motor Space Information

In this section, the motion-copying system in the work space [81] is shown. The information in the motor space is transformed into the work space information, and the bilateral control is implemented in the work space. Because the human motion is stored as the work space information, different devices can be used at the motion reproduction phase.

2.2.1 Motion-Saving System

The motion-saving system is a control system when human motion is recorded. It is constructed by a master-slave type haptic device, and it is on the basis of the bilateral control based on acceleration control [34]. By the bilateral control with high transparency, the summation of the master and slave forces maintains 0 in order to realize the "law of action and reaction" between the master and slave systems. On the other hand, the position error between the master and slave systems maintains 0. As a result, a human operator in the master side can feel as if he/she is touching the real environment.

The control structure of the motion-saving system shown in Fig. 2-4 is the same as the basic method [65]. In Fig. 2-4, $\boldsymbol{\theta} = [\theta_1\ \theta_2\ \cdots]^{\mathrm{T}}$, $\boldsymbol{T} = [T_1\ T_2\ \cdots]^{\mathrm{T}}$ stand for the angle and torque in the actuator space; $\boldsymbol{x} = [x\ y\ z\ \cdots]^{\mathrm{T}}$, $\boldsymbol{F} = [F_x\ F_y\ F_z\ \cdots]^{\mathrm{T}}$ stand for the position and force in the work space; superscript $^{\mathrm{ref}}$, $^{\mathrm{res}}$, and $^{\mathrm{ext}}$ stand for the reference, response, and external torque (or force), respectively; subscript $_{\mathrm{M}}$, $_{\mathrm{S}}$, $_{\mathrm{C}}$, and $_{\mathrm{D}}$ stand for the master system, slave system, common mode, and differential mode, respectively; $\hat{}$ stands for the estimated value. $\boldsymbol{J}_{\mathrm{aco}}$ stands for Jacobian matrix, and $\boldsymbol{Q}$ stands for quarry matrix [98, 99]. Disturbance observer (DOB) [35, 36] is implemented in each motor locally to cancel unexpected disturbance, and reaction force observer (RFOB) is implemented in each motor to estimate force response without force sensor.

The information about the actuator space $(\boldsymbol{\theta}, \boldsymbol{T})$ is transformed into the work space information $(\boldsymbol{x}, \boldsymbol{F})$ by Jacobian matrix. This transformation depends on the structure of the haptic devices. The coordinate of the actuator space information is not the same between the master and slave devices when the configurations of these haptic devices are different. On the other hand, the information in the work space is the unique coordinate. Hence, the bilateral control is able to be implemented in this space. In this method, the bilateral control is implemented in each axis respectively. Then, the operator's motion is recorded as the information in the work space.

2.2.2 Motion-Loading System

Fig. 2-5 shows a control structure of the motion-loading system. The basic structure of this system is similar to the bilateral control based on the work space information, too. However, the master system does not exist in real world. Instead of the master system, the position and force information stored in the motion data memory is used as the virtual master system. The motion-loading system is equivalent to the unilateral control, because the virtual system is not affected according to the response of the motion reproduction. In other words, the slave system is controlled by a position controller and a force controller simultaneously.

In general, both position and force controls cannot be achieved at the same time because these controls have different control aims. In particular, the control aim of position controller is that the position response corresponds with the position command even if the external force is applied to the motor. On the other hand, the control aim of the force controller is that the applied force to the environment corresponds with the force command even if the environmental position is arbitrary. Hence, these control aims can not achieved simultaneously. However, there is an exceptive case. This case is that position and force commands have the relation on the basis of environmental impedance written as

$$\boldsymbol{F}_{\mathrm{cmd}} = \boldsymbol{Z}_{\mathrm{env}} \boldsymbol{x}_{\mathrm{cmd}} \tag{2.1}$$

where Z_{env} stands for the environmental impedance; and subscript $_{\mathrm{cmd}}$ stands for the stored information. In the motion-copying system, the recorded position and force information meets condition of (2.1),

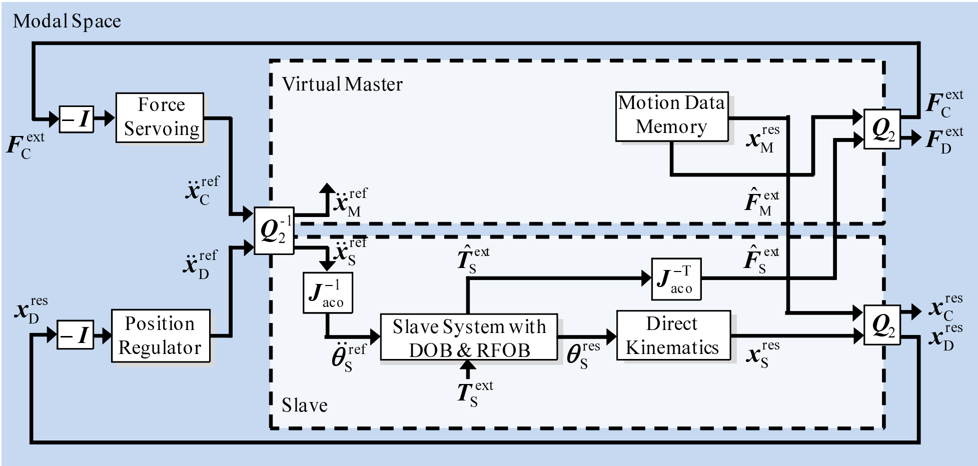

Fig. 2-5: Control structure of motion-loading system based on work space information.

because the slave system contacts with a real environment actually in the motion-saving system. Hence, in the motion-loading system, these two control aims are achieved only when the environmental condition is the same as it in the motion-saving system.

As mentioned above, not only free motion but also contact motion is recorded and reproduced. In this way, the slave motor reproduces the recorded operator's motions at any time. Thus, even if the structure of the device used in the motion-loading system is different from it in the motion-saving system, the recorded motion is reproduced precisely. It is because that the work space is the unique coordinate which does not depend on the configurations of the haptic devices.

2.2.3 Modeling of Experimental Systems

In the experiments in this section, two types of devices were used: a serial-link device and a parallel-link device. The models of these devices are shown in Fig. 2-6. The "contact point" stands for the point which is operated by human operator or contacts with an environment. In this research, gravity term is neglected because both devices are located horizontally. In this subsection, the equations about these models are described.

Serial-Link Device

Fig. 2-6 (a) shows a model of the serial-link device, where m and l stand for the mass and length of link; subscript $_1$ and $_2$ stand for links 1 and 2. In this device, two direct-drive (DD) motors are mounted

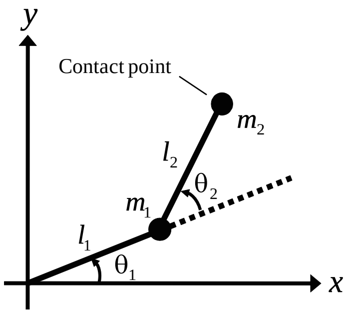

(a) Serial-link device.

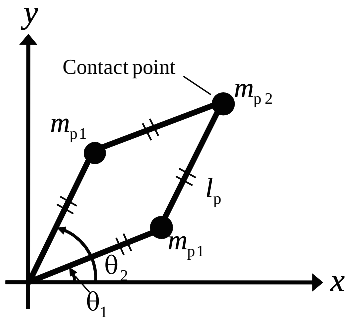

(b) Parallel-link device.

Fig. 2-6: Models of devices used in experiment for motion-copying system based on work space information.

in each joints. The dynamics of this device is described as

$$\begin{aligned} \boldsymbol{T} &= \boldsymbol{M}_{2\text{lk}}\ddot{\boldsymbol{\theta}} + \boldsymbol{H}_{2\text{lk}} \\ &= \begin{bmatrix} M_{2\text{lk}\,11} & M_{2\text{lk}\,12} \\ M_{2\text{lk}\,21} & M_{2\text{lk}\,22} \end{bmatrix} \ddot{\boldsymbol{\theta}} + \begin{bmatrix} H_{2\text{lk}\,1} \\ H_{2\text{lk}\,2} \end{bmatrix} \end{aligned} \tag{2.2}$$

$$\begin{cases} M_{2\text{lk}\,11} = (m_1 + m_2)l_1^2 + m_2 l_2^2 + 2m_2 l_1 l_2 \cos\theta_2 + J_{\text{n}} \\ M_{2\text{lk}\,12} = m_2 l_2^2 + m_2 l_1 l_2 \cos\theta_2 \\ M_{2\text{lk}\,21} = m_2 l_2^2 + m_2 l_1 l_2 \cos\theta_2 \\ M_{2\text{lk}\,22} = m_2 l_2^2 + J_{\text{n}} \end{cases} \tag{2.3}$$

$$\begin{cases} H_{2\text{lk}\,1} = -m_2 l_1 l_2 \dot{\theta}_2^2 \sin\theta_2 - 2m_2 l_1 l_2 \dot{\theta}_1 \dot{\theta}_2 \sin\theta_2 \\ H_{2\text{lk}\,2} = m_2 l_1 l_2 \dot{\theta}_1^2 \sin\theta_2 \end{cases} \tag{2.4}$$

where $\boldsymbol{M}_{2\text{lk}}$, $\boldsymbol{H}_{2\text{lk}}$, and J_{n} stand for the moment matrix, nonlinear term, and inertia moment of the rotor, respectively. The position of the contact point is derived as

$$\begin{bmatrix} x \\ y \end{bmatrix} = \begin{bmatrix} l_1 \cos\theta_1 + l_2 \cos(\theta_1 + \theta_2) \\ l_1 \sin\theta_1 + l_2 \sin(\theta_1 + \theta_2) \end{bmatrix}. \tag{2.5}$$

Hence, the velocity of contact point is obtained by

$$\begin{aligned} \begin{bmatrix} \dot{x} \\ \dot{y} \end{bmatrix} &= \boldsymbol{J}_{\text{aco}\,2\text{lk}} \begin{bmatrix} \dot{\theta}_1 \\ \dot{\theta}_2 \end{bmatrix} \\ &= \begin{bmatrix} J_{2\text{lk}\,11} & J_{2\text{lk}\,12} \\ J_{2\text{lk}\,21} & J_{2\text{lk}\,22} \end{bmatrix} \begin{bmatrix} \dot{\theta}_1 \\ \dot{\theta}_2 \end{bmatrix} \end{aligned} \tag{2.6}$$

$$\begin{cases} J_{2\mathrm{lk}\,11} = -l_1 \sin\theta_1 - l_2 \sin(\theta_1+\theta_2) \\ J_{2\mathrm{lk}\,12} = -l_2 \sin(\theta_1+\theta_2) \\ J_{2\mathrm{lk}\,21} = l_1 \cos\theta_1 + l_2 \cos(\theta_1+\theta_2) \\ J_{2\mathrm{lk}\,22} = l_2 \cos(\theta_1+\theta_2) \end{cases} \tag{2.7}$$

where $\boldsymbol{J}_{\mathrm{aco}\,2\mathrm{lk}}$ stands for Jacobian matrix of this device. The relationship of the force F_x, F_y and the torque T_1, T_2 is shown as

$$\begin{bmatrix} F_x \\ F_y \end{bmatrix} = \boldsymbol{J}^{\mathrm{T}}_{\mathrm{aco}\,2\mathrm{lk}} \begin{bmatrix} T_1 \\ T_2 \end{bmatrix}. \tag{2.8}$$

The acceleration references $\ddot{x}^{\mathrm{ref}}$, $\ddot{y}^{\mathrm{ref}}$ are transformed into the actuator space:

$$\begin{bmatrix} \ddot{\theta}_1^{\mathrm{ref}} \\ \ddot{\theta}_2^{\mathrm{ref}} \end{bmatrix} = \boldsymbol{J}^{-1}_{\mathrm{aco}\,2\mathrm{lk}} \begin{bmatrix} \ddot{x}^{\mathrm{ref}} \\ \ddot{y}^{\mathrm{ref}} \end{bmatrix}. \tag{2.9}$$

The information in the actuator space is transformed into the work space by (2.5) and (2.8). Then, the acceleration references calculated by the bilateral control are transformed into the actuator space by (2.9).

Parallel-Link Device

Fig. 2-6 (b) shows a model of the parallel-link device. Two DD motors are mounted on the base of the parallel-link device. In this device, the lengths of all links are the same, and those are written by l_{p}. $m_{\mathrm{p}\,1}$ and $m_{\mathrm{p}\,2}$ stand for the mass of joints. The dynamics of this device is described as

$$\begin{aligned} \boldsymbol{T} &= \boldsymbol{M}_{\mathrm{p}}\ddot{\boldsymbol{\theta}} + \boldsymbol{H}_{\mathrm{p}} \\ &= \begin{bmatrix} M_{\mathrm{p}\,11} & M_{\mathrm{p}\,12} \\ M_{\mathrm{p}\,21} & M_{\mathrm{p}\,22} \end{bmatrix} \ddot{\boldsymbol{\theta}} + \begin{bmatrix} H_{\mathrm{p}\,1} \\ H_{\mathrm{p}\,2} \end{bmatrix} \end{aligned} \tag{2.10}$$

$$\begin{cases} M_{\mathrm{p}\,11} = (m_{\mathrm{p}\,1} + m_{\mathrm{p}\,2}) l_{\mathrm{p}}^2 + J_{\mathrm{n}} \\ M_{\mathrm{p}\,12} = m_{\mathrm{p}\,2} l_{\mathrm{p}}^2 \cos(\theta_2 - \theta_1) \\ M_{\mathrm{p}\,21} = m_{\mathrm{p}\,2} l_{\mathrm{p}}^2 \cos(\theta_2 - \theta_1) \\ M_{\mathrm{p}\,22} = (m_{\mathrm{p}\,1} + m_{\mathrm{p}\,2}) l_{\mathrm{p}}^2 + J_{\mathrm{n}} \end{cases} \tag{2.11}$$

$$\begin{cases} H_{\mathrm{p}\,1} = -m_{\mathrm{p}\,2} l_{\mathrm{p}}^2 \dot{\theta}_2^2 \sin(\theta_2 - \theta_1) \\ H_{\mathrm{p}\,2} = m_{\mathrm{p}\,2} l_{\mathrm{p}}^2 \dot{\theta}_1^2 \sin(\theta_2 - \theta_1) \end{cases} \tag{2.12}$$

where $\boldsymbol{M}_{\mathrm{p}}$ and $\boldsymbol{H}_{\mathrm{p}}$ stands for the moment matrix and nonlinear term. The position of the contact point is derived as

$$\begin{bmatrix} x \\ y \end{bmatrix} = \begin{bmatrix} l_{\mathrm{p}} \cos\theta_1 + l_{\mathrm{p}} \cos\theta_2 \\ l_{\mathrm{p}} \sin\theta_1 + l_{\mathrm{p}} \sin\theta_2 \end{bmatrix}. \tag{2.13}$$

Hence, the velocity of the contact point is obtained by

$$\begin{aligned}\begin{bmatrix}\dot{x}\\ \dot{y}\end{bmatrix} &= \boldsymbol{J}_{\mathrm{aco\,p}}\begin{bmatrix}\dot{\theta}_1\\ \dot{\theta}_2\end{bmatrix}\\ &= \begin{bmatrix}J_{\mathrm{p}\,11} & J_{\mathrm{p}\,12}\\ J_{\mathrm{p}\,21} & J_{\mathrm{p}\,22}\end{bmatrix}\begin{bmatrix}\dot{\theta}_1\\ \dot{\theta}_2\end{bmatrix}\end{aligned} \tag{2.14}$$

$$\begin{cases} J_{\mathrm{p}\,11} = -l_{\mathrm{p}}\sin\theta_1\\ J_{\mathrm{p}\,12} = -l_{\mathrm{p}}\sin\theta_2\\ J_{\mathrm{p}\,21} = l_{\mathrm{p}}\cos\theta_1\\ J_{\mathrm{p}\,22} = l_{\mathrm{p}}\cos\theta_2\end{cases} \tag{2.15}$$

where $\boldsymbol{J}_{\mathrm{aco\,p}}$ stands for Jacobian matrix of this device. The relationship between the force F_x, F_y and the torque T_1, T_2 is shown as

$$\begin{bmatrix}F_x\\ F_y\end{bmatrix} = \boldsymbol{J}^{\mathrm{T}}_{\mathrm{aco\,p}}\begin{bmatrix}T_1\\ T_2\end{bmatrix}. \tag{2.16}$$

The acceleration references $\ddot{x}^{\mathrm{ref}}$, $\ddot{y}^{\mathrm{ref}}$ are transformed into the actuator space:

$$\begin{bmatrix}\ddot{\theta}_1^{\mathrm{ref}}\\ \ddot{\theta}_2^{\mathrm{ref}}\end{bmatrix} = \boldsymbol{J}^{-1}_{\mathrm{aco\,p}}\begin{bmatrix}\ddot{x}^{\mathrm{ref}}\\ \ddot{y}^{\mathrm{ref}}\end{bmatrix}. \tag{2.17}$$

The information in the actuator space is transformed into the work space by (2.13) and (2.16). Then, the acceleration references generated by the bilateral control are transformed into the actuator space by (2.17).

2.2.4 Experiments

Experimental Setup

Fig. 2-7 shows the experimental systems. In the motion-saving system, two same-type serial devices shown in Fig. 2-7 (a) were used as the master and slave systems. In the motion-loading system, motion reproductions about two cases were conducted: using the serial-link device and a parallel-link device shown in Fig. 2-7 (b). The parameters of the serial-link device and parallel-link device are shown in Table 2.1 and Table 2.2, respectively. In each system, the same-type DD rotary motors were mounted. The angle responses were measured by the rotary encoders, and the torque responses were estimated by RTOB without torque sensors. Control program was implemented in RTAI (the RealTime Application Interface for Linux) 3.7. The experimental parameters are shown in Table 2.3.

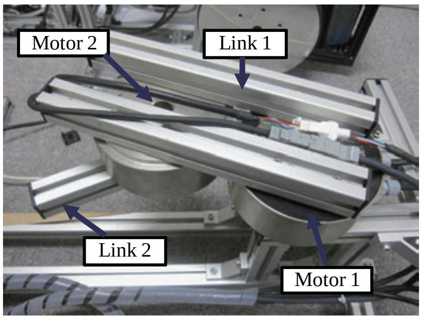

(a) Serial-link device.

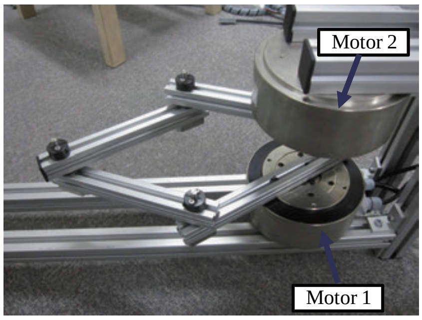

(b) Parallel-link device.

Fig. 2-7: Experimental systems for motion-copying system based on work space information.

Table 2.1: Parameters of serial-link device.

Parameter	Description	Value
m_1	Mass 1	1.5 kg
m_2	Mass 2	0.15 kg
l_1	Length of link 1	0.14 m
l_2	Length of link 2	0.16 m
$g_{\mathrm{dis}\,1}$	Cut-off frequency of DOB (motor 1)	80 rad/s
$g_{\mathrm{dis}\,2}$	Cut-off frequency of DOB (motor 2)	300 rad/s
$g_{\mathrm{r}\,1}$	Cut-off frequency of RFOB (motor 1)	80 rad/s
$g_{\mathrm{r}\,2}$	Cut-off frequency of RFOB (motor 2)	300 rad/s

Table 2.2: Parameters of parallel-link device.

Parameter	Description	Value
$m_{\mathrm{p}\,1} + m_{\mathrm{p}\,2}$	Mass of model	0.15 kg
l_{p}	Length of links	0.14 m
$g_{\mathrm{dis}\,\mathrm{p}}$	Cut-off frequency of DOB	900 rad/s
$g_{\mathrm{r}\,\mathrm{p}}$	Cut-off frequency of RFOB	900 rad/s

In the motion-saving system, human operated the master system, and the slave system contacted with an environment. At the same time, operator's motion was recorded to the motion data memory as the position and force information in the work space. In this experiment, human motion included both constrained motion and unconstrained motion. In the motion-loading system, the recorded information was loaded from the motion data memory and operator's motion was reproduced. In this experiment, the environmental location was mostly the same between the motion-saving and motion-loading systems.

Table 2.3: Experimental parameters for motion-copying system based on work space.

Parameter	Description	Value
T_s	Sampling time	100 μs
	Resolution of motor	260000 pulse/r
K_{tn}	Torque coefficient	1.18 Nm/Arms
J_n	Inertia moment of motor	0.0028 kgm^2
K_p	Position gain	8100
K_d	Velocity gain	180
K_f	Force gain	1.0
g_{pd}	Cut-off frequency of pseudo-derivation	1000 rad/s

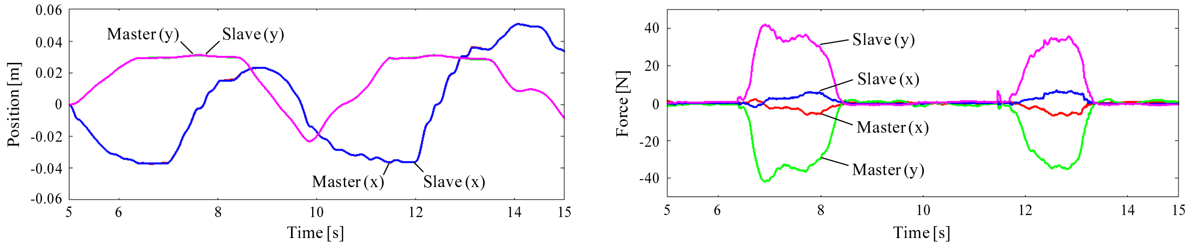

(a) Position responses. (b) Force responses.

Fig. 2-8: Experimental results of motion-saving system in work space

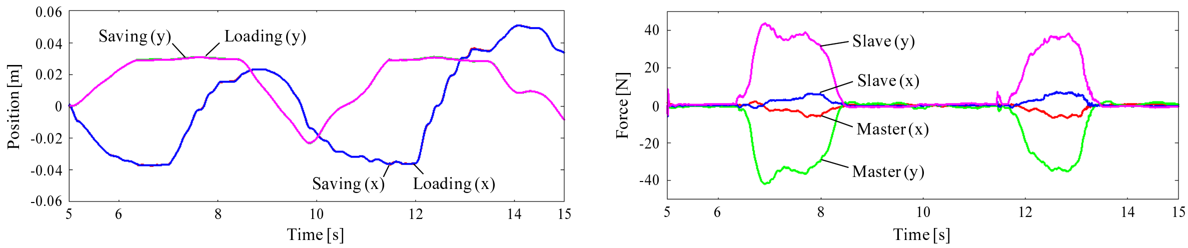

(a) Position responses. (b) Force responses.

Fig. 2-9: Experimental results of motion-loading system with serial-link device.

The motors were actuated by angle control during first 5 s in order to move to initial angle shown in

$$\begin{bmatrix} \theta_{\mathrm{ini}\,1} \\ \theta_{\mathrm{ini}\,2} \end{bmatrix} = \begin{bmatrix} 0 \\ \frac{\pi}{2} \end{bmatrix}. \tag{2.18}$$

After 5 s, the motion-saving and motion-loading steps were conducted.

Experimental Results

The experimental results of the motion-saving system are shown in Fig. 2-8, and the results of the motion-loading system are shown in Figs. 2-9 and 2-10. In particular, Fig. 2-9 shows the experimental

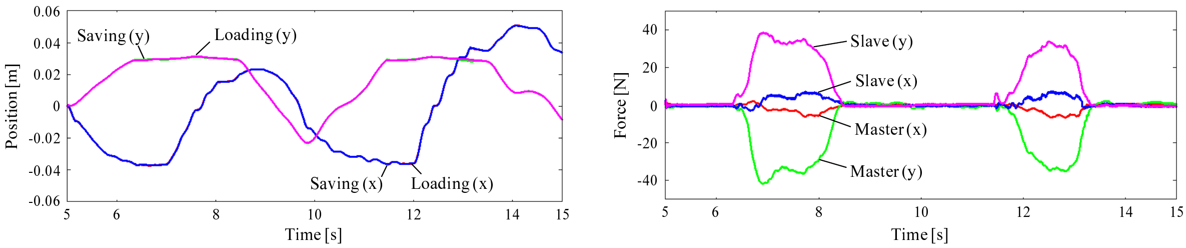

(a) Position responses. (b) Force responses.

Fig. 2-10: Experimental results of motion-loading system with parallel-link device.

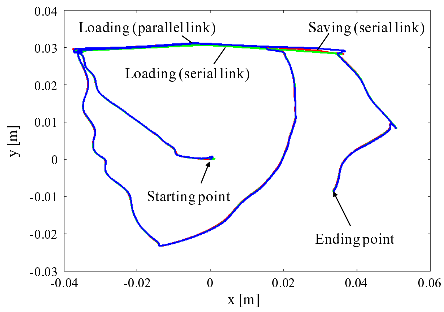

Fig. 2-11: Trajectories of tip point.

results with the serial-link device, and Fig. 2-10 shows the experimental results with the parallel-link device. In all figures, only information in the work space is represented, and the responses of the motion-saving or motion-loading steps are shown (after 5 s). (a) and (b) show the position and force responses, respectively. In addition, both x axis information and y axis information are drawn in one figure. The trajectories of the tip position are shown in Fig. 2-11. In Fig. 2-11, the responses of the recorded motion, reproduced motion with the serial-link device, and reproduced motion with the parallel-link device are shown.

Fig. 2-9 shows that the recorded motion was reproduced by using the haptic devices with the same configurations based on the work space information. Furthermore from Fig. 2-10, it is said that the recorded motion was reproduced even if the configurations of the haptic devices are different. In both figures, the position tracking is realized accurately in the unconstrained motion. However, the recorded motion is not realized accurately in the constrained motion. The main reason of this phenomenon is that the environmental location is not completely the same as the motion-saving phase which is expressed in Fig. 2-11. For achieving the accurate reproduction, it is necessary to set the same environmental condition.

Table 2.4: Correlation between recorded motion and reproduced motion.

	Serial-link device	Parallel-link device
Position (x)	1.000000	1.000000
Position (y)	0.999981	0.999923
Force (x)	1.000000	1.000000
Force (y)	0.998815	0.995842

Then, the evaluation of the experimental results using correlation coefficient is shown. The goal of the motion reproduction is that the responses in the motion-saving and motion-loading systems are the same value. Hence it can be said that if correlation coefficient between the responses in the motion-saving and motion-loading steps is large value, the ideal reproduction is attained. The correlation coefficient is obtained by

$$R = \frac{\sum_{i=1}^{n}(a_i^{\mathrm{sav}} - \overline{a}^{\mathrm{sav}})(a_i^{\mathrm{ld}} - \overline{a}^{\mathrm{ld}})}{\sqrt{\sum_{i=1}^{n}(a_i^{\mathrm{sav}} - \overline{a}^{\mathrm{sav}})^2}\sqrt{\sum_{i=1}^{n}(a_i^{\mathrm{ld}} - \overline{a}^{\mathrm{ld}})^2}} \tag{2.19}$$

where R, a, $\overline{a}$, and n stand for the correlation coefficient, response, average of response, and amount of data, respectively. Superscript $^{\mathrm{sav}}$ and $^{\mathrm{ld}}$ stand for the recorded response and reproduced response. The correlation coefficient about each response is shown in Table 2.4. It is shown that the value of the correlation coefficients are large value in both reproductions. Hence it is said that the accurate reproductions were achieved. In this experiments, the y directional motion is more complicated than the x directional motion. Hence, the coefficients about y direction are smaller compared with the coefficients about x direction. From these experimental results, the validity of the proposal is confirmed.

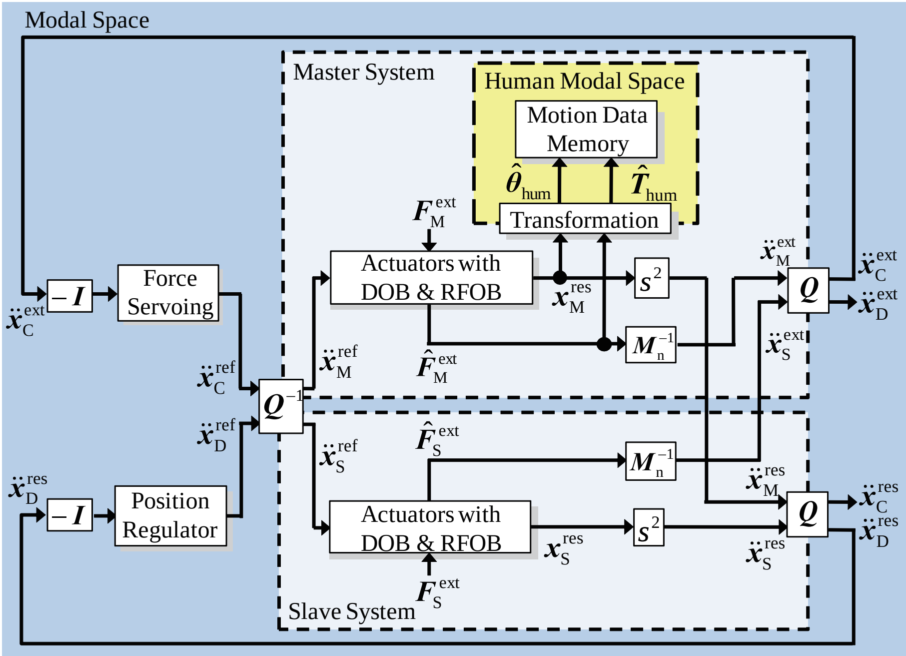

Fig. 2-12: Control structure of motion-saving system based on finger modal space.

2.3 Specialized Coordinate for Finger Motion

In this section, the specialized coordinate for finger motion is introduced. Here, it is assumed that an exoskeleton haptic device is used in the motion-saving system and an endoskeleton haptic device is used in the motion-loading system. In this application, the human motions should be treated in the human modal space because the information acquired by the endoskeleton-type device is not human own motion. Hence, the coordinate of the human model is more appropriate than work space in this application. In order to acquire the human own motion, it is necessary to estimate the human motion from device's information. Then, the estimated human motion is reproduced by the endoskeleton-type haptic device which imitates the humans body. In this section, the method of preservation and reproduction of the human motion on the basis of the human modal space [82] is proposed. By this proposal, it is realized that the human motion is recorded and reproduced by using the haptic systems with different configurations.

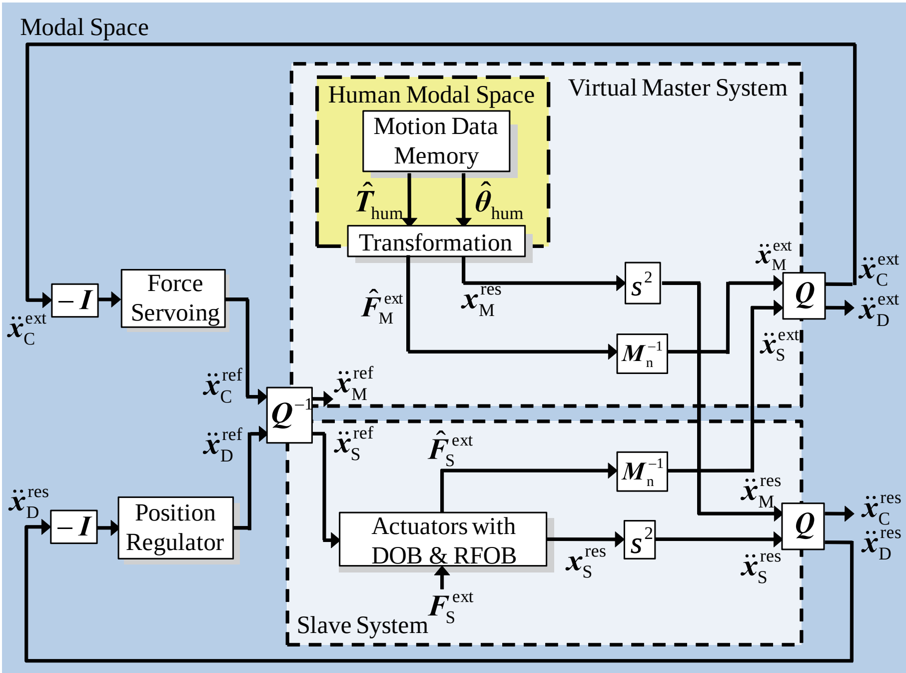

Fig. 2-13: Control structure of motion-loading system based on finger modal space.

2.3.1 Motion-Saving System

A block diagram of the motion-saving system is shown in Fig. 2-12. The introduced block diagram is similar to the basic motion-saving system. In this figure, $\hat{\boldsymbol{\theta}}_{\rm hum}$ and $\hat{\boldsymbol{T}}_{\rm hum}$ stand for the estimated angle and estimated torque in the human modal space. The bilateral control based on the acceleration control is implemented in each actuator. In the motion-saving system, position and force information in the actuator space is transformed into the human modal space by the transformation matrix which depends on the configurations of saving devices. When the joint model is used as the human model, the variables of $\hat{\boldsymbol{\theta}}_{\rm hum}$ and $\hat{\boldsymbol{T}}_{\rm hum}$ stand for the joint angle and joint torque of the human joint. In this way, the operator's motion is recorded to the motion data memory as the estimated value in the human modal space. In this method, the unified space between the motion-saving and motion-loading systems is human modal space.

2.3.2 Motion-Loading System

Fig. 2-13 shows the control structure of the motion-loading system. The introduced system is similar to the basic structure, too. Here, the recorded information is transformed into the actuator space by the transformation matrix which depends on the configuration of the device. The slave system in the motion-

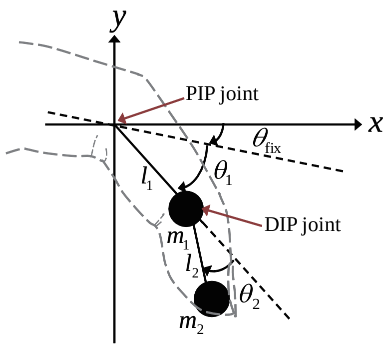

Fig. 2-14: Finger model used in experiment for motion-copying system based on human model.

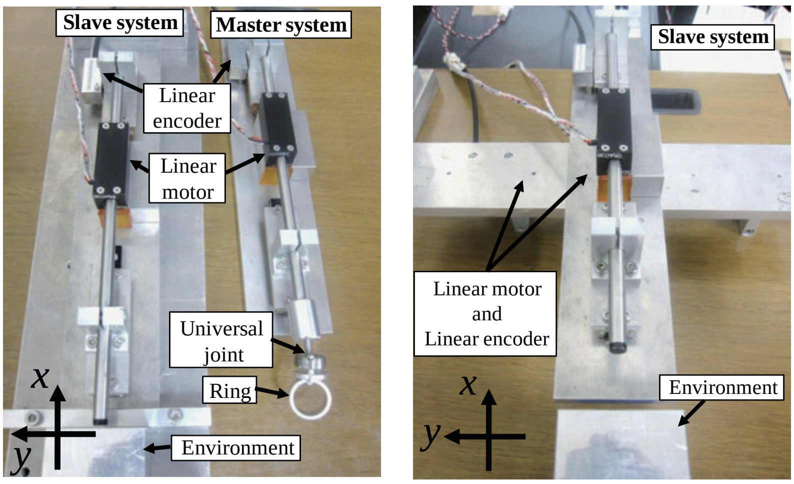

(a) Motion-saving system. (b) Motion-loading system.

Fig. 2-15: Experimental system for motion-copying system based on human model.

loading system is controlled by transformed information. In this way, the recorded human motion is reproduced.

In this method, the controllers of the motion-saving and motion-loading systems are implemented in the actuator space. Of course, it is possible to implement the controllers after transformation into the human modal space.

2.3.3 Modeling of Experimental System

In the experiments conducted in this research, finger motion is focused. The human operator moves his finger through the device which imitates the exoskeleton-type device, and the device which imitates the endoskeleton-type device reproduces the recorded human motion. We assume that the operator moves

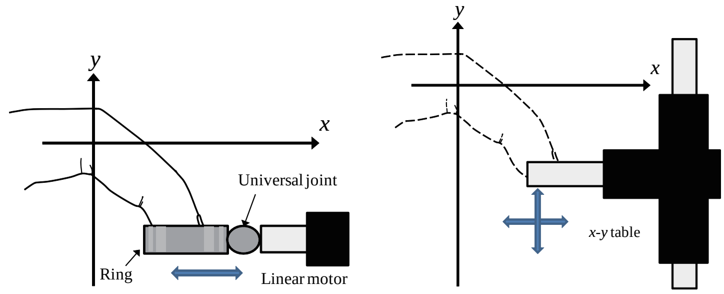

(a) Motion-saving system. (b) Motion-loading system.

Fig. 2-16: Simplified models of experimental systems for motion-copying system based on human model.

only PIP (proximal interphalangeal) joint and DIP (distal interphalangeal) joint, and the other joint is fixed. In addition, we assume that the finger model is used two-mass model in this research, and the simplified diagram is shown in Fig. 2-14. Links 1 and 2 are regarded as the middle phalanx and the distal phalanx, respectively. In Fig. 2-14, θ, m, and l stand for the angle of joint, mass of link, and length of the link; subscript $_1$, $_2$ and $_{\rm fix}$ stand for link 1, link 2, and angle of the proximal phalanx which is fixed, respectively. In this subsection, the modeling of the experimental systems is conducted.

Experimental systems in the motion-saving and motion-loading steps are shown Fig. 2-15 (a) and (b), respectively. The device shown Fig. 2-15 (a) imitates the exoskeleton-type device. In the motion-saving system, human puts on the ring which is connected on the linear motor by the universal joint in the master system. Only x axis position and force are obtained by the linear actuator. Here, it is assumed that the ring contacts with the finger tip. Hence, this device acquires the information of the finger tip. In the motion-loading system, the end effector of the x-y table reproduces the trajectory and the applied force of the finger tip point. The device shown Fig. 2-15 (b) imitates the endoskeleton-type device. The models of these devices are shown in Fig. 2-16.

Modeling of Device Used in Motion-Saving System

In the motion-saving system, the finger model has two DOF, but the haptic device has one DOF. So, the finger joint information is not obtained without a restraint condition. Here, the finger joint information is obtained under the condition that the DIP joint is a passive DOF that follows the PIP joint through tendons connection [100] which is represented as

$$\theta_{2\,\mathrm{MS}} = \frac{4}{5}\theta_{1\,\mathrm{MS}} \tag{2.20}$$

where subscript $_{\mathrm{MS}}$ stands for the motion-saving system. From this condition, the tip position is written by

$$\begin{bmatrix} x_{\mathrm{MS}} \\ y_{\mathrm{MS}} \end{bmatrix} = \begin{bmatrix} l_1 \cos(\theta_{1\,\mathrm{MS}} + \theta_{\mathrm{fix}}) + l_2 \cos(\frac{9}{5}\theta_{1\,\mathrm{MS}} + \theta_{\mathrm{fix}}) \\ -l_1 \sin(\theta_{1\,\mathrm{MS}} + \theta_{\mathrm{fix}}) - l_2 \sin(\frac{9}{5}\theta_{1\,\mathrm{MS}} + \theta_{\mathrm{fix}}) \end{bmatrix} \tag{2.21}$$

where x_{MS} and y_{MS} stand for the positions of the absolute coordinate. Newton-Raphson method is used in order to estimate the joint angle, because it is very difficult to calculate the analytic solution about $\theta_{1\,\mathrm{MS}}$ and $\theta_{2\,\mathrm{MS}}$.

The joint torque responses are obtained by

$$\begin{aligned} \begin{bmatrix} T_{1\,\mathrm{MS}} \\ T_{2\,\mathrm{MS}} \end{bmatrix} &= \boldsymbol{J}^{\mathrm{T}}_{\mathrm{aco\,MS}} \begin{bmatrix} F_{x\,\mathrm{MS}} \\ F_{y\,\mathrm{MS}} \end{bmatrix} \\ &= \boldsymbol{J}^{\mathrm{T}}_{\mathrm{aco\,MS}} \begin{bmatrix} 0 \\ F_{y\,\mathrm{MS}} \end{bmatrix} \end{aligned} \tag{2.22}$$

where subscript $_x$ and $_y$ stand for x axis and y axis, respectively. $\boldsymbol{J}_{\mathrm{aco}}$ stands for Jacobian matrix, and it is shown as

$$\boldsymbol{J}_{\mathrm{aco\,MS}} = \begin{bmatrix} J_{11\,\mathrm{MS}} & J_{12\,\mathrm{MS}} \\ J_{21\,\mathrm{MS}} & J_{22\,\mathrm{MS}} \end{bmatrix} \tag{2.23}$$

$$\begin{cases} J_{11\,\mathrm{MS}} = -l_1 \sin(\theta_{1\,\mathrm{MS}} + \theta_{\mathrm{fix}}) - l_2 \sin(\frac{9}{5}\theta_{1\,\mathrm{MS}} + \theta_{\mathrm{fix}}) \\ J_{12\,\mathrm{MS}} = -l_2 \sin(\frac{9}{5}\theta_{1\,\mathrm{MS}} + \theta_{\mathrm{fix}}) \\ J_{21\,\mathrm{MS}} = -l_1 \cos(\theta_{1\,\mathrm{MS}} + \theta_{\mathrm{fix}}) - l_2 \cos(\frac{9}{5}\theta_{1\,\mathrm{MS}} + \theta_{\mathrm{fix}}) \\ J_{22\,\mathrm{MS}} = -l_2 \cos(\frac{9}{5}\theta_{1\,\mathrm{MS}} + \theta_{\mathrm{fix}}) \end{cases} . \tag{2.24}$$

The information acquired by the actuators are transformed into the finger modal space by these equations. Then, the estimated joint angle and torque are recorded to the motion data memory.

Modeling of Device Used in Motion-Loading System

In the motion-loading system, the end effector of the x-y table reproduces the recorded motion of the finger tip. The tip position is written by

$$\begin{bmatrix} x_{\mathrm{ML}} \\ y_{\mathrm{ML}} \end{bmatrix} = \begin{bmatrix} l_1 \cos(\theta_{1\,\mathrm{ML}} + \theta_{\mathrm{fix}}) + l_2 \cos(\theta_{1\,\mathrm{ML}} + \theta_{2\,\mathrm{ML}} + \theta_{\mathrm{fix}}) \\ -l_1 \sin(\theta_{1\,\mathrm{ML}} + \theta_{\mathrm{fix}}) - l_2 \sin(\theta_{1\,\mathrm{ML}} + \theta_{2\,\mathrm{ML}} + \theta_{\mathrm{fix}}) \end{bmatrix} \tag{2.25}$$

where subscript $_{\mathrm{ML}}$ stands for the value used in the motion-loading system. Then, the recorded torque are transformed by

$$\begin{bmatrix} F_{x\,\mathrm{ML}} \\ F_{y\,\mathrm{ML}} \end{bmatrix} = \boldsymbol{J}^{-\mathrm{T}}_{\mathrm{aco\,ML}} \begin{bmatrix} T_{1\,\mathrm{ML}} \\ T_{2\,\mathrm{ML}} \end{bmatrix} . \tag{2.26}$$

Table 2.5: Experimental parameters of motion-copying system based on human model.

Parameter	Description	Value
T_{s}	Sampling time	100 μs
K_{tn}	Force coefficient	3.3 N/A
M_{n}	Mass	0.24 kg
K_{p}	Position gain	10000
K_{d}	Velocity gain	200
K_{f}	Force gain	8
g_{pd}	Cut-off frequency of pseudo-derivation	2000 rad/s
g_{dis}	Cut-off frequency of disturbance observer	700 rad/s
g_{r}	Cut-off frequency of reaction force observer	700 rad/s

Jacobian matrix of the motion-loading system is described by

$$\boldsymbol{J}_{\mathrm{aco\,ML}} = \begin{bmatrix} J_{11\,\mathrm{ML}} & J_{12\,\mathrm{ML}} \\ J_{21\,\mathrm{ML}} & J_{22\,\mathrm{ML}} \end{bmatrix} \tag{2.27}$$

$$\begin{cases} J_{11\,\mathrm{ML}} = -l_1 \sin(\theta_{1\,\mathrm{ML}} + \theta_{\mathrm{fix}}) - l_2 \sin(\theta_{1\,\mathrm{ML}} + \theta_{2\,\mathrm{ML}} + \theta_{\mathrm{fix}}) \\ J_{12\,\mathrm{MS}} = -l_2 \sin(\theta_{1\,\mathrm{MS}} + \theta_{2\,\mathrm{ML}} + \theta_{\mathrm{fix}}) \\ J_{21\,\mathrm{MS}} = -l_1 \cos(\theta_{1\,\mathrm{MS}} + \theta_{\mathrm{fix}}) - l_2 \cos(\theta_{1\,\mathrm{MS}} + \theta_{2\,\mathrm{ML}} + \theta_{\mathrm{fix}}) \\ J_{22\,\mathrm{MS}} = -l_2 \cos(\theta_{1\,\mathrm{MS}} + \theta_{2\,\mathrm{ML}} + \theta_{\mathrm{fix}}) \end{cases} \tag{2.28}$$

From these equations, the recorded finger motion data are transformed into the actuator space.

2.3.4 Experiments

Experimental Setup

In order to verify the validity of the proposed method, the experiments were conducted. The experimental systems shown in Fig. 2-15 are composed of the linear motors and the position encoders whose resolution is 100 nm. The environment used in this experiments is an aluminum block. In these experiments, the position information were measured by the position encoder, and the force responses were estimated by the RFOB without force sensors. The control program was implemented in RTAI 3.7. The experimental parameters are shown in Table 2.5, and the parameters about the finger model is set as Table 2.6.

In the motion-saving system, the human operator put on the haptic device shown in Fig. 2-15 (a), and he moved only PIP and DIP joints. The slave system contacted with an environment, and human operator felt the reaction force from an environment because the bilateral control is implemented. At the same time, operator's motion was recorded to the motion data memory on the basis of the human modal

Table 2.6: Parameters of finger model for motion-copying system based on human model.

Parameter	Description	Value
l_1	Length of link 1	0.025 m
l_2	Length of link 2	0.025 m
m_1	Mass of link 1	0.012 kg
m_2	Mass of link 2	0.012 kg
θ_{fix}	Fixed angle	0.524 rad
$\theta_{1\ \text{ini}}$	Initial angle of PIP joint	0.087 rad
$\theta_{2\ \text{ini}}$	Initial angle of DIP joint	0.070 rad

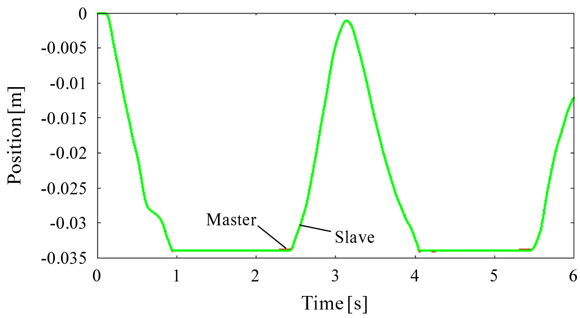

(a) Position responses.

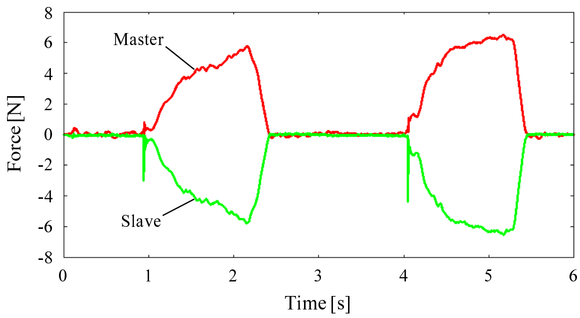

(b) Force responses.

Fig. 2-17: Experimental results of motion-saving system in actuator space.

information. Then, in the motion-loading system, the recorded motion is reproduced by the device shown in Fig. 2-15 (b). The information in the human modal space is transformed into the actuator space, and the slave system is controlled by transformed information.

Experimental Results

Figs. 2-17 and 2-18 show the experimental results of the motion-saving system. Fig. 2-17 (a) and (b) indicate the position responses and the force responses acquired by the linear actuators. The responses of the master and slave systems are depicted in one figure. Then, the movement of the operator's finger joint is estimated from the responses of the master system. Fig. 2-18 (a) and (b) indicate the estimated angle and torque in the finger modal space, which are estimated by Newton-Raphson method and (2.22) respectively. In these figures, the responses of PIP joint and DIP joint are described. The responses shown in this figure were recorded to the motion data memory. Fig. 2-19 shows the experimental results of the motion reproduction. (a) and (b) indicate position responses and force responses, and both information about x axis and y axis are depicted. In Fig. 2-19, the "virtual master" means the responses of the recorded motion, which is in the motion data memory. This figure shows that the motion acquired

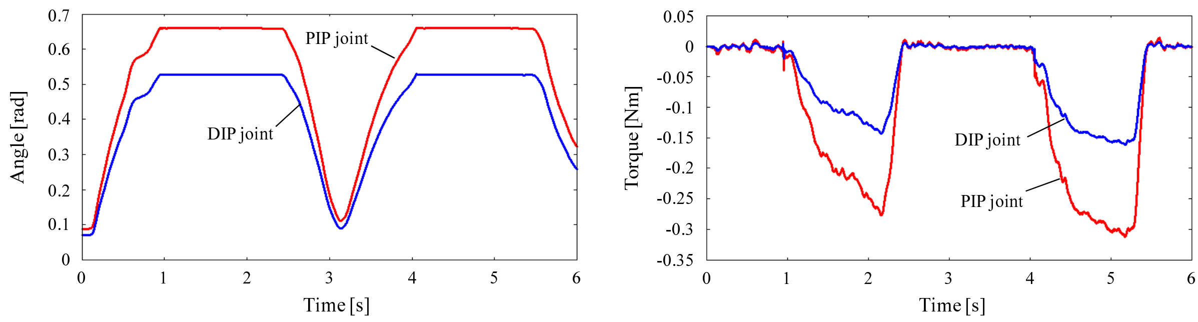

(a) Angle responses. (b) Torque responses.

Fig. 2-18: Estimated finger motion.

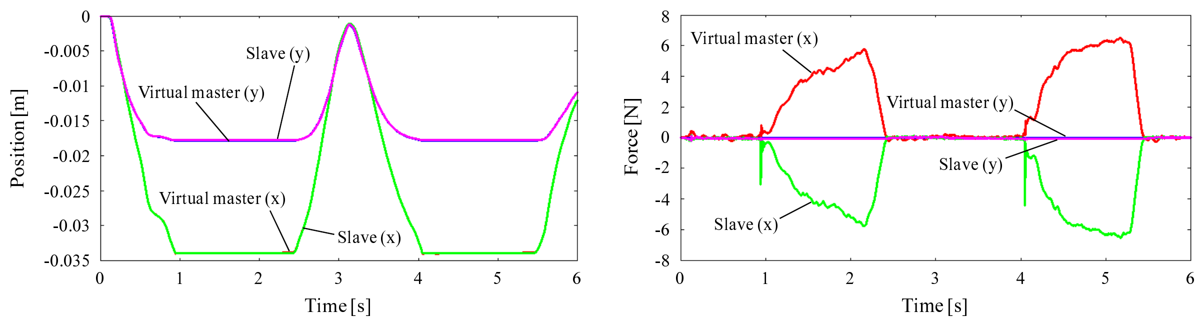

(a) Position responses. (b) Force responses.

Fig. 2-19: Experimental results of motion reproduction using motion-copying system based on human model.

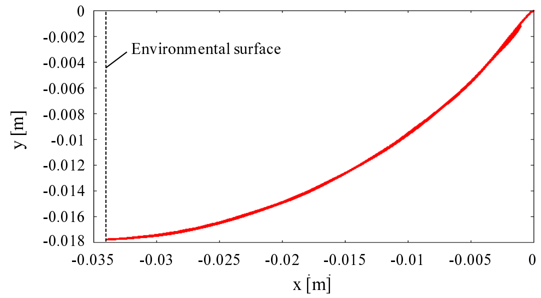

Fig. 2-20: Trajectory of finger tip.

in the motion-saving system is reproduced by the device with different configurations through the finger modal space. The information about x axis is unknown in the motion-saving system, but it is reproduced through the estimated finger motion. It is expressed in Fig. 2-20. The trajectory of the tip point is reproduced. From these figures, the availability of the proposal is verified.

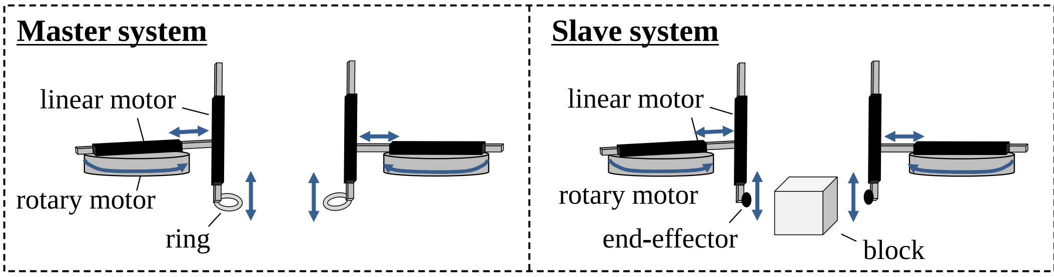

Fig. 2-21: Simplified figure of the experimental system.

2.4 Specialized Coordinate for Picking Up and Moving Motion

In this section, the motion modal space is introduced as specialized coordinate for complicated motion. The basic concept is similar to function mode [101,102]. Human motions are composed of "do something with a tool to an target object"; (e.g.)"writing with a pen," "drinking in a cup," "throwing a ball," etc. The picking up and moving motion is focused here as a complicated motion, and the specialized coordinate for such motion is described. By the introduced coordinate, the human motion is separated into motion elements. In the following chapter, the appropriate controller is implemented in each motion element axis according to the aim of each motion element.

2.4.1 Modeling and Coordinate Transformation

In order to deal with a human motion, coordinate transformation from motor space information to motion-mode space information is necessary. After the transformation, the human motion can be controlled by separated motions. This section describes a modeling of the experimental system, and two coordinate transformation is provided; between the motor space and work space; between the work space and motion-mode space.

Modeling

The simplified figure of the experimental system is shown in Fig. 2-21. One unit of the experimental device is constructed three motors; a rotary motor (horizontal) and two linear motors (horizontal and vertical). In each motor, a disturbance observer (DOB) is implemented locally. The master system (or the slave system) is constructed by two device units. In the master system, an operator inserts his/her finger to rings and move his/her finger. On the contrary, in the slave system, an end-effector is controlled

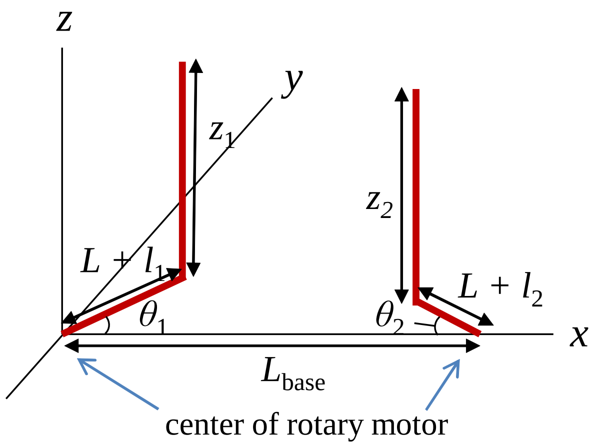

(a) x-y-z axis view.

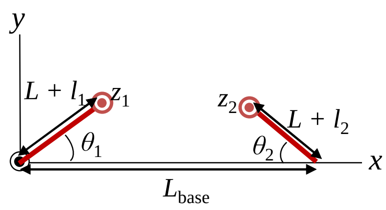

(b) x-y axis view.

Fig. 2-22: Modelings of the experimental systems.

by the master system and it contacts with an environment. Model of the system is shown in Fig. 2-22 where L stands for length between center of the rotary motor to the end-effector (horizontal direction); L_{base} stands for length between rotary motors of two device units; θ stands for angle response of rotary motor located horizontally; l stands for position response of linear motor located horizontally; z stands for position response of linear motor located vertically; and subscript $_1$ and $_2$ stand for device unit 1, which is for thumb, and device unit 2, which is for first finger respectively.

Coordinate Transformation between Motor Space and Work Space

First, information in the motor space is transformed into work space information. Generally, Jacobian matrix is used for the coordinate transformation. Eqs. (2.29) – (2.31) show equations to transform position, velocity, and force information:

$$\boldsymbol{P}_{\mathrm{work}} = \begin{bmatrix} x_{\mathrm{tmb}} \\ y_{\mathrm{tmb}} \\ z_{\mathrm{tmb}} \\ x_{\mathrm{fst}} \\ y_{\mathrm{fst}} \\ z_{\mathrm{fst}} \end{bmatrix} = \begin{bmatrix} (L+l_1)\cos\theta_1 \\ (L+l_1)\sin\theta_1 \\ z_1 \\ L_{\mathrm{base}} - (L+l_2)\cos\theta_2 \\ (L+l_2)\sin\theta_2 \\ z_2 \end{bmatrix}, \tag{2.29}$$

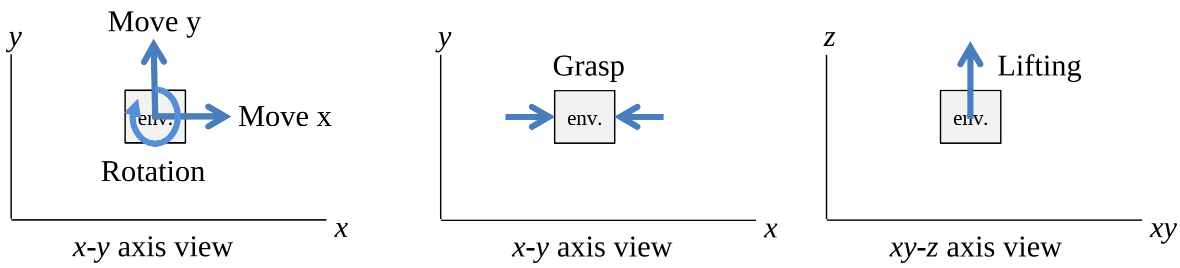

Fig. 2-23: Motion mode.

$$\dot{\boldsymbol{P}}_{\text{work}} = \boldsymbol{J}_{aco,work}\dot{\boldsymbol{P}}_{\text{motor}} = \begin{bmatrix} \cos\theta_1 & -(L+l_1)\sin\theta_1 & 0 & 0 & 0 & 0 \\ \sin\theta_1 & (L+l_1)\cos\theta_1 & 0 & 0 & 0 & 0 \\ 0 & 0 & 1 & 0 & 0 & 0 \\ 0 & 0 & 0 & -\cos\theta_2 & (L+l_2)\sin\theta_2 & 0 \\ 0 & 0 & 0 & \sin\theta_2 & (L+l_2)\cos\theta_2 & 0 \\ 0 & 0 & 0 & 0 & 0 & 1 \end{bmatrix} \begin{bmatrix} \dot{l}_1 \\ \dot{\theta}_1 \\ \dot{z}_1 \\ \dot{l}_2 \\ \dot{\theta}_2 \\ \dot{z}_2 \end{bmatrix}, \tag{2.30}$$

$$\boldsymbol{F}_{\text{work}} = \boldsymbol{J}_{aco,work}^{-T}\boldsymbol{F}_{\text{motor}}, \tag{2.31}$$

where $\boldsymbol{P}$ and $\boldsymbol{F}$ stands for the position matrix and force matrix respectively; $\boldsymbol{J}_{\text{aco}}$ stands for Jacobian matrix; subscript $_{\text{tmb}}$ and $_{\text{fst}}$ stand for thumb and first finger respectively; and subscript $_{\text{motor}}$ and $_{\text{work}}$ stand for the motor-space information and work-space information, respectively. The equivalent mass matrix in the work space is shown below:

$$\boldsymbol{M}_{\text{eq,work}}\ddot{\boldsymbol{P}}_{\text{work}} = \boldsymbol{F}_{\text{work}}, \tag{2.32}$$

where

$$\boldsymbol{M}_{\text{eq,work}} = \boldsymbol{J}_{\text{aco,work}}^{-T}\boldsymbol{M}_{\text{motor}}\boldsymbol{J}_{\text{aco,work}}^{-1}. \tag{2.33}$$

In Eqs. (2.32) and (2.33), $\boldsymbol{M}$ stands for the mass matrix and subscript $\boldsymbol{M}_{\text{eq}}$ stands for the equivalent mass matrix.

Coordinate Transformation between Work Space and Motion-Mode Space

In order to deal with human motions, a coordinate transformation from work space to motion-mode space is shown. In this section, the following six motion-mode axes are defined as Fig. 2-23.

move-x: target object's linear motion on x axis;

move-y: target object's linear motion on y axis;

rotation: target object's rotary motion;

grasp: grasping motion for target object;

lifting: target object's linear motion on vertical axis;

z-difference: height difference between end-effectors of thumb and first finger.

These axes are on the basis of the relation of two end-effectors. Hence, they do not stand for the movement of the target object directly. When the devices grasp the target object, axes of the move-x, move-y, rotation, lifting, z-difference indicate the movement of the target object. Note that, in order to simplify the motion, the "z-difference" axis is controlled by position controller which command is 0. As a result, height of the end effectors of two-device units is held as the same. Hence, the human motions are expressed by remaining five axes in this research.

The transformation between work space and motion-mode space is similar as above subsection. Eqs. 2.29 – 2.31 show equations to transform the position, velocity, and force information;

$$\boldsymbol{P}_{\rm mode} = \begin{bmatrix} p_{{\rm mv}-x} \\ p_{{\rm mv}-y} \\ p_{\rm rot} \\ p_{\rm grsp} \\ p_{\rm lift} \\ p_{z-{\rm dif}} \end{bmatrix} = \begin{bmatrix} \frac{x_{\rm tmb}+x_{\rm fst}-L_{\rm base}}{2} \\ \frac{y_{\rm tmb}+y_{\rm fst}}{2} \\ \tan^{-1}\frac{y_{\rm fst}-y_{\rm tmb}}{x_{\rm fst}-x_{\rm tmb}} \\ \sqrt{(x_{\rm fst}-x_{\rm tmb})^2+(y_{\rm fst}-y_{\rm tmb})^2} \\ \frac{z_{\rm tmb}+z_{\rm fst}}{2} \\ \frac{z_{\rm tmb}-z_{\rm fst}}{2} \end{bmatrix}, \tag{2.34}$$

$$\dot{\boldsymbol{P}}_{\rm mode} = \boldsymbol{J}_{aco,mode}\dot{\boldsymbol{P}}_{\rm work} = \begin{bmatrix} \frac{1}{2} & 0 & 0 & \frac{1}{2} & 0 & 0 \\ 0 & \frac{1}{2} & 0 & 0 & \frac{1}{2} & 0 \\ A & B & 0 & -A & -B & 0 \\ C & D & 0 & -C & -D & 0 \\ 0 & 0 & \frac{1}{2} & 0 & 0 & \frac{1}{2} \\ 0 & 0 & \frac{1}{2} & 0 & 0 & -\frac{1}{2} \end{bmatrix} \begin{bmatrix} \dot{x}_{\rm tmb} \\ \dot{y}_{\rm tmb} \\ \dot{z}_{\rm tmb} \\ \dot{x}_{\rm fst} \\ \dot{y}_{\rm fst} \\ \dot{z}_{\rm fst} \end{bmatrix}, \tag{2.35}$$

$$\begin{aligned} A &= \frac{y_{\rm fst}-y_{\rm tmb}}{(x_{\rm fst}-x_{\rm tmb})^2-(y_{\rm fst}-y_{\rm tmb})^2}, \quad & B &= -\frac{x_{\rm fst}-x_{\rm tmb}}{(x_{\rm fst}-x_{\rm tmb})^2-(y_{\rm fst}-y_{\rm tmb})^2}, \\ C &= -\frac{x_{\rm fst}-x_{\rm tmb}}{\sqrt{(x_{\rm fst}-x_{\rm tmb})^2+(y_{\rm fst}-y_{\rm tmb})^2}}, \quad & D &= -\frac{y_{\rm fst}-y_{\rm tmb}}{\sqrt{(x_{\rm fst}-x_{\rm tmb})^2+(y_{\rm fst}-y_{\rm tmb})^2}}, \end{aligned} \tag{2.36}$$

$$\boldsymbol{F}_{\rm mode} = \boldsymbol{J}_{aco,mode}^{-T}\boldsymbol{F}_{\rm work}, \tag{2.37}$$

where p stands for position; subscript ${}_{{\rm mv}-x}$, ${}_{{\rm mv}-y}$, ${}_{\rm rot}$, ${}_{\rm grsp}$, ${}_{\rm lift}$, and ${}_{z-{\rm dif}}$ stand for axis of "move-x mode," axis of "move-y mode," axis of "rotation mode," axis of "grasp mode," axis of "lifting mode,"

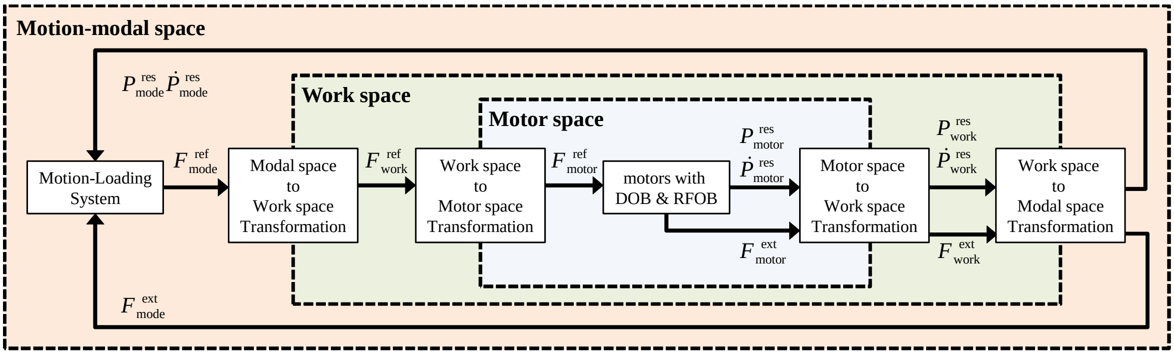

Fig. 2-24: Coordinate transformation.

and axis of "z-difference" respectively; and subscript $_{\mathrm{mode}}$ stands for motion-mode space information. The equivalent mass matrix in the motion-mode space is shown as

$$\boldsymbol{M}_{\mathrm{eq,mode}}\ddot{\boldsymbol{P}}_{\mathrm{mode}} = \boldsymbol{F}_{\mathrm{mode}}, \tag{2.38}$$

where

$$\boldsymbol{M}_{\mathrm{eq,mode}} = \boldsymbol{J}_{\mathrm{aco,mode}}^{-T}\boldsymbol{M}_{\mathrm{work}}\boldsymbol{J}_{\mathrm{aco,mode}}^{-1}. \tag{2.39}$$

From eqs. (2.29)–(2.39), the information of the motor space is transformed into the information of the motion-mode space shown in fig. 2-24. In this section, the MCS is implemented in each axis in motion-mode space. In addition, work space observer [103–105] is implemented in the motion-mode space not to interfere with each modal axis.

2.4.2 Experiments

Experimental Setup

In this section, the validity of the proposed method is verified by experiments. Fig. 2-25 shows the experimental system used in the experiments. This system is constructed by the master and slave systems, and each system is composed of two-device units. The device unit is constructed by three motors; a rotary motor (horizontal) and two linear motors (horizontal and vertical). In the motion-saving step, both of the master and slave systems were used. A human operator operates the master system, and the end effector in the slave system grasped an environment shown Fig. 2-26.

The position response was measured by the position encoder or the rotary encoder, and the force response was estimated by reaction force observer (RFOB) without force sensors. The control program

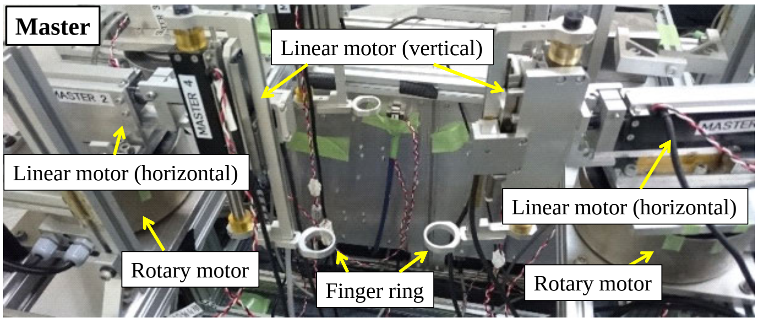

(a) Master system.

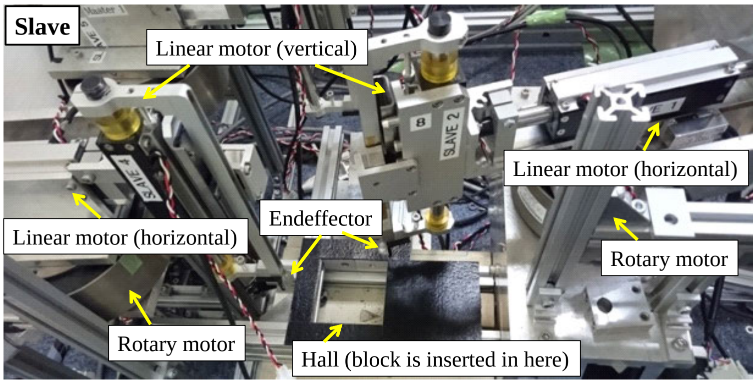

(b) Slave system.

Fig. 2-25: Experimental systems for reproduction with motion mode.

Fig. 2-26: Target environment (Cork block).

was written in C language under RTAI 3.7. The parameters used in these experiments are shown in Table 2.7.

Experimental Results of Motion Recording

Figs. 2-27 and 2-28 show the experimental results of the motion recording. The responses of the master and slave systems are depicted in the figure. The left figures show the position responses and the

Table 2.7: Experimental parameters for reproduction with motion mode.

Parameter	Description	Value
$T_{\rm s}$	Sampling time	200 μs
L	length between center of the rotary motor to the end-effector	0.16 m
$L_{\rm base}$	length between rotary motors of two device units	0.41 m
$K_{\rm fn}$	Force coefficient of linear motor	40.0 N/A
$M_{\rm n}$	Mass of linear motor	0.3 kg
$g_{\rm pd,l}$	Cut-off frequency of pseudo-derivation of linear motor	600 rad/s
$g_{\rm dis,l}$	Cut-off frequency of disturbance observer of linear motor	600 rad/s
$K_{\rm tn}$	Torque coefficient of rotary motor	1.18 Nm/A
$I_{\rm n}$	Inertia around rotary motor	0.00288 kgm^2
$g_{\rm pd,r}$	Cut-off frequency of pseudo-derivation of rotary motor	250 rad/s
$g_{\rm dis,r}$	Cut-off frequency of disturbance observer of rotary motor	250 rad/s
$K_{\rm p,move}$	Position gain for move-x and move-y axes	3600
$K_{\rm d,move}$	Velocity gain for move-x and move-y axes	120
$K_{\rm f,move}$	Force gain for move-x and move-y axes	5
$K_{\rm p,rot}$	Position gain for rotation axis	1600
$K_{\rm d,rot}$	Velocity gain for rotation axis	80
$K_{\rm f,rot}$	Force gain for rotation axis	2
$K_{\rm p,grsp}$	Position gain for grasp axis	3600
$K_{\rm d,grsp}$	Velocity gain for grasp axis	120
$K_{\rm f,grsp}$	Force gain for grasp axis	5
$K_{\rm p,lift}$	Position gain for lifting and z-diff axes	3600
$K_{\rm d,lift}$	Velocity gain for lifting and z-diff axes	120
$K_{\rm f,lift}$	Force gain for lifting axis	0.8
$g_{\rm wob}$	Cut-off frequency of work space observer	500 rad/s
$m_{\rm obj1}$	Weight of cork block	0.05 kg
$l_{\rm obj1}$	Side length of cork block	0.055 m

right figures show the force responses. The responses of the motion-modal space are shown, because the MCS controllers are implemented in the motion-modal space. It is shown from figures that the operator grasped the block at first; then he lifted the block; moved the block at y direction; moved the block at x direction; rotated the block; and finally got his finger off of the block. These figures show that the responses of master and slave systems are almost the same because the ideal bilateral control is implemented. Note that z-different axis was controlled by position controller to keep height of the devices.

Experimental Results of Motion Reproduction

Figs. 2-29 and 2-30 show the experimental results of the motion reproduction. The responses of the recorded data and reproduced data are depicted in the figure. The left figures show the position responses and the right figures show the force responses. It is shown that recorded motion was reproduced. The error between recorded data and reproduced data is caused by difference of environmental condition. As

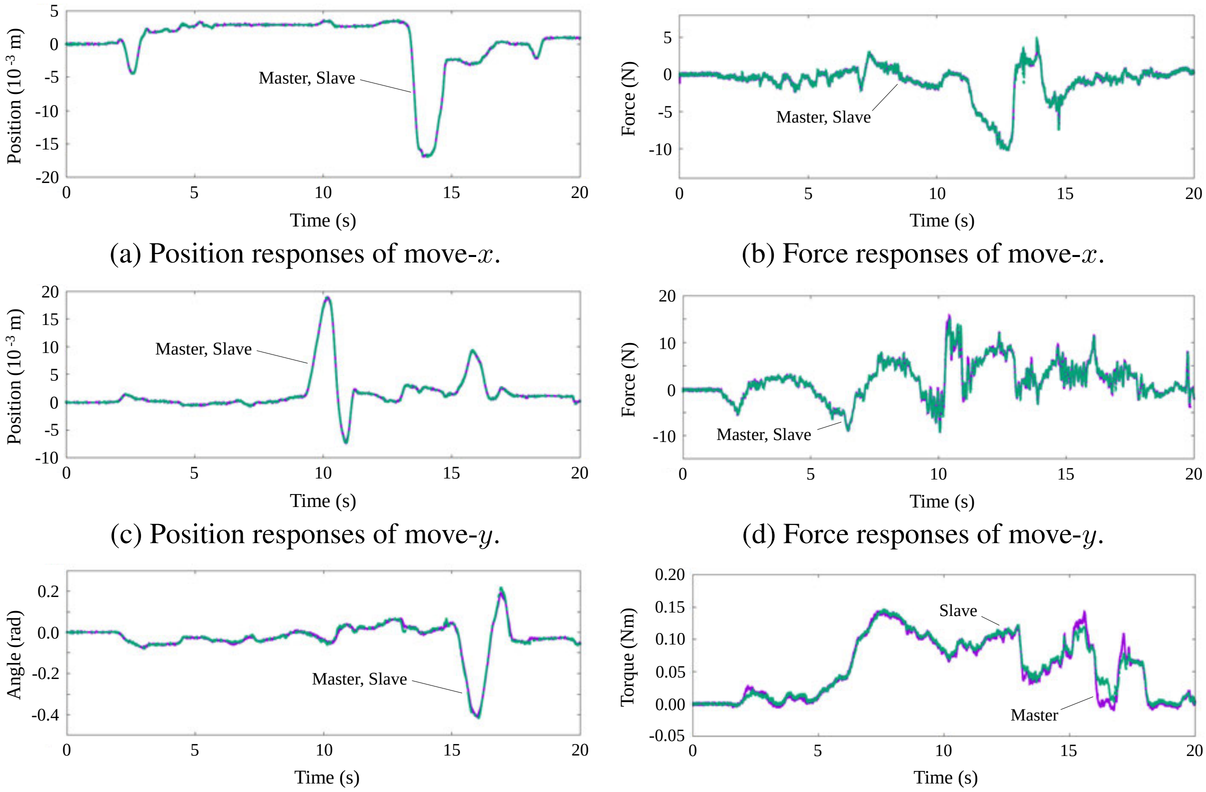

(a) Position responses of move-x. (b) Force responses of move-x.

(c) Position responses of move-y. (d) Force responses of move-y.

(e) Angle responses of rotation. (f) Torque responses of rotation.

Fig. 2-27: Experimental result of motion recording based on motion mode. (1/2)

described in section 2.2, the completely same environmental condition is needed for perfect reproduction. However, it is impossible to satisfy such condition. In particular in this experimental system, the device is slightly warped, and the initial location of the device and target object is not completely the same. Hence, the completely same response could not be achieved because environmental condition is little bit different from motion recording phase.

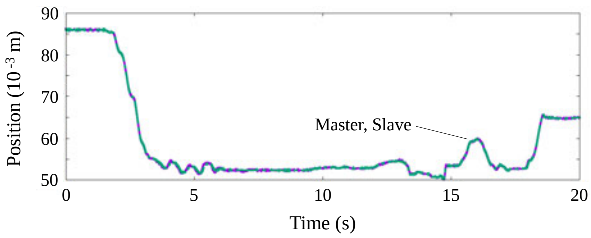

(a) Position responses of grasping.

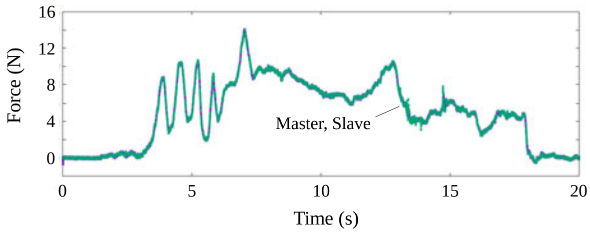

(b) Force responses of grasping.

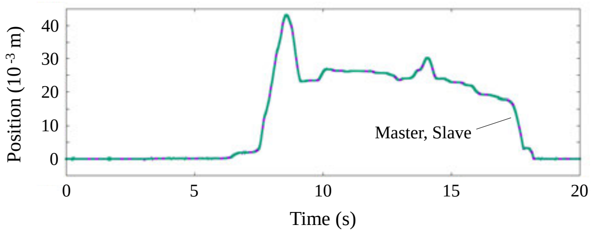

(c) Position responses of lifting.

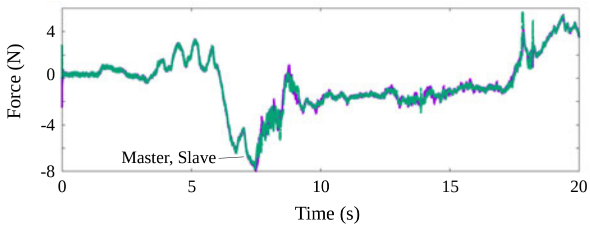

(d) Force responses of lifting.

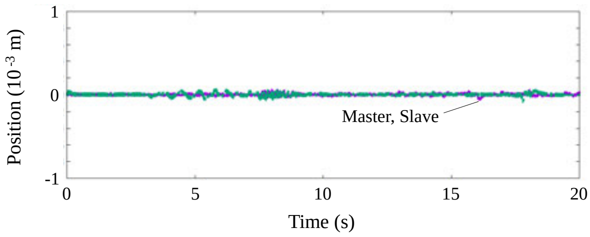

(e) Position responses of z-difference.

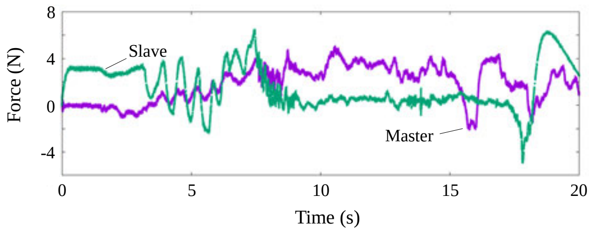

(f) Force responses of z-difference.

Fig. 2-28: Experimental result of motion recording based on motion mode. (2/2)

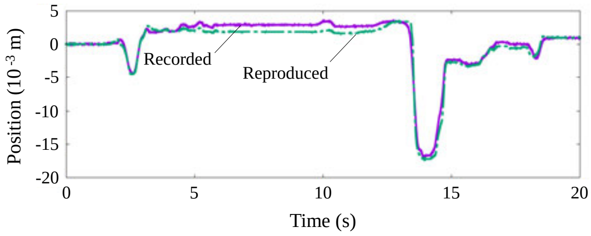

(a) Position responses of move-x.

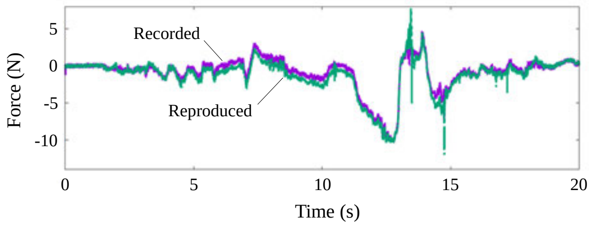

(b) Force responses of move-x.

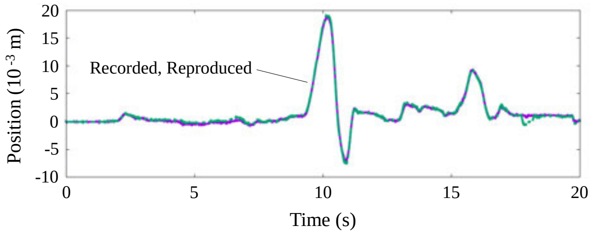

(c) Position responses of move-y.

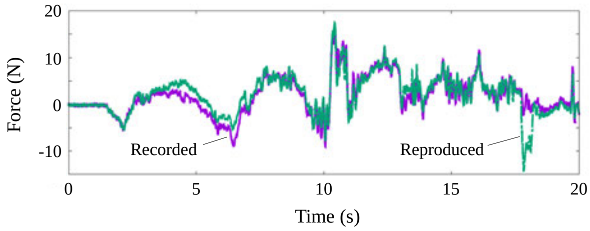

(d) Force responses of move-y.

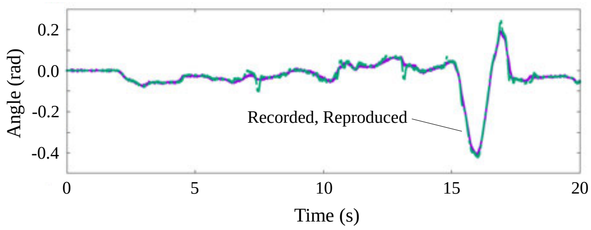

(e) Angle responses of rotation.

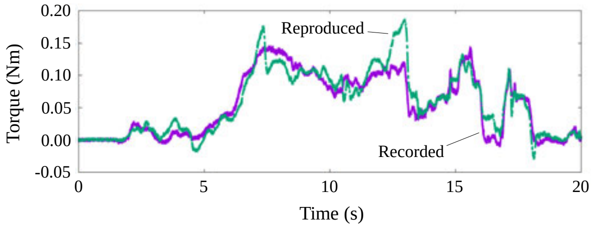

(f) Torque responses of rotation.

Fig. 2-29: Experimental result of motion reproduction based on motion mode. (1/2)

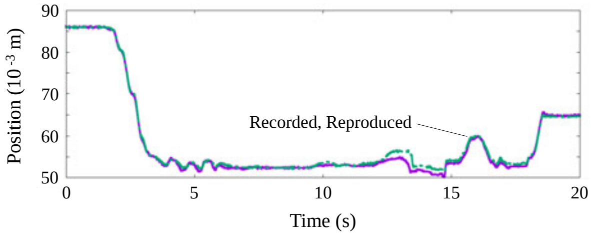

(a) Position responses of grasping.

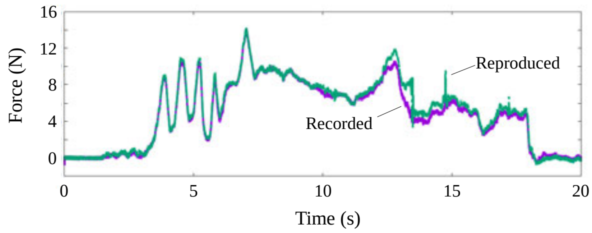

(b) Force responses of grasping.

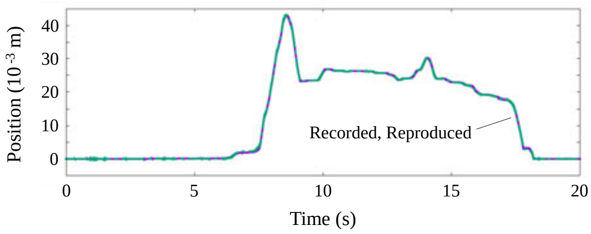

(c) Position responses of lifting.

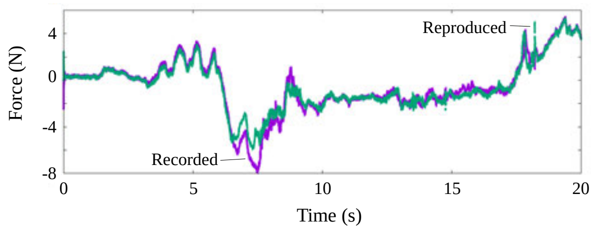

(d) Force responses of lifting.

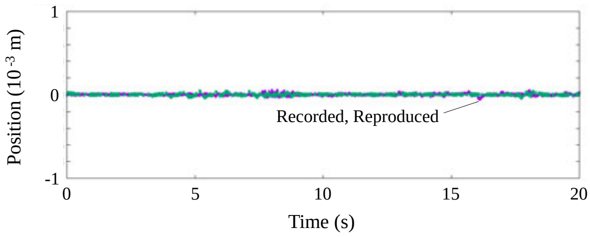

(e) Position responses of z-difference.

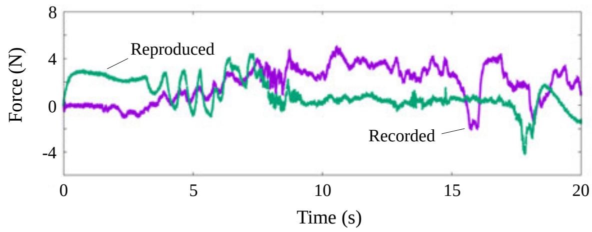

(f) Force responses of z-difference.

Fig. 2-30: Experimental result of motion reproduction based on motion mode. (2/2)

2.5 Summary

In this chapter, coordinate transformation from motor space to common space was described and two concepts were introduced; abstraction and specialization. Under the concept of the coordinate transformation, three types of coordinates were discussed. First in section 2.2, the work space was chosen as the common coordinate to abstract the motion data which depend on a hardware structure. By this transformation, motion data could be reproduced even if the structures of the haptic devices are different. Then, the human modal space and the motion modal space were introduced to specialize motion data for applications in section 2.3 and section 2.4, respectively. The human modal space was introduced to treat human motion on the basis of human model. It was assumed that an exoskeleton haptic device is used in motion recording and an endoskeleton haptic device is used in motion reproduction. On the other hand, the motion modal space was introduced to separate motion elements from the human motion. By this transformation, the appropriate control methods could be implemented in each motion element. In each section, the validity of the proposed methods was shown by the experimental results. These coordinate transformations are used in the following chapter.

For ideal motion reproduction, it is more desirable to deal with the motion data in the relative coordinate to the environment. It is because that the human motion targets the external environment. Hence, if the environmental location is changed, it is expected that relation between the environment and the origin of the coordinate is maintained. As described in section 2.4, the motion mode is not the coordinate of the movement of the target object, but the coordinate of the movement of the end-effectors. In this case, the motion mode does not completely depend on the structure of the devices because the relation of the initial position between two end-effectors depends on the structure of the device. If we want to construct the system which is not affected by the device at all, it is necessary to deal with the motion data in the relative coordinate to the object. In addition, it is more desirable to consider the relation between the target object and the external environment, too.

Chapter 3

Integrated Reproduction of Motion Components

3.1 Background and Overview of This Chapter

For the future applications of the motion-copying system, it is important to reproduce many motions from fewer recorded motions. For example, in industrial processing, there are some processes such as the cutting process, boring process, and polishing process. Of course, the motions for each process are different. Hence, the skills required for them are also different. If the integrated reproduction is achieved, expert motions for each process can be recorded separately as motion components and then integrated and reproduced as a single motion by robots. As a result, the many motions can be constructed from the recorded motion components. As mentioned above, the proposed system couples the recorded motions temporally and an integrated motion reproduction can be achieved using it.

In this chapter, methods to connect two recorded motions in time series and reproduce in a single motion are proposed. The concept of the integrated reproduction is shown in Fig. 3-1. The recorded two motions are integrated temporally, and the integrated motion is reproduced in one motion.

In the previous studies about motion teaching to humanoid robots, some postures are recorded and they are interpolated. As a result, one motion is generated by interpolation of the postures [106, 107]. In other words, motion is just a set of the postures. On the other hand, there are few researches that one motion is generated by motion components [108]. Because boundaries of the motion components are just a posture, the same concept of the interpolation can be used at the motion-copying system.

In this chapter, two coupling methods are proposed. The method described in section 3.2 assumes that

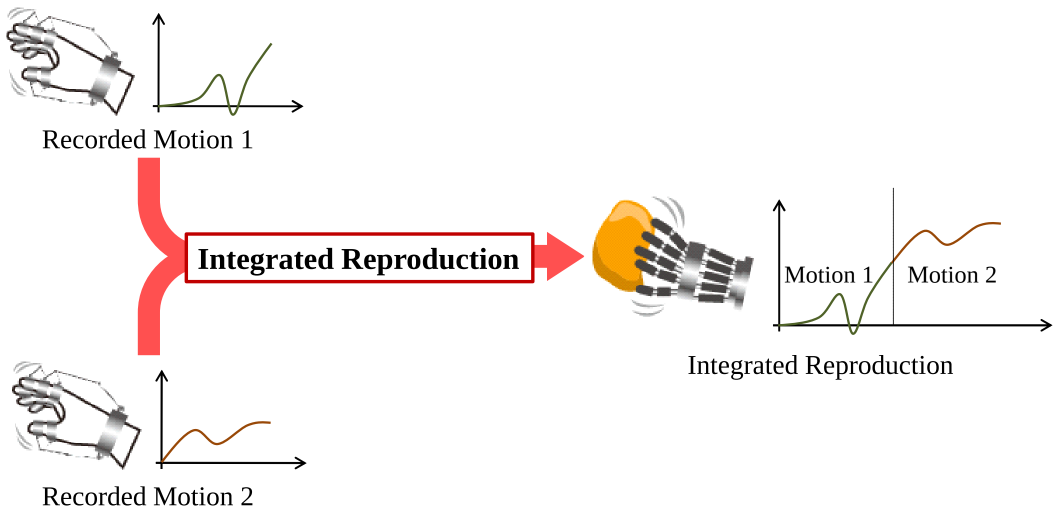

Fig. 3-1: Concept of integrated reproduction of motion elements.

human motions are dealt with position and force information [83–85]. In this method, interpolated data are calculate and inserted between two motions to connect them smoothly. Concept of this method is same as the motion teaching of the humanoid robots. The other method described in section 3.3 assumes that human motions are dealt with acceleration information [86]. In this method, general interpolation method cannot be used, because position information is not used as the motion data. Instead of it, equivalent velocities of the two motions are connected by adding acceleration between two motions. These two methods depend on the format of motion data. We can choose motion data format according to the aim or the environmental condition of motion reproduction. These proposed methods can apply to the basic motion-copying system [65] and the motion-copying system based on acceleration information [91]. By the integrated reproduction, the motions in separated process are recorded independently, and whole task is realized by connect any motion components of each process. In each section, experimental results show the validity of the proposed methods.

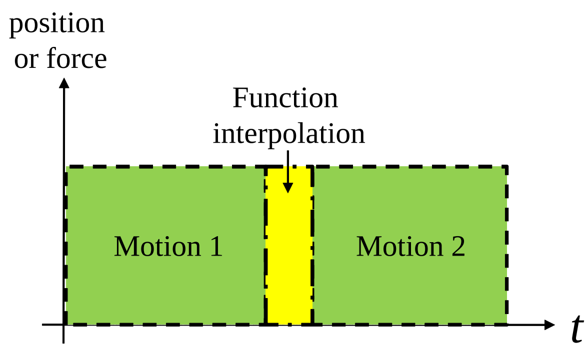

Fig. 3-2: Simplified diagram of integrated reproduction based on position and force information.

3.2 Integrated Reproduction Based on Position and Force Information

In this section, a method of integrating two recorded motions and of reproducing the integrated motion in a single motion [83–85] is described. When recorded motions are integrated directly, the abrupt change occurs between each motion because the commands of connection point are not continuous. To avoid such case, the recorded position and force data are interpolated to connect the motions smoothly. Fig. 3-2 shows the concept of the proposed method. In this section, the proposed method is implemented in the system described in section 2.3.

3.2.1 Control Structure

In order to avoid the abrupt change, a coupling interval is inserted between the two recorded motions and the recorded motions are interpolated during the coupling interval. In this paper, cubic interpolation is used to consider the effects of second-order derivation on the data. Further, it is assumed that the position of an environment is known.

The angle command θ_{cmd} and the torque command T_{cmd} during the coupling interval are

$$\theta_{\mathrm{cmd}} = a_\theta + b_\theta(t-t_1) + c_\theta(t-t_1)^2 + d_\theta(t-t_1)^3 \tag{3.1}$$

$$T_{\mathrm{cmd}} = a_T + b_T(t-t_1) + c_T(t-t_1)^2 + d_T(t-t_1)^3, \tag{3.2}$$

where t and t_1 stand for time and time when the first motion ends; $a, \cdots, d$ stand for coefficient of $t^0, \cdots, t^3$; and subscripts $_\theta$ and $_T$ stand for angle command and torque command, respectively. The coefficients used in Eqs. (3.1) and (3.2) are calculated by

$$\begin{cases} a_\theta = \theta_1^{\mathrm{end}} \\ b_\theta = \dot{\theta}_1^{\mathrm{end}} \\ c_\theta = \dfrac{3(\theta_2^{\mathrm{beg}} - \theta_1^{\mathrm{end}})}{(t_2 - t_1)^2} - \dfrac{\dot{\theta}_2^{\mathrm{beg}} + 2\dot{\theta}_1^{\mathrm{end}}}{t_2 - t_1} \\ d_\theta = -\dfrac{2(\theta_2^{\mathrm{beg}} - \theta_1^{\mathrm{end}})}{(t_2 - t_1)^3} + \dfrac{\dot{\theta}_2^{\mathrm{beg}} + \dot{\theta}_1^{\mathrm{end}}}{(t_2 - t_1)^2} \end{cases} \tag{3.3}$$

$$\begin{cases} a_T = T_1^{\mathrm{end}} \\ b_T = \dot{T}_1^{\mathrm{end}} \\ c_T = \dfrac{3(T_2^{\mathrm{beg}} - T_1^{\mathrm{end}})}{(t_2 - t_1)^2} - \dfrac{\dot{T}_2^{\mathrm{beg}} + 2\dot{T}_1^{\mathrm{end}}}{t_2 - t_1} \\ d_T = -\dfrac{2(T_2^{\mathrm{beg}} - T_1^{\mathrm{end}})}{(t_2 - t_1)^3} + \dfrac{\dot{T}_2^{\mathrm{beg}} + \dot{T}_1^{\mathrm{end}}}{(t_2 - t_1)^2} \end{cases}, \tag{3.4}$$

where t_2 stands for time when the second motion begins; and superscript $^{\mathrm{end}}$ and $^{\mathrm{beg}}$ stand for last value of recorded motion and first value of recorded motion, respectively. t_2 is obtained by

$$t_2 = t_1 + t_{\mathrm{cpl}}, \tag{3.5}$$

where t_{cpl} stands for length of the coupling interval. A designer can set t_{cpl} depending on the applications. If the working efficiency of an assembly process requires to be good, t_{cpl} should be set to a value that is as small as possible. On the other hand, if the proposed method is applied to a human support field such as a power-assisted system, t_{cpl} should be set to a value such that the operator does not feel discomfort.

3.2.2 Experiments

In this sub-section, the validity of the proposed method is verified by experiments. Here, finger motion is considered, and the operator's motions are recorded and reproduced. The model of the experimental system is described in the section 2.3.

Experimental Setup

The experimental systems are shown in Fig. 3-3. These systems are constructed using motor systems, which are composed of linear motors and position encoders whose resolutions are 100 nm. An aluminum

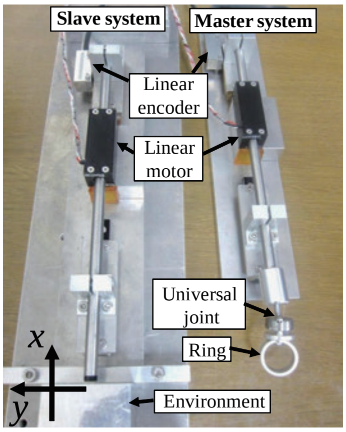

(a) Motion-saving system.

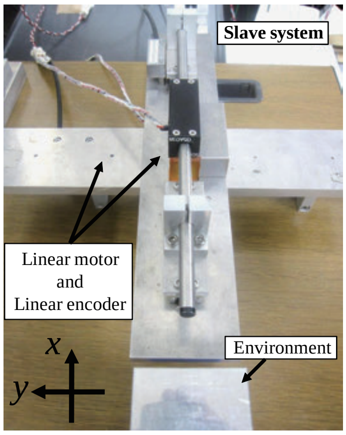

(b) Motion-loading system.

Fig. 3-3: Experimental system for motion-copying system based on human model.

Table 3.1: Experimental parameters of integrated reproduction based on position and force information.

Parameter	Description	Value
T_s	Sampling time	100 μs
K_{tn}	Force coefficient	3.3 N/A
M_n	Mass	0.24 kg
K_p	Position gain	10000
K_d	Velocity gain	200
K_f	Force gain	12
g_{pd}	Cut-off frequency of pseudo-derivation	5000 rad/s
g_{dis}	Cut-off frequency of disturbance observer	700 rad/s
g_r	Cut-off frequency of reaction force observer	700 rad/s

block was used in the experiments. The position information was measured by a position encoder and the force response was estimated by the RFOB without force sensors. The control program was implemented in RTAI 3.7. The experimental parameters are listed in Table 3.1, and the parameters of the finger model are listed in Table 3.2.

The experimental system used for the motion-saving system is shown in Fig. 3-3 (a). This experimental system is composed of master and slave systems. The linear motors are actuated only in the y-axial direction. A human operator wears the ring, which is connected to the universal joint, and moves the master system; the slave system is teleoperated. When the end effector of the slave system contacts an environment, the human operator feels a reaction force from the environment resembling that experienced by touching a real environment. The information acquired by the master system is transformed

Table 3.2: Parameters of finger model for velification of integrated reproduction based on position and force information.

Parameter	Description	Value
l_1	Length of link 1	0.025 m
l_2	Length of link 2	0.025 m
m_1	Mass of link 1	0.012 kg
m_2	Mass of link 2	0.012 kg
θ_{fix}	Fixed angle	0.524 rad
$\theta_{1\ \text{ini}}$	Initial angle of PIP joint	0.087 rad
$\theta_{2\ \text{ini}}$	Initial angle of DIP joint	0.070 rad

into finger modal space and recorded to the motion data memory.

In this research, two types of motions were recorded separately. First, an unconstrained motion was recorded. This motion is the one in which the end effector does not contact the environment. Hence, the position response of the master system tracks that of the slave system. Second, a constrained motion was recorded. This motion is the one in which the end effector contacts the environment and the operator applies an external force on to the environment. The unconstrained motion was recorded as “motion 1,” and the constrained motion was recorded as “motion 2.” The durations of both the motions were 5 s.

The experimental system for the motion-loading system is shown in Fig. 3-3 (b). This system is an x-y table composed of two linear actuator systems. The distance between the initial position of the end effector and the environment was set to 0.03 m.

In the motion-loading system, two recorded motions were integrated in a time series and reproduced as a single motion. The recorded motions were interpolated during the coupling interval in the finger modal space. Then, the integrated motion was transformed into commands for the position and force controllers and reproduced on the basis of these commands. The coupling interval between two motions was set to 0.5 s.

Experimental Results of Motion Recording

Figs. 3-4 and 3-5 show the experimental results of the motion-saving system. The responses of the master and slave systems are depicted in the figure, (a) and (b) respectively show the position responses and force responses acquired by the linear actuators in the real world. Then, the movement of the operator’s finger joint is estimated from the responses of the master system. (c) and (d) respectively show the estimated angle and torque in the finger modal space, which are estimated by the Newton-Raphson method and using Eq. (2.22). In these figures, the responses of the PIP and DIP joints are

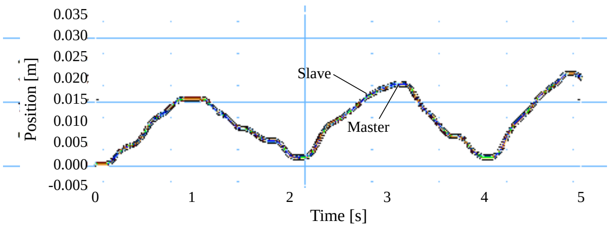

(a) Position responses.

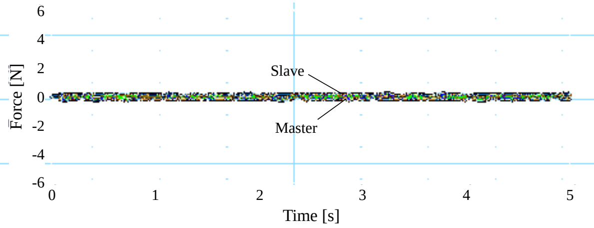

(b) Force responses.

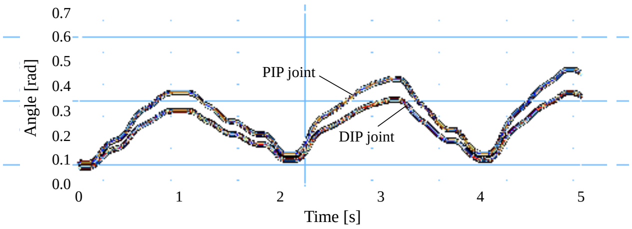

(c) Estimated angle.

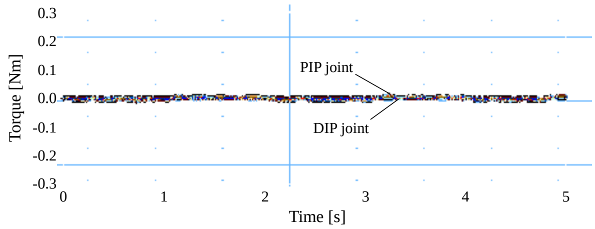

(d) Estimated torque.

Fig. 3-4: Experimental results of motion recording of motion 1 for velification of integrated reproduction based on position and force information.

depicted. Fig. 3-4 shows the results for motion 1 (unconstrained motion). The position responses vary significantly, but the force responses do not vary as much because the end effector does not contact the environment. On the other hand, Fig. 3-5 shows the results for motion 2 (constrained motion). This figure shows that the operator applied a force to the environment twice. The responses shown in Fig. 3-4 (c) and (d) and in Fig. 3-5 (c) and (d) were recorded to the motion data memory.

Experimental Results of Motion Reproduction

Fig. 3-6 shows the experimental result of the integrated motion reproduction of the two recorded motions. In the figure, (a) and (b) respectively show the position and force responses and the information about both the x axis and the y axis is shown. (c) and (d) respectively show the estimated responses about the PIP joint and the DIP joint. In Fig. 3-6, the virtual master system stands for the responses of the recorded motion in the motion data memory. The errors for each response are described in Fig. 3-7: (a) shows the angle error and (b) shows the torque error. These figures reveal two things. First, the two recorded motions were integrated and reproduced as a single motion. In particular, motion 1 was reproduced in the first 5.0 s and the recorded motion 2 was reproduced in the last 5.0 s. Between the two motions, the coupling interval was inserted. Fig. 3-7 shows that the errors between the responses of the motion-saving and motion-loading systems are sufficiently small. Second, the motion acquired by the

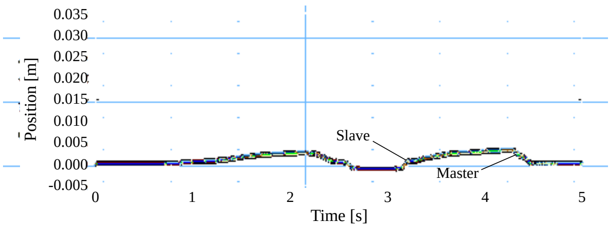

(a) Position responses.

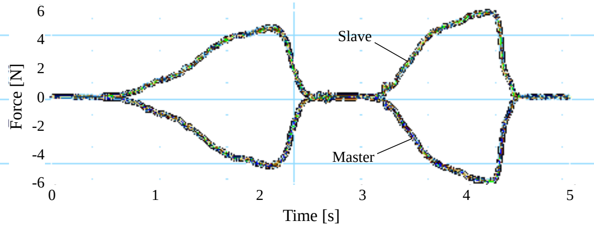

(b) Force responses.

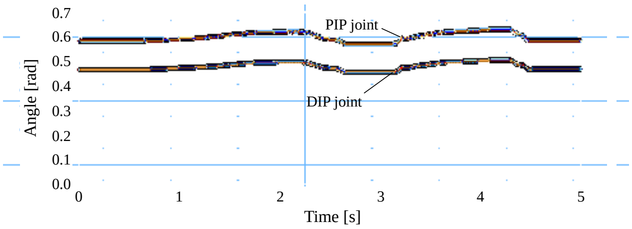

(c) Estimated angle.

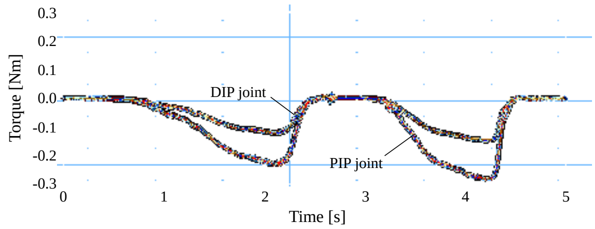

(d) Estimated torque.

Fig. 3-5: Experimental results of motion recording of motion 2 for velification of integrated reproduction based on position and force information.

motion-saving system was reproduced using devices with different configurations through the conversion of data point into the finger modal space. Even though the information of the motion about the x axis was unknown in the motion-saving system, it was estimated through the finger motion data and reproduced using a different device.

Next, the evaluation of the experimental results using a correlation coefficient is discussed. The goal of motion reproduction is that the responses of the motion-saving and motion-loading systems should be the same. Hence, it can be said that if the correlation coefficient between the responses of the motion-saving and motion-loading systems is large, ideal motion reproduction is achieved. The correlation coefficient is obtained by the equation:

$$R = \frac{\sum_{i=1}^{n}(a_i^{\mathrm{sav}} - \overline{a}^{\mathrm{sav}})(a_i^{\mathrm{ld}} - \overline{a}^{\mathrm{ld}})}{\sqrt{\sum_{i=1}^{n}(a_i^{\mathrm{sav}} - \overline{a}^{\mathrm{sav}})^2}\sqrt{\sum_{i=1}^{n}(a_i^{\mathrm{ld}} - \overline{a}^{\mathrm{ld}})^2}}, \tag{3.6}$$

where R, a^{sav}, a^{ld}, $\bar{\ }$, and n stand for correlation coefficient, recorded response, and reproduced responses, average, and amount of data, respectively.

The correlation coefficients for each response are listed in Table 3.3. It can be seen that the values of the correlation coefficients are large for both reproductions. Hence, it can be concluded that accurate reproductions were achieved. From these experimental results, the validity of the proposed method is confirmed. The haptic systems were coupled spatially and temporally.

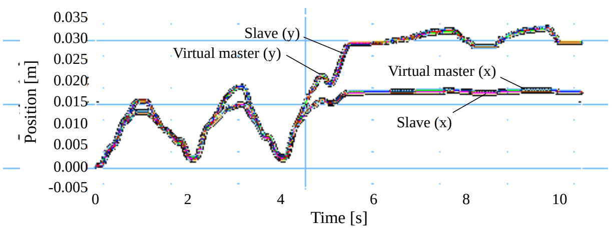

(a) Position responses.

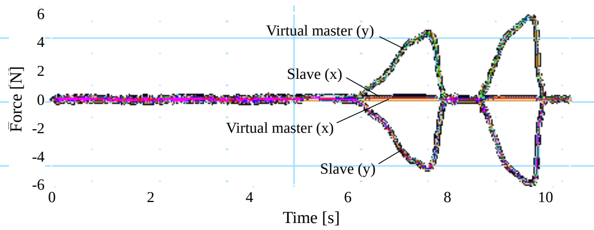

(b) Force responses.

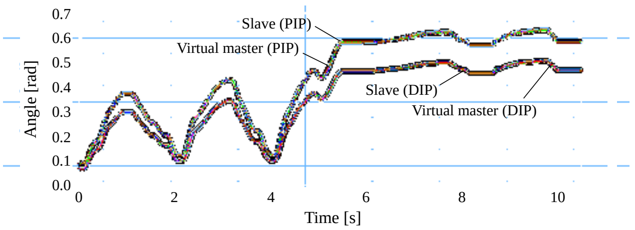

(c) Estimated angle.

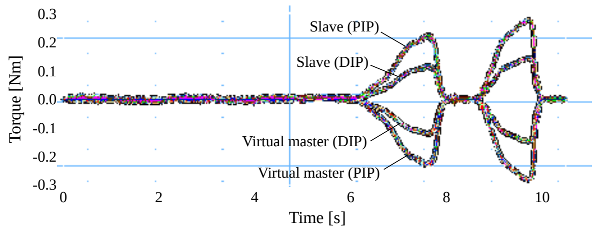

(d) Estimated torque.

Fig. 3-6: Experimental results of integrated motion reproduction for velification of integrated reproduction based on position and force information.

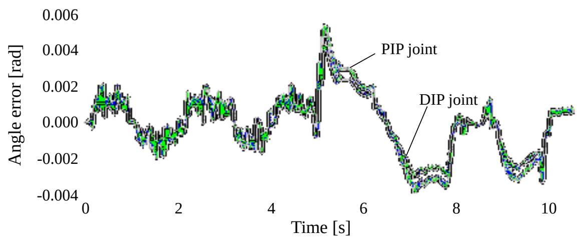

(a) Angle error.

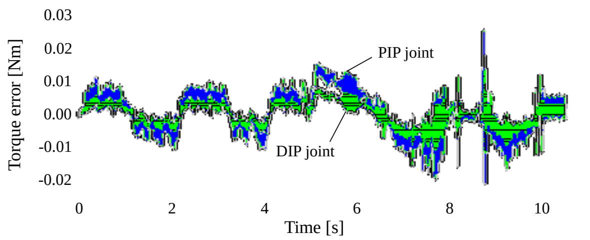

(b) Torque error.

Fig. 3-7: Angle and force errors during motion reproduction for velification of integrated reproduction based on position and force information.

Table 3.3: Correlation between recorded motion and reproduced motion.

	Correlation coefficient
Angle (θ_1)	0.999948
Angle (θ_2)	0.999948
Torque (T_1)	0.997864
Torque (T_2)	0.998050

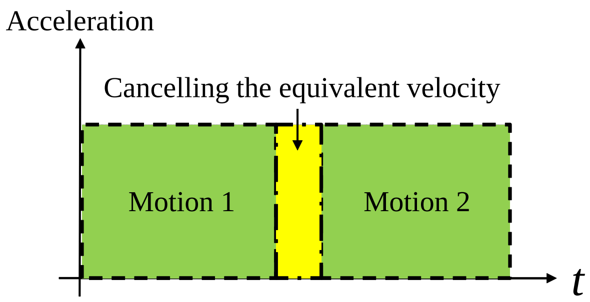

Fig. 3-8: Simplified diagram of integrated reproduction based on acceleration information.

3.3 Integrated Reproduction Based on Acceleration Information

In this section, two human motions are stored to the motion data memory as the acceleration information, and they are integrated in time series and reproduced [86]. In the case when two motions are connected directly, the second motion is not reproduced because an actuator has the haptic energy at the end of the first motion. Therefore, an integration method of the recorded haptic information considering haptic energy is proposed. Fig. 3-8 shows the concept of the proposed method. In this section, the proposed method is implemented in the system described in section 2.2.

3.3.1 Control Structure

In the case that two motions are connected directly, the second motion is not reproduced precisely since the actuator has the haptic energy at the end of the first motion. Concretely speaking, the applied force becomes larger or tip velocity becomes faster in the second motion. Therefore, two motion components need to be integrated considering the continuity of the equivalent haptic energy.

In this research, the equivalent velocity $\dot{x}^{\rm equ}$ which is the integration of the acceleration reference of the recorded motion is assumed to the haptic energy:

$$\dot{x}^{\rm equ} = \int \ddot{x}^{\rm ref} dt. \tag{3.7}$$

The equivalent velocity can be assumed to the haptic energy since the acceleration response corresponds with the reference by DOB. The acceleration response expresses the behavior of the device which include both position variation and applied force. In order to cancel the haptic energy which is comprehended the end of first motion, the rated acceleration of the actuator is applied during appropriate time period:

$$\ddot{x}^{\rm ref} = -{\rm sgn}(\dot{x}^{\rm equ}_{\rm end\,1} - \dot{x}^{\rm equ}_{\rm beg\,2})\ddot{x}^{\rm cpl} \tag{3.8}$$

where $\mathrm{sgn}(\bullet)$ shows the signum function; $\ddot{x}^{\mathrm{cpl}}$ denotes the acceleration added during coupling time; subscript $_{\mathrm{end}\,1}$ and $_{\mathrm{beg}\,2}$ stand for equivalent velocity when the first motion ends and the second motion begins, respectively. The amount of the coupling time is obtained as

$$i = \frac{\left|\dot{x}^{\mathrm{equ}}_{\mathrm{end}\,1} - \dot{x}^{\mathrm{equ}}_{\mathrm{beg}\,2}\right|}{\left|\ddot{x}^{\mathrm{cpl}}\right| T_{\mathrm{s}}} \tag{3.9}$$

where i and T_{s} denote the amount of samples and sampling time period, respectively. Here, $\dot{x}^{\mathrm{equ}}_{\mathrm{end}\,1}$, $\dot{x}^{\mathrm{equ}}_{\mathrm{beg}\,2}$, and T_{s} are the constant parameters which depend on the recorded motion and sampling time period of the system. On the other hand, either i or $\ddot{x}^{\mathrm{cpl}}$ is variable, and the other one is constant. It depends on the application. If we want to set the coupling time as short as possible, $\ddot{x}^{\mathrm{cpl}}$ is set as constant of max acceleration of the system, and i is calculated by Eq. (3.9). On the other hand, if the coupling time is defined by application, i is set constant, and $\ddot{x}^{\mathrm{cpl}}$ is calculated by Eq. (3.9). After cancelling the equivalent velocity, the second motion is reproduced. As a result, the integrated reproduction of human motions is attained.

3.3.2 Experiments

In this sub-section, the validity of the proposed method is verified by experiments. The model of the experimental system is described in the section 2.2.

Experimental Setup

Fig. 3-9 shows experimental systems. Two devices were used in the motion-saving system, and only one device was used in the motion-loading system. The parameters of the serial-link device is shown in Table 3.4. In each system, the same-type DD rotary motors were mounted. The angle responses were measured by the rotary encoders, and the torque responses were estimated by RTOB without torque sensors. Control program was implemented in RTAI 3.7. The experimental parameters are shown in Table 3.5.

In this experiment, the method described in section 3.2 was implemented in x axis, and the proposed method was implemented in y axis. In the motion-saving phase, human operates the master, and the slave was teleoperated and contacted with the environment. The environment was almost located parallel to the x axis. At the same time, the position and force responses of the x axis of the master system were recorded. On the other hand, the acceleration reference of the y axis of the slave system was recorded into the motion data memory. In addition, the equivalent velocity of the y axis of the slave system when

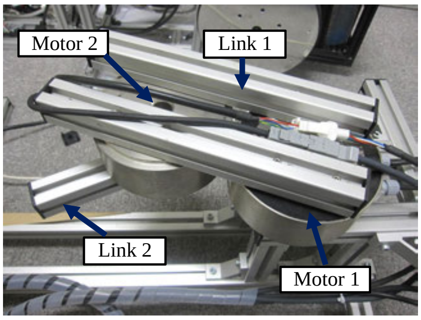

Fig. 3-9: Experimental system for velification of integrated reproduction based on acceleration information.

Table 3.4: Parameters of serial-link device for velification of integrated reproduction based on acceleration information.

Parameter	Description	Value
m_1	Mass 1	2.5 kg
m_2	Mass 2	0.3 kg
l_1	Length of link 1	0.14 m
l_2	Length of link 2	0.14 m
$g_{\mathrm{dis}\,1}$	Cut-off frequency of DOB (motor 1)	80 rad/s
$g_{\mathrm{dis}\,2}$	Cut-off frequency of DOB (motor 2)	200 rad/s
$g_{\mathrm{r}\,1}$	Cut-off frequency of RFOB (motor 1)	300 rad/s
$g_{\mathrm{r}\,2}$	Cut-off frequency of RFOB (motor 2)	500 rad/s

Table 3.5: Experimental parameters for velification of integrated reproduction based on acceleration information.

Parameter	Description	Value
T_{s}	Sampling time	100 μs
	Resolution of motor	260000 pulse/r
K_{tn}	Torque coefficient	1.18 Nm/Arms
J_{n}	Inertia moment of motor	0.00288 kgm^2
K_{p}	Position gain	4900
K_{d}	Velocity gain	140
K_{f}	Force gain	0.6
g_{pd}	Cut-off frequency of pseudo-derivation	400 rad/s
g_{wob}	Cut-off frequency of WOB	400 rad/s

the motion begins and ends were recorded to the motion data memory, too. In these experiments, two motions were recorded: an unconstrained motion and a constrained motion. Each motion was recorded during 5 seconds.

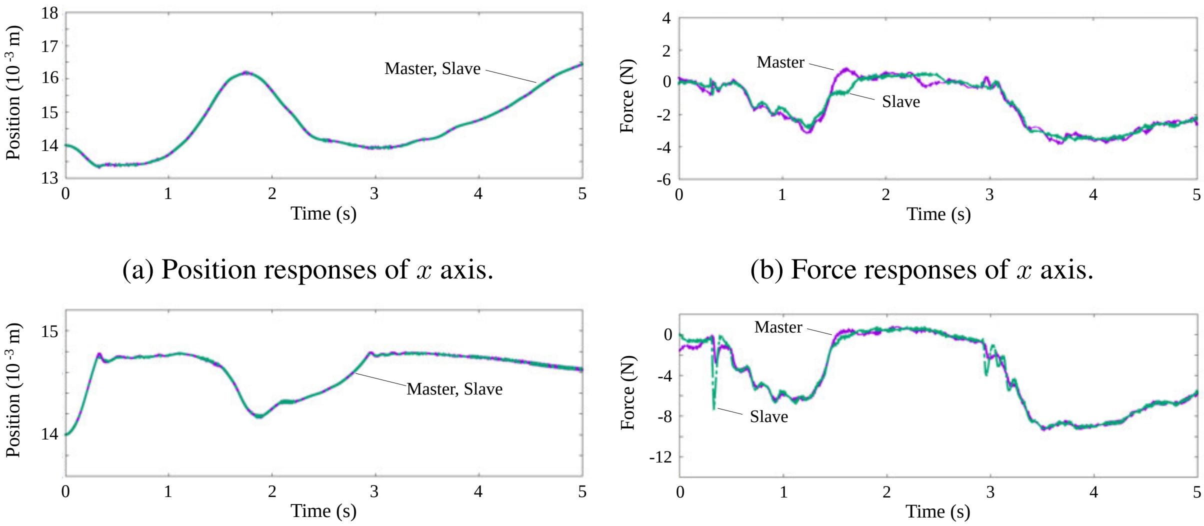

(a) Position responses of x axis.

(b) Force responses of x axis.

(c) Position Responses of y axis.

(d) Force Responses of y axis.

Fig. 3-10: Experimental results of recorded motion 1 for velification of integrated reproduction based on acceleration information.

In the motion-loading phase, the integrated reproduction of the recorded motions was conducted. Concretely speaking, first, the motion 1 was reproduced, then the motion 2 was reproduced. Here, two patterns of the reproductions were conducted: without proposed method and with proposed method. In the case that the proposed method was used, the braking force was applied in order to connect the haptic energy between the end of the motion 1 and the beginning of the motion 2. In this experiment, the coupling time was 0.5 s. The acceleration added during coupling time was calculated during the motion reproduction by Eq. (3.9).

Experimental Results of Motion Recording

Figs. 3-10 and 3-11 show the experimental results of the motion 1 and the motion 2 in the motion-saving step. In these figures, (a) and (b) show the position responses and the force responses of x axis; and (c) and (d) show the position responses and the force responses of y axis, respectively. From these results, it turns out that the bilateral force feedback control is successfully realized. These motions were recorded as the digital information to the motion data memory. In the motion 2, the data during 3 s to 5 s were recorded. In this experiment, the proposed method was implemented at only y axis. Therefore, acceleration of the y axis was stored, and both position and force of the x axis were stored.

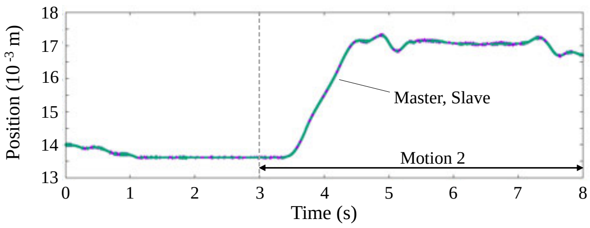

(a) Position responses of x axis.

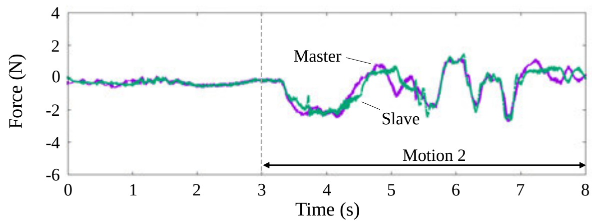

(b) Force responses of x axis.

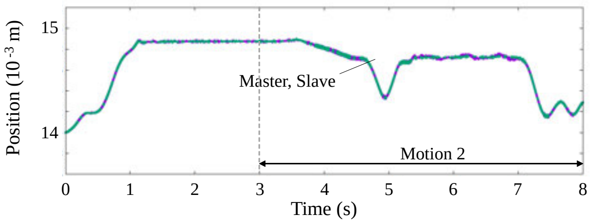

(c) Position Responses of y axis.

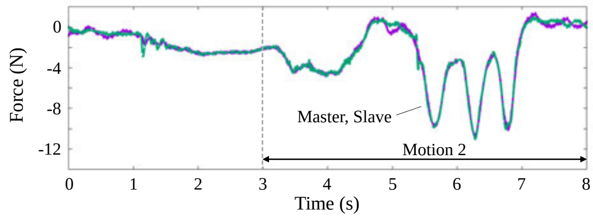

(d) Force Responses of y axis.

Fig. 3-11: Experimental results of recorded motion 2 for velification of integrated reproduction based on acceleration information.

Experimental Results of Motion Reproduction

Fig. 3-12 shows the experimental results of the integrated reproduction without proposed method. In this figure, the responses of the reproduction and recorded motion are depicted. Fig. 3-13 shows the position and force error of 3-12. Only results of y axis are shown in Fig. 3-13, because the proposed method was implemented at y axis. It turns out that both the position and force responses are not reproduced as the recorded ones in the motion 2. The reason why the recorded motion could not be reproduced is that the equivalent velocities of the end of the motion 1 and beginning of the motion 2 did not correspond with. In this case, the device applied force to the wall at the end of motion 1. After that, the acceleration was added according to the motion 2. As a result, strong force was applied to the environment because the remaining equivalent velocity was not canceled.

On the contrary, Fig. 3-14 shows the experimental results of the integrated reproduction with proposed method, and Fig. 3-15 shows the position and force error of 3-14. Only results of y axis are shown in Fig. 3-15, because the proposed method was implemented at y axis. It turns out that 2nd motion was reproduced. The remained energy was canceled during coupling period, and the energy at the beginning motion 2 was corresponding between motion recording and motion reproduction. As mentioned above, the integrated reproduction for unknown environmental location is attained by using the proposed

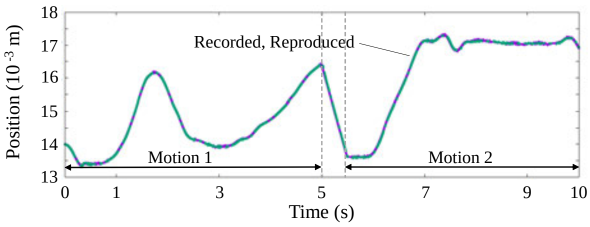

(a) Position responses of x axis.

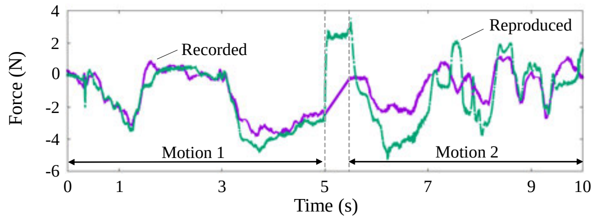

(b) Force responses of x axis.

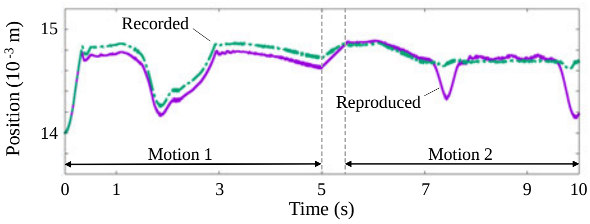

(c) Position Responses of y axis.

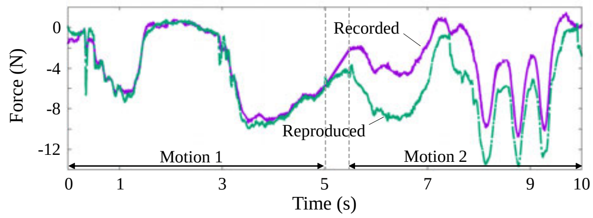

(d) Force Responses of y axis.

Fig. 3-12: Experimental results of integrated motion reproduction without proposed method for velification of integrated reproduction based on acceleration information.

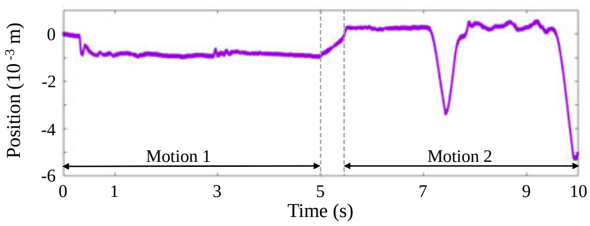

(a) Position Error.

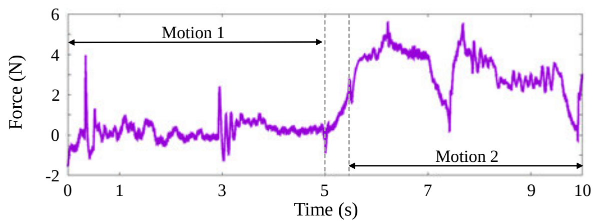

(b) Force Error.

Fig. 3-13: Error of motion reproduction at y axis without proposed method for velification of integrated reproduction based on acceleration information.

method.

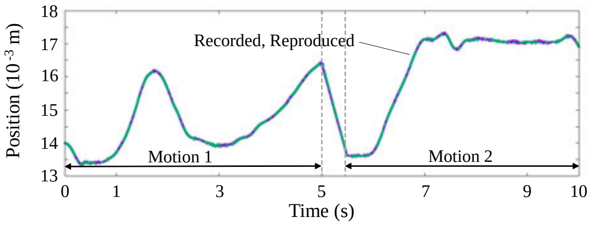

(a) Position responses of x axis.

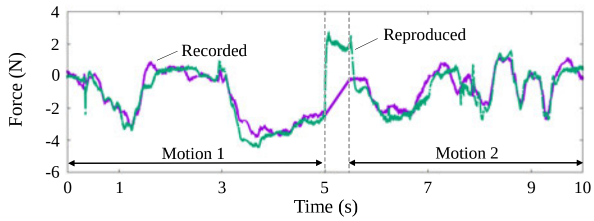

(b) Force responses of x axis.

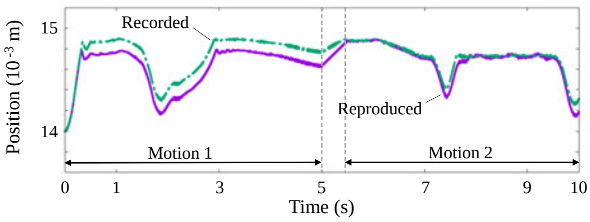

(c) Position Responses of y axis.

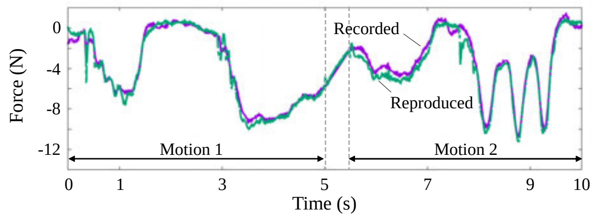

(d) Force Responses of y axis.

Fig. 3-14: Experimental results of integrated motion reproduction with proposed method for velification of integrated reproduction based on acceleration information.

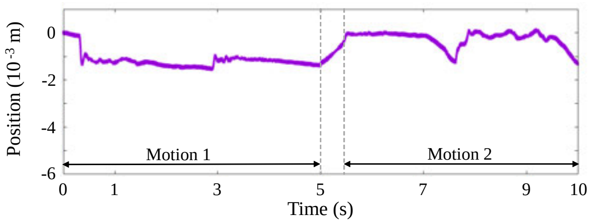

(a) Position Error.

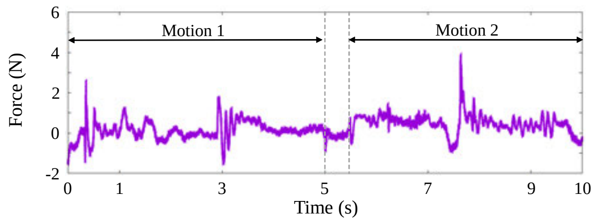

(b) Force Error.

Fig. 3-15: Error of motion reproduction at y axis with proposed method for velification of integrated reproduction based on acceleration information.

3.4 Summary

The purpose of this chapter was that one motion was reproduced from some motion components by connecting them time series. By the proposal, the recorded two motions are integrated temporally, and the integrated motion is reproduced in one motion. In this chapter, two coupling methods were proposed.

In section 3.2, the integrated reproduction method based on interpolation was proposed. This method is for the motion-copying system using position and force information. In this method, the coupling time was inserted and the interpolation was implemented during it. By the method, the coupling time in which two motions are connected is able to be set shorter, because the tracking performance is improved.

On the other hand, the integrated reproduction method considering haptic energy was proposed in section 3.3. This method is for the motion-copying system using acceleration information. In this method, equivalent velocity of the two motions were connected by adding acceleration between two motions.

The proposed coupling methods depend on the reproduction method of latter motion. When the latter reproduction method is the basic motion-loading system which is based on position and force information, the interpolation method described in section 3.2 should be used. On the other hand, the method that cancels the equivalent velocity described in section 3.3 should be used when the latter reproduction method is the acceleration-based motion-copying system.

In each section, the validity of the proposed methods was shown by the experimental results. By these methods, it is expected to reproduce many motions by combining motion components.

Chapter 4

Motion-Copying System with Adaptation for Difference of Environment

4.1 Background and Overview of This Chapter

It is known that motion-copying system needs the completely same environment between motion recording phase and motion reproducing phase [87–89]. In this chapter, the method to adapt the environmental difference is described.

By using the motion reproduction method based on only position information like as motion capture based method [6–9], the recorded motion can be reproduced only when the environmental location is completely the same. However, the recorded motion cannot be reproduced when the environmental location is different. On the other hand, by using the motion reproduction method based on only force information [12], applied force for environment is reproduced but trajectory of the position is not reproduced. The motion-copying system is hybrid control of the position and force. By using position-force hybrid system, adaptively for the minute change of the environment is improve [109–111]. However, robustness for drastically different environment between motion recording and motion reproduction is decreased by adding the force information to the recorded motion. For the future applications of the motion-copying system, it is important to reproduce recorded motions even if the environmental condition is different. In this chapter, the adaptation methods for motion-copying system when a target environment is different are proposed.

In this chapter, two types of difference of environmental condition are discussed. Concept of adaptation for difference of environment is shown in Fig. 4-1.

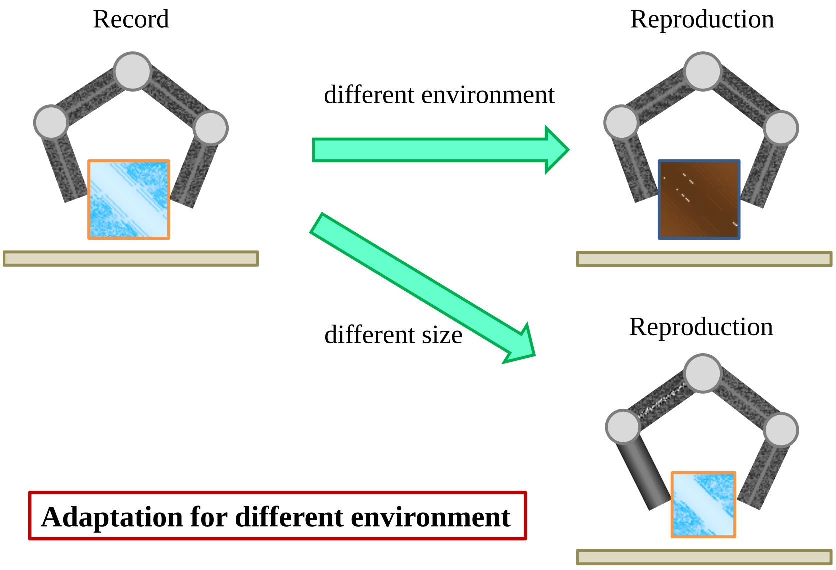

Fig. 4-1: Concept of adaptation for difference of environment.

First, motion reproduction method when target environmental size is different [91–94] is proposed in section 4.2. Both position and force cannot be reproduced at the same time when environmental location is different. Here, the motion reproduction which does not depend on the base of the position is achieved. There are some researches of motion reproduction when the environmental location is different in one-degree-of-freedom system [87,88]. The method described in this section can be grouped the same category of them. This method can be used under the condition that the environmental location is changed in the same direction of the motion. Therefore, the grasping axis is suitable for utilizing these methods [112].

Then, motion reproduction method when target environmental material is different [95] is proposed in section 4.3. Here, we assume that the motion-copying system is applied to the application of "peg-in-hole." There are some researches which the external environment is difference [89]. However, most of them treat the simple motion which just contacts with the constrained environment such as a wall. On the other hand, this section shows the method for more complicated application. In order to reproduce the same task of the recorded motion, the effect from the difference of the target environment is omitted. As a result, the task of the recorded motion is successfully reproduced. In each section, experimental results show the validity of the proposed methods.

4.2 Motion-Copying System Based on Acceleration Information

In this section, a motion-copying system based on acceleration information [91–94] is proposed. If motion information includes the position information, the reproduced motion depends on the initial position because the position information is a relative information. Here, the human motion is regarded as the acceleration information. The acceleration information is absolute value which expresses the amount of change. Therefore, the recorded motion does not depend on the initial position.

4.2.1 Control Structure

Figs. 4-2 and 4-3 show the control structures of the proposed motion-saving and motion-loading systems, where x and F stand for the position and force; superscripts $^{\mathrm{ref}}$, $^{\mathrm{res}}$, $^{\mathrm{ext}}$, and $^{\mathrm{sav}}$ stand for the reference, response, external force, and recorded response; subscripts $_{\mathrm{M}}$, $_{\mathrm{S}}$, $_{\mathrm{C}}$, and $_{\mathrm{D}}$ stand for the master system, slave system, common mode, and differential mode; $\hat{}$ stands for the estimated value; $\boldsymbol{Q}$ stands for quarry matrix. The structure of the motion-saving system is the same as the basic method [65] The motion-loading system is constructed by an actuator and the acceleration controller with the disturbance observer (DOB). The recorded human motion is reproduced by substituting stored data for acceleration reference of the slave system. In the basic method, position and force responses of the master system are recorded, and a human motion is reproduced by the virtual master system constructed by the stored data. On the other hand, in the proposed method, acceleration reference of the slave system $\ddot{x}_{\mathrm{S}}^{\mathrm{ref}}$ is used. Thus, the amount of data becomes half compared with the basic method. Furthermore, it is easy to implement the proposed motion-loading system because the structure of the introduced system is very simple.

In the basic method, the position and force responses correspond with the stored information. Therefore, the recorded motion is reproduced. Thus, the reproduced motion is affected by the initial position because position information indicates the deflection based on the initial position. As a result, when the environmental position is different in the motion-loading system, the motion which targets at an environment is not achieved.

On the other hand, the acceleration information is dealt with in the proposed method. The equivalent acceleration about the behavior of the motor $\ddot{x}^{\mathrm{equ}}$ corresponds with acceleration reference $\ddot{x}^{\mathrm{ref}}$ by DOB as

$$\ddot{x}^{\mathrm{ref}} = \ddot{x}^{\mathrm{equ}}. \tag{4.1}$$

The equivalent acceleration is used as the movement of the end-effector and/or applied force to an en-

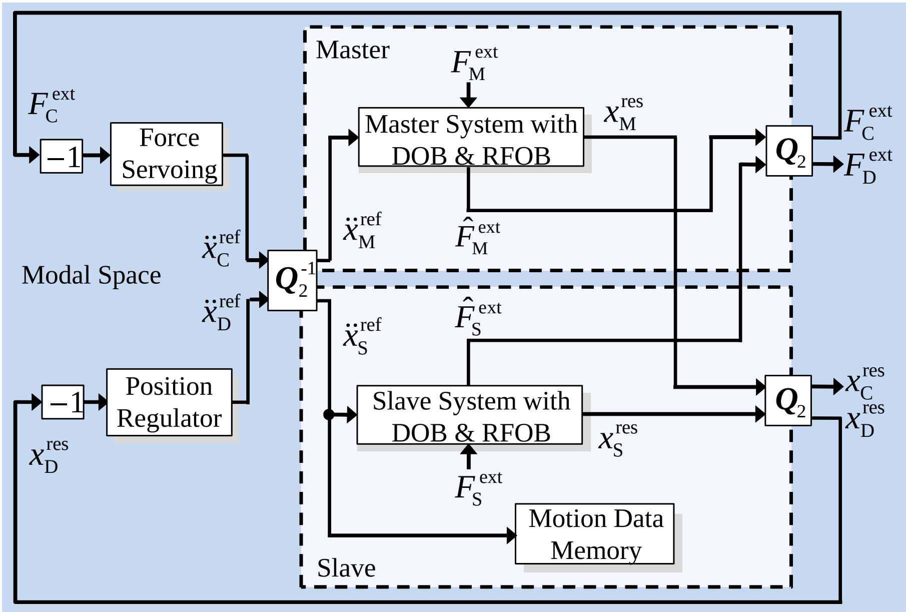

Fig. 4-2: Block diagram of proposed motion-saving system.

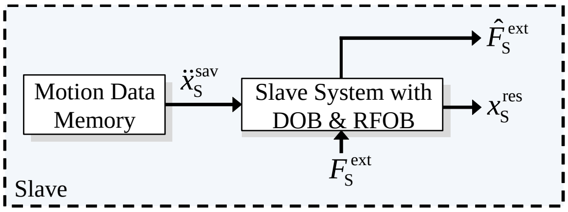

Fig. 4-3: Block diagram of proposed motion-loading system.

vironment. Therefore, to record the acceleration reference is the same meaning of to record the whole behavior of the system which includes position and force information. In the motion-loading system, the recorded acceleration is reproduced. Hence, the recorded motion is reproduced when the environmental condition is completely the same as the motion-saving system. In the case that the environmental position is nearer, the equivalent acceleration about the movement of end-effector's position is used as the applied force. On the other hand, when the environmental position is farther, the equivalent acceleration about the applied force is used as the movement of the end-effector. Then, the recorded motion is reproduced since the position and force responses correspond with them in the motion-saving system. In other words, while the relative condition for an environment is the same as the motion-saving system,

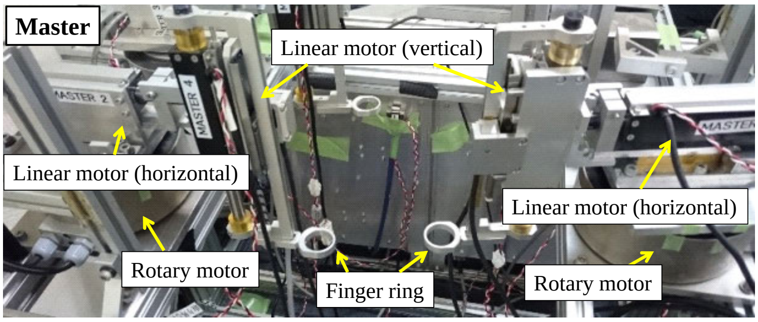

(a) Master system.

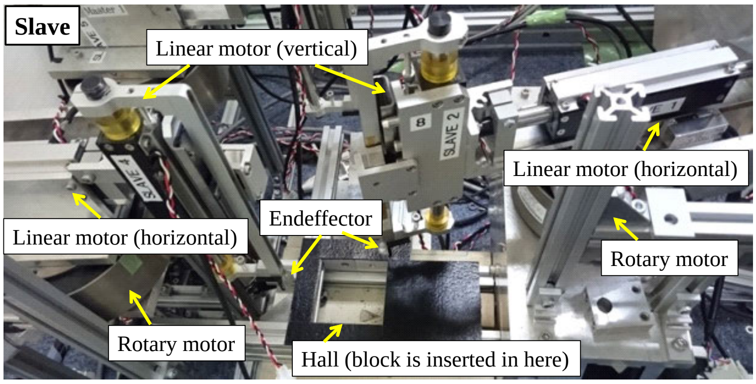

(b) Slave system.

Fig. 4-4: Experimental systems for verification of motion-copying system based on acceleration information.

the recorded motion is reproduced. The condition is shown as

$$x^{\mathrm{sav}}_{\mathrm{env}} - x^{\mathrm{sav}}_{\mathrm{res}} = x^{\mathrm{ld}}_{\mathrm{env}} - x^{\mathrm{ld}}_{\mathrm{res}} \tag{4.2}$$

where superscript $^{\mathrm{sav}}$ and $^{\mathrm{ld}}$ stand for the value in the motion-saving system and motion-loading system, respectively.

4.2.2 Experiments

In this sub-section, the validity of the proposed method is verified by experiments. The model of the experimental system is described in the section 2.4. In this research, the proposed method is implemented only grasp axis. The other axes were controlled by the normal motion-copying system [65].

Fig. 4-5: Target environment for verification of motion-copying system based on acceleration information (Cork block).

Table 4.1: Experimental cases for verification of motion-copying system based on acceleration information.

Case No.	target object	with/without proposed method
1	larger cork cube	without proposed method
2	smaller cork cube	without proposed method
3	larger cork cube	with proposed method
4	smaller cork cube	with proposed method

Experimental Setup

Fig. 4-4 shows the experimental system used in the experiments. This system is constructed by the master and slave systems, and each system is composed of two-device units. The device unit is constructed by three motors; a rotary motor (horizontal) and two linear motors (horizontal and vertical). In the motion-saving step, both of the master and slave systems were used. A human operator operates the master system, and the end effector in the slave system grasped an environment shown Fig. 4-5. The position response was measured by the position encoder or the rotary encoder, and the force response was estimated by reaction force observer (RFOB) without force sensors. The control program was written in C language under RTAI 3.7.

In this experiment, two kinds of cork blocks were used. One of the target object is a cork cube 55 mm on each side, and the other is a cork cube 45 mm on each side. In addition, it was assumed that the environmental position was unknown. In the motion recording step, the human operator grasped the block at first; then, lifted the block; moved the block at y direction; and took down the block. Then, the stored motion was reproduced as Table 4.1.

The parameters used in these experiments are shown in Table 4.2.

Table 4.2: Experimental parameters for verification of motion-copying system based on acceleration information.

Parameter	Description	Value
$T_{\rm s}$	Sampling time	200 μs
L	length between center of the rotary motor to the end-effector	0.16 m
$L_{\rm base}$	length between rotary motors of two device units	0.41 m
$K_{\rm fn}$	Force coefficient of linear motor	40.0 N/A
$M_{\rm n}$	Mass of linear motor	0.3 kg
$g_{\rm pd,l}$	Cut-off frequency of pseudo-derivation of linear motor	600 rad/s
$g_{\rm dis,l}$	Cut-off frequency of disturbance observer of linear motor	600 rad/s
$K_{\rm tn}$	Torque coefficient of rotary motor	1.18 Nm/A
$I_{\rm n}$	Inertia around rotary motor	0.00288 kgm^2
$g_{\rm pd,r}$	Cut-off frequency of pseudo-derivation of rotary motor	250 rad/s
$g_{\rm dis,r}$	Cut-off frequency of disturbance observer of rotary motor	250 rad/s
$K_{\rm p,move}$	Position gain for move-x and move-y axes	3600
$K_{\rm d,move}$	Velocity gain for move-x and move-y axes	120
$K_{\rm f,move}$	Force gain for move-x and move-y axes	5
$K_{\rm p,rot}$	Position gain for rotation axis	1600
$K_{\rm d,rot}$	Velocity gain for rotation axis	80
$K_{\rm f,rot}$	Force gain for rotation axis	2
$K_{\rm p,grsp}$	Position gain for grasp axis	3600
$K_{\rm d,grsp}$	Velocity gain for grasp axis	120
$K_{\rm f,grsp}$	Force gain for grasp axis	5
$K_{\rm p,lift}$	Position gain for lifting and z-diff axes	3600
$K_{\rm d,lift}$	Velocity gain for lifting and z-diff axes	120
$K_{\rm f,lift}$	Force gain for lifting axis	0.8
$g_{\rm wob}$	Cut-off frequency of work space observer	500 rad/s
$m_{\rm obj1}$	Weight of cork block (large)	0.05 kg
$l_{\rm obj1}$	Side length of cork block(large)	0.055 m
$m_{\rm obj2}$	Weight of cork block (small)	0.03 kg
$l_{\rm obj2}$	Side length of cork block (small)	0.045 m

Experimental Results of Motion Recording

Fig. 4-6 shows the experimental results of the motion recording. The responses of the master and slave systems are depicted in the figure. The left figures show the position responses and the right figures show the force responses. In addition, the dotted line of (g) mean the block surface. The responses of the motion-modal space are shown, because the MCS controllers are implemented in the motion-modal space. It is shown from figures that the operator grasped the block at first; then he lifted the block; moved the block at y direction; and took down the block. These figures show that the responses of master and slave systems are almost the same because the ideal bilateral control is implemented.

Experimental Results of Motion Reproduction

Fig. 4-7 shows the experimental results of the motion reproduction in case 1. The responses of the recorded motion and reproduced motion are depicted in the figure. The left figures show the position responses and the right figures show the force responses. In addition, the dotted line of (g) mean the block surface. The recorded motion was reproduced in all axes because the environment was the same between motion recording and motion reproduction. Note that the small error of the x axis is from the tracking performance of the controllers, and it is not a problem because amount is small.

Fig. 4-8 shows the experimental results of the motion reproduction in case 2. The responses of the recorded motion and reproduced motion are depicted in the figure. The left figures show the position responses and the right figures show the force responses. In addition, the dotted line of (g) mean the block surface. It is shown by Fig. 4-8 (g) and (h) that both position and force error occurred in grasp axis when the constrained motion. It is because that the environmental position in the grasp axis was different. The normal motion-copying system is a hybrid control, hence it needs completely the same environment.

Fig. 4-9 shows the experimental results of the motion reproduction in case 3. The responses of the recorded motion and reproduced motion are depicted in the figure. The left figures show the position responses and the right figures show the force responses. The recorded motion was reproduced in all axes even if the proposed method was used in the case of the same environment between motion recording and motion reproduction. It is shown by Figs. 4-7 and 4-9 that both basic motion-loading system and proposed motion-loading system based on acceleration information can be used under the condition when the environmental condition is the same. However, there is the position error in grasp axis after 9 s in Fig. 4-9, it is because that the operator finished the operation and took his hand off the device. As a result, the system maintained the acceleration of the end of the motion.

Fig. 4-10 shows the experimental results of the motion reproduction in case 2. The responses of the recorded motion and reproduced motion are depicted in the figure. The left figures show the position responses and the right figures show the force responses. In addition, the dotted line of (g) mean the block surface. It is shown by Fig. 4-10 (g) and (h) that the ideal motion reproduction is achieved. Since the condition between the slave system and the target object was identical with that of motion-saving system (since time t is about 3 s), the responses of the slave system corresponded with the recorded motion. In particular, the position response had the offset which was caused by the deflections of the environmental position (10 mm), and force response corresponded with recorded one. As mentioned above, the validity of the proposed method is confirmed.

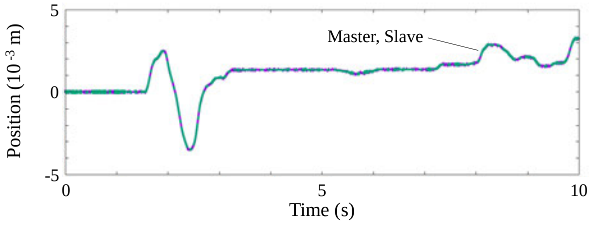

(a) Position responses of x axis.

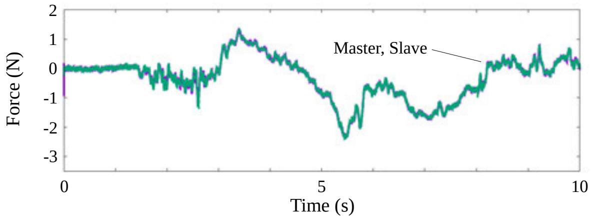

(b) Force responses of x axis.

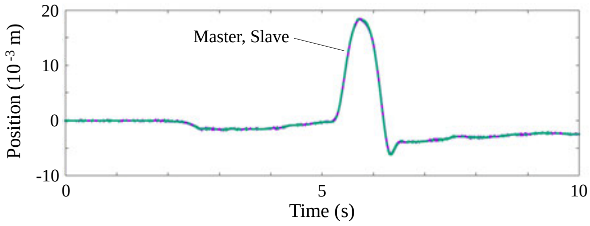

(c) Position responses of y axis.

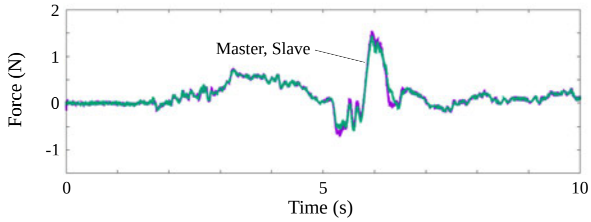

(d) Force responses of y axis.

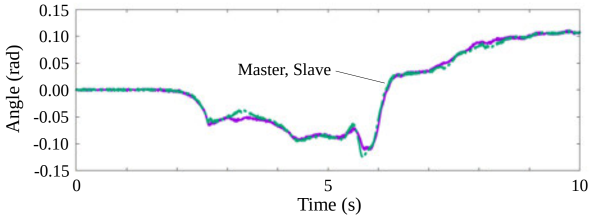

(e) Angle responses of rotation axis.

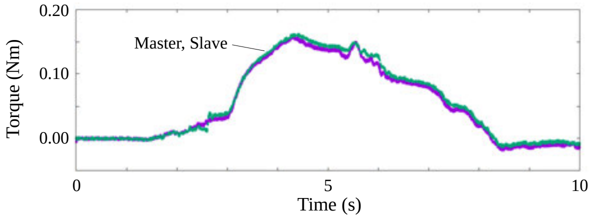

(f) Torque responses of rotation axis

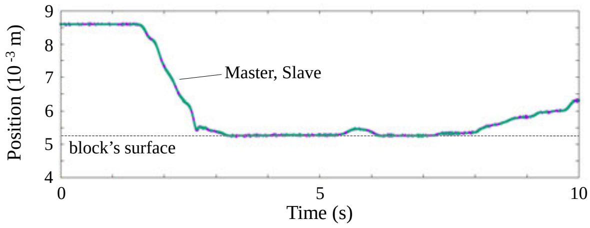

(g) Position responses of grasp axis.

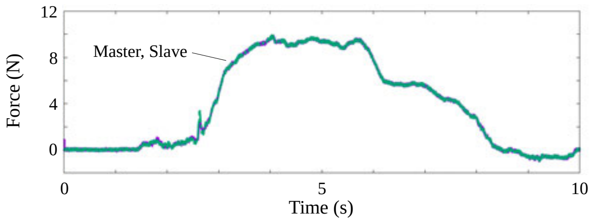

(h) Force responses of grasp axis.

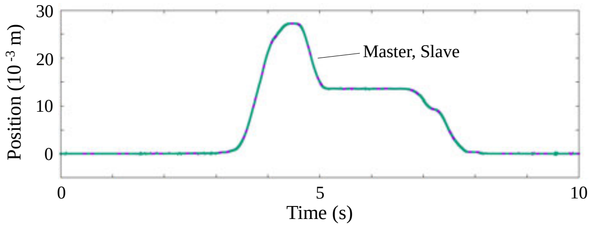

(i) Position responses of lifting axis.

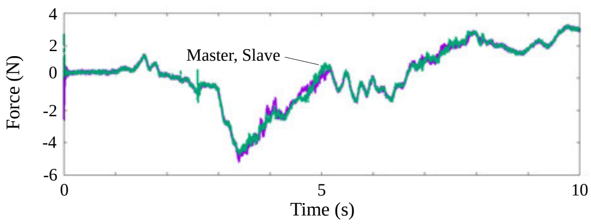

(j) Force responses of lifting axis.

Fig. 4-6: Experimental results of motion recording for verification of motion-copying system based on acceleration information.

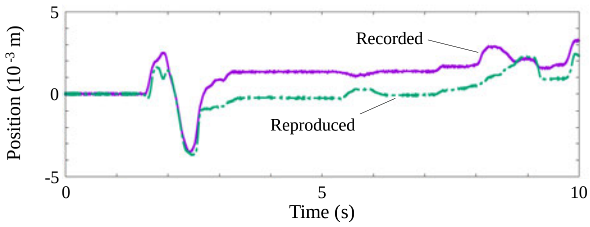

(a) Position responses of x axis.

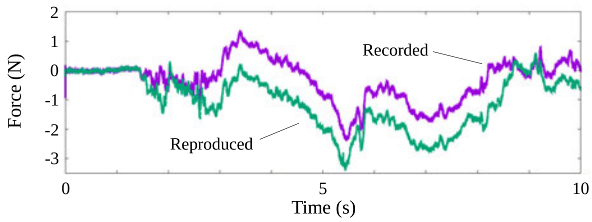

(b) Force responses of x axis.

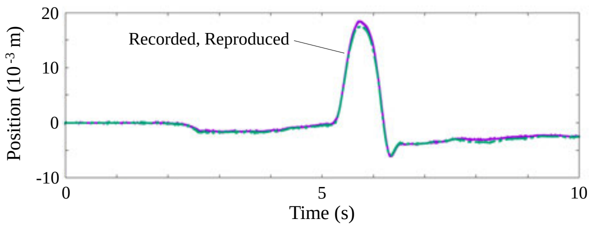

(c) Position responses of y axis.

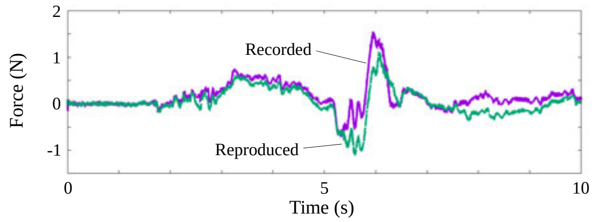

(d) Force responses of y axis.

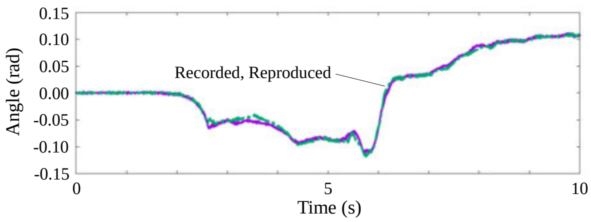

(e) Angle responses of rotation axis.

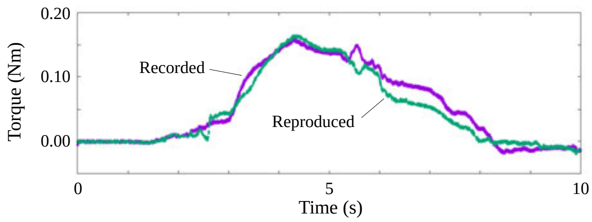

(f) Torque responses of rotation axis

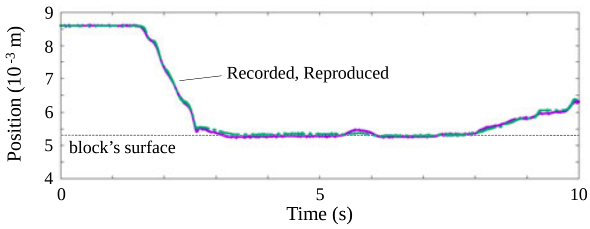

(g) Position responses of grasp axis.

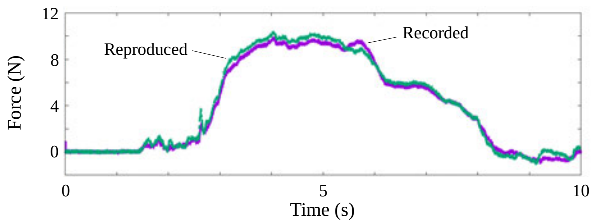

(h) Force responses of grasp axis.

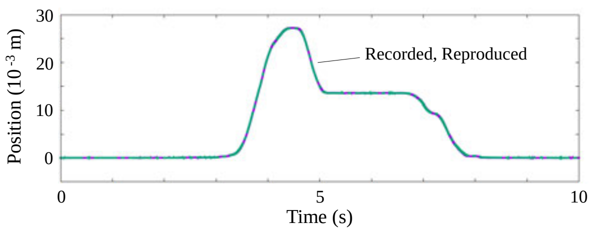

(i) Position responses of lifting axis.

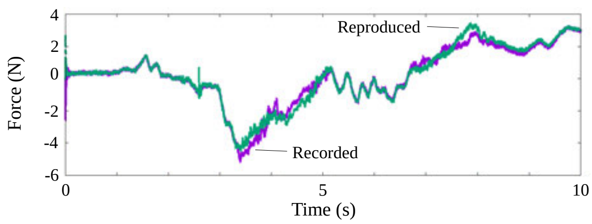

(j) Force responses of lifting axis.

Fig. 4-7: Experimental results of motion reproduction in case 1 (same target environment, without proposed method) for verification of motion-copying system based on acceleration information.

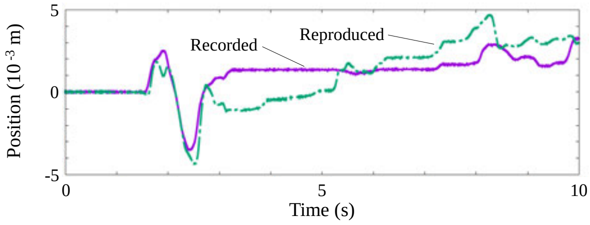

(a) Position responses of x axis.

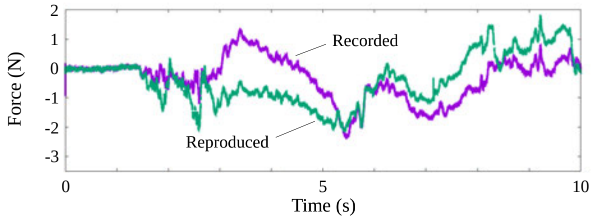

(b) Force responses of x axis.

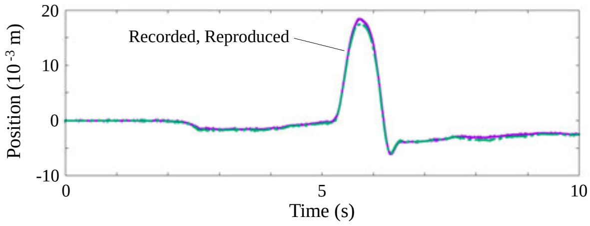

(c) Position responses of y axis.

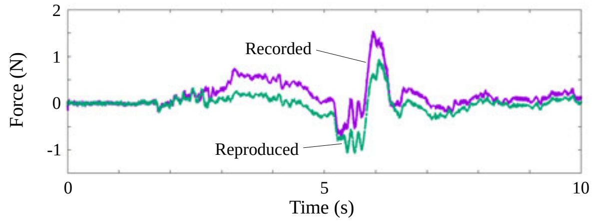

(d) Force responses of y axis.

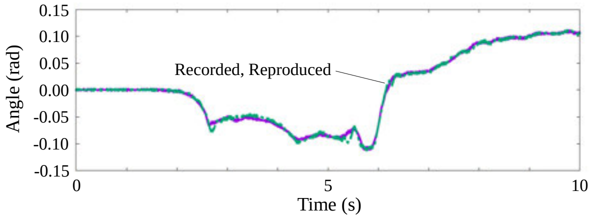

(e) Angle responses of rotation axis.

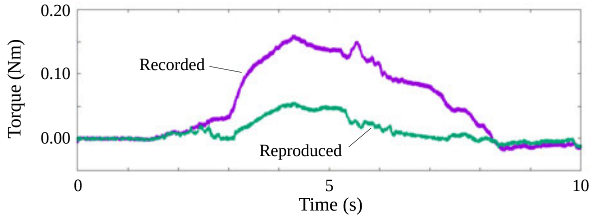

(f) Torque responses of rotation axis

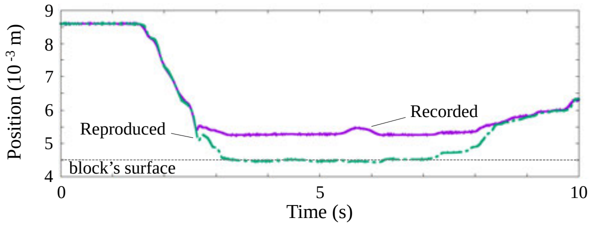

(g) Position responses of grasp axis.

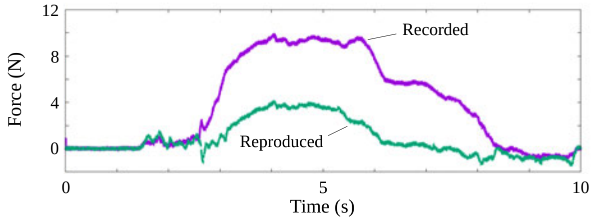

(h) Force responses of grasp axis.

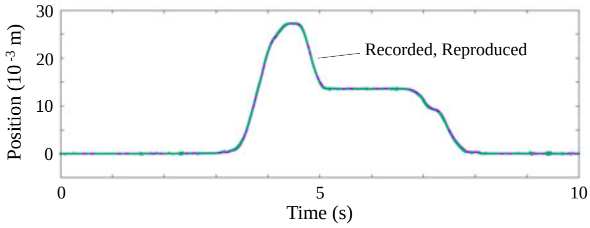

(i) Position responses of lifting axis.

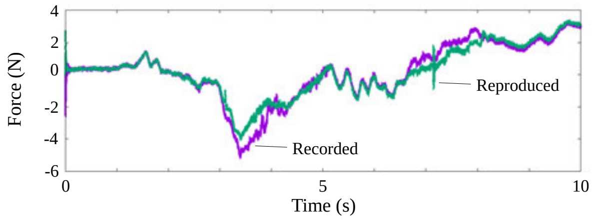

(j) Force responses of lifting axis.

Fig. 4-8: Experimental results of motion reproduction in case 2 (different target environment, without proposed method) for verification of motion-copying system based on acceleration information.

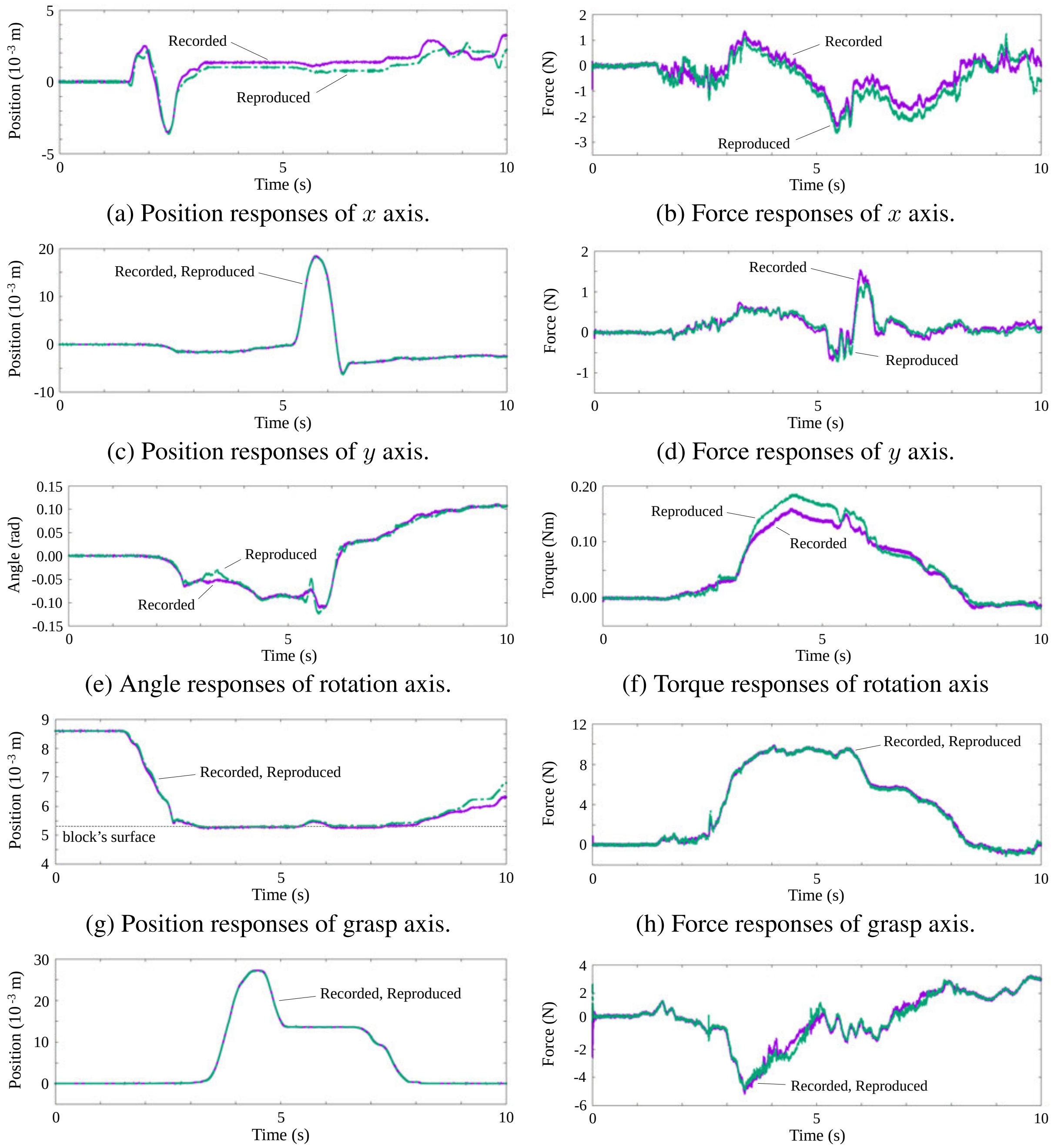

(a) Position responses of x axis.

(b) Force responses of x axis.

(c) Position responses of y axis.

(d) Force responses of y axis.

(e) Angle responses of rotation axis.

(f) Torque responses of rotation axis

(g) Position responses of grasp axis.

(h) Force responses of grasp axis.

(i) Position responses of lifting axis.

(j) Force responses of lifting axis.

Fig. 4-9: Experimental results of motion reproduction in case 3 (same target environment, with proposed method) for verification of motion-copying system based on acceleration information.

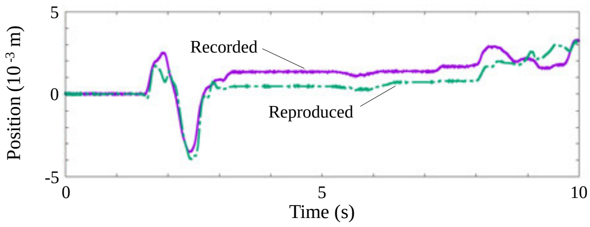

(a) Position responses of x axis.

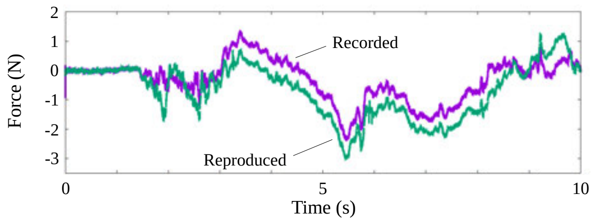

(b) Force responses of x axis.

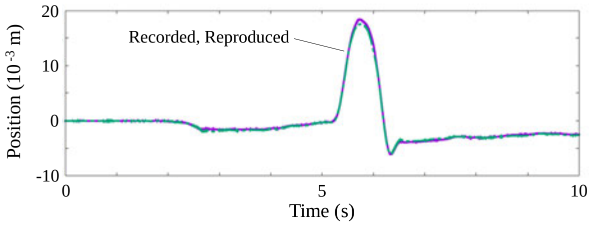

(c) Position responses of y axis.

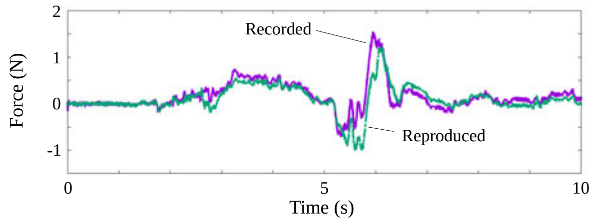

(d) Force responses of y axis.

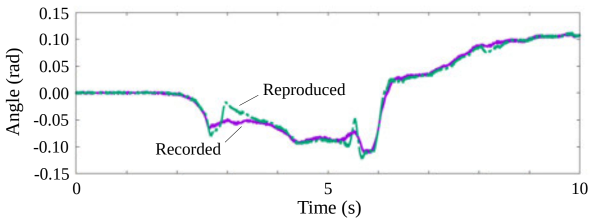

(e) Angle responses of rotation axis.

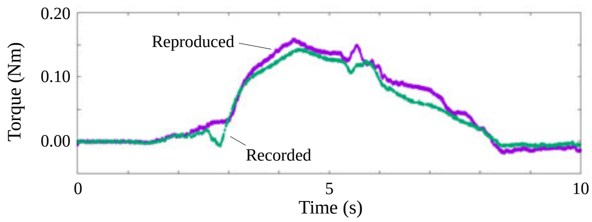

(f) Torque responses of rotation axis

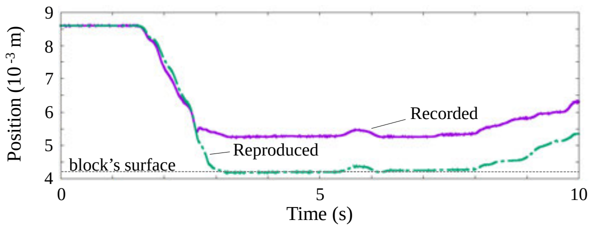

(g) Position responses of grasp axis.

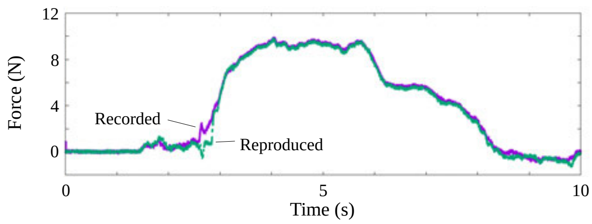

(h) Force responses of grasp axis.

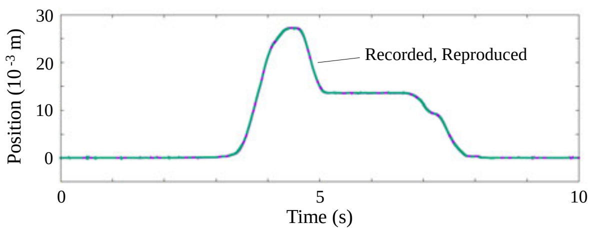

(i) Position responses of lifting axis.

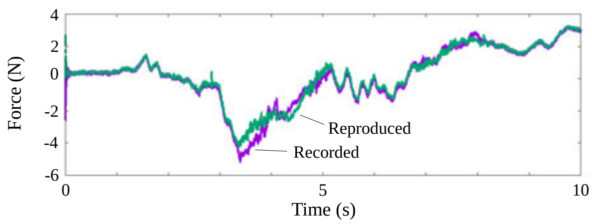

(j) Force responses of lifting axis.

Fig. 4-10: Experimental results of motion reproduction in case 5 (different target environment, with proposed method) for verification of motion-copying system based on acceleration information.

4.3 Adaptive Motion Reproduction for Different Target Object

In this section, the motion reproduction method when target environmental material is different [95] is proposed. We focus a motion which includes motions to pick up a block, to move the block near the hole, get down the block, move while being in contact with the external environment, and to insert the block into a hole. The goal of this section is to achieve recorded “peg-in-hole” motion even if a target block is different. In particular, we deal with the case which weight and material of the blocks are different. Here, the effect from the difference of the target environment is omitted, and the task of the recorded motion is successfully reproduced.

4.3.1 Control Structure

The application of this research is “peg-in-hole” task which includes following motion;

(1) to grasp a block;

(2) to pick up a block;

(3) to move the block near the hole;

(4) to get down the block;

(5) to move while being in contact with the external environment (search the hole);

(6) to insert the block into a hole;

which is shown in Fig. 4-11.

In this task, it is known by the pre-experiment that searching motion with hand feeling is important. The relations of the initial positions of device, target object, and external environment are not completely the same between motion recording and reproduction. By carrying out searching motion with hybrid control, the target object can be inserted into the hole even if the environmental location is slightly different. When the target environment is different, applied force during searching motion is different. As a result, the recorded task cannot be reproduced. In this research, we assume that applied force is separated to force affected by the difference of a target object and common force which is not affected by it. In this section, the former one is denoted as f^{eff}, and the latter one is denoted as f^{com}. The applied force during motion is written as

$$f^{\mathrm{com}} = f^{\mathrm{cmd}} - f^{\mathrm{eff}}, \tag{4.3}$$

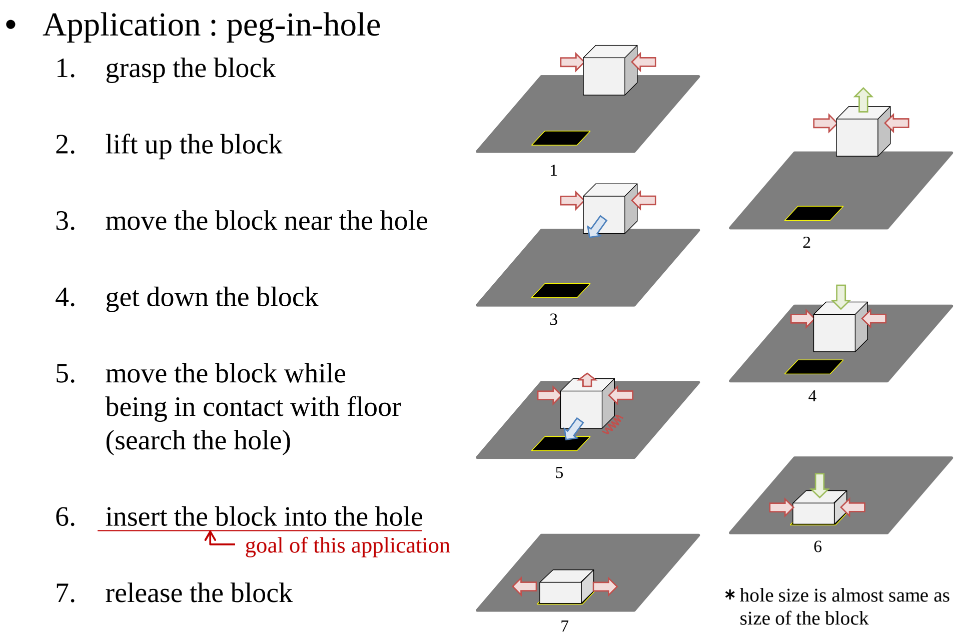

Fig. 4-11: Motion procedure of the application.

where superscript $^{\text{cmd}}$ stands for the recorded information. Important point is to correspond with f^{com} between motion recording and motion reproduction. When the target object is different, f^{eff} is different. As a result, the recorded task is not reproduced because f^{com} is different. In order to correspond with f^{com}, compensation force f^{cmp} is added when the target object is different;

$$f^{\text{com}} = f^{\text{cmd}} - (f^{\text{eff}} - f^{\text{cmp}}). \tag{4.4}$$

Eqs. (4.3) and (4.4) are general for the motions to act external environment using target object such as writing with pen and so on.

In this application, condition of the different target object affects two kind of applied force. One of them is the applied vertical force to floor, and the other is the horizontal force. In particular, the former force is affected by the weight difference of the object, and latter force is affected by the friction difference of the object. By compensating force in each axis, the recorded task is reproduced.

Human can apply the same force to the floor even if a weight of a tool is different, because human can compensate difference of the weight. Hence, the weight compensator is implemented in a lifting axis. In the steady state of the lifting motion, difference between the stored force and reproduced force is the difference of the weight of the target object,

$$F_{\mathrm{lift}}^{\mathrm{cmp}} = \frac{1}{n}\sum_{i=0}^{n}(F_{\mathrm{lift},i}^{\mathrm{rcd}} - F_{\mathrm{lift},i}^{\mathrm{rpd}}) \tag{4.5}$$

where n stands for sample number during steady state of the lifting motion; and superscript ${}^{\mathrm{cmp}}$, ${}^{\mathrm{rcd}}$, and ${}^{\mathrm{rpd}}$ stand for the compensation value, recorded value and response in motion-recording phase, respectively. In this research, n is defined by the motion date in the motion recording in advance.

In the task, friction force is different because the target environment is different between the motion recording and motion reproduction steps. Hence, it is necessary to compensate the force difference on the basis of the friction force. In this paper, the difference of Coulomb friction is dealt with, because it is simplified model of friction. The compensation force is described as

$$F_{\mathrm{mv}}^{\mathrm{cmp}} = \mu_{\mathrm{mv}}^{\mathrm{est}} N, \tag{4.6}$$

where N stands for the normal force between the object and the floor, and subscript ${}_{\mathrm{mv}}$ stands for move-x and move-y axes. The friction coefficient $\mu_{\mathrm{mv}}^{\mathrm{est}}$ is calculated by

$$\mu_{\mathrm{mv}}^{\mathrm{est}} = \frac{1}{n}\sum_{i=0}^{n}\frac{(F_{\mathrm{mv},i}^{\mathrm{rcd}} - F_{\mathrm{mv},i}^{\mathrm{rpd}})}{N_i}. \tag{4.7}$$

The force difference based on the friction difference is estimated while the force of lifting axis is steady. Note that this estimation needs to be conducted while the weight compensation is in effect.

By the above equations, the recorded force is compensated and the motion applying the same force to the external environment is achieved. In the future, it is desired to use better method to estimate the compensation force. However, the simplified method is used as a first step of the research. F^{cmp} is calculated during motion reproduction and added it after the calculation. The time period during calculation is defined in advance in this research. In the future, it is expected that the system recognizes the feature of the motion, and the system decides when the compensation value is calculated and when the compensation value is added to the command.

Finally, the controller of the motion-loading system is shown in Fig. 4-12, where $\boldsymbol{P}$, $\boldsymbol{F}$, and veM_{eq} stand for position matrix, force matrix, and equivalent mass matrix: superscript ${}^{\mathrm{res}}$, ${}^{\mathrm{cmd}}$, ${}^{\mathrm{ext}}$, and ${}^{\mathrm{ref}}$ stand for response, command, external value, and reference: subscript mode stands for value of motion modal space: $\boldsymbol{K}_{\mathrm{p}}$, $\boldsymbol{K}_{\mathrm{d}}$, and $\boldsymbol{K}_{\mathrm{f}}$ stand for proportion gain matrix, derivation gain matrix, and force gain matrix, respectively; and $\boldsymbol{F}^{\mathrm{cmp}}$ stand for force compensation matrix which elements are described by Eqs. (4.5) and (4.6). Each of these matrices is diagonal matrix.

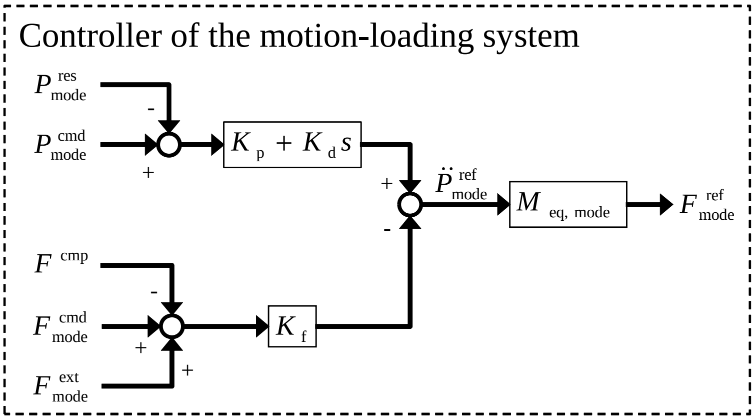

Fig. 4-12: Controller of the proposed method.

4.3.2 Experiments

In this sub-section, the validity of the proposed method is verified by experiments. The model of the experimental system is described in the section 2.4.

Experimental Setup

Fig. 4-13 shows the experimental system used in the experiments. This system is constructed by the master and slave systems, and each system is composed of two-device units. The device unit is constructed by three motors; a rotary motor (horizontal) and two linear motors (horizontal and vertical). In the motion-recording step, both of the master and slave systems were used. A human operator operates the master system, and the end effector in the slave system brought the block and inserted the block into the hole. In particular, motion procedure is i) grasping a block; ii) picking up a block; iii) moving the block near the hole; iv) getting down the block; v) moving while being in contact with the external environment (search the hole); vi) inserting the block into a hole. On the contrary, only the slave system was used in the motion-reproducing step. The recorded motion was reproduced by the slave system. Then, the device picked up the block and inserted the block into the hole as if it is recorded motion. The goal of this application is that the block exists in the hole after the motion reproduction. The target object is shown in Fig. 4-14. In the motion-recording step, the acrylic block was used. Then in the motion-reproducing step, both the acrylic block and the cork block were used. Size of the hole and the block are almost the same, but they are not completely the same. In this experiment, 4 patterns of motion reproduction, which is shown in Table 4.3, were carried out.

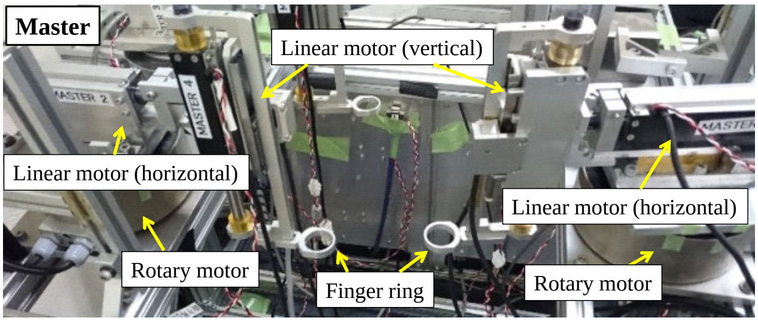

(a) Master system.

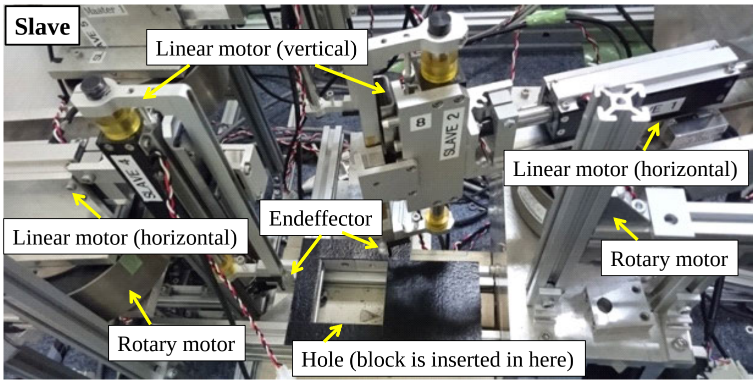

(b) Slave system.

Fig. 4-13: Experimental systems for verification of adaptive motion-loading system for environmental difference.

Table 4.3: Experimental cases for verification of adaptive motion-loading system for environmental difference.

Case No.	target object	with/without proposed method
1	acrylic cube (the same object)	without proposed method
2	cork cube (the different object)	without proposed method
3	acrylic cube (the same object)	with proposed method
4	cork cube (the different object)	with proposed method

In this experiment, the different controllers are implemented in each axis during motion reproduction;

move-x: MCS controller with compensation force;

move-y: MCS controller with compensation force;

rotation: normal MCS controller;

grasp: force controller;

lifting: MCS controller with compensation force.


(a) Acrylic block.

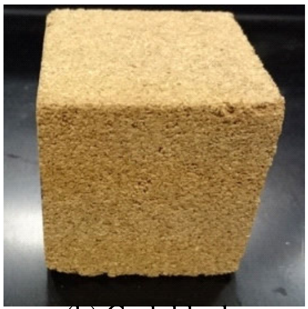
(b) Cork block.

Fig. 4-14: Target environments for verification of adaptive motion-loading system for environmental difference.

The position response was measured by the position encoder or the rotary encoder, and the force response was estimated by reaction force observer (RFOB) [39] without force sensors. The control program was written in C language under RTAI 3.7. The parameters used in these experiments are shown in Table 4.4.

Experimental Results of Motion Recording

Fig. 4-15 shows the experimental result of the motion recording. The responses of the master and slave systems are depicted in the figure. The left figures show the position responses and the right figures show the force responses. The responses of the motion-modal space are shown, because the bilateral controllers are implemented in the motion-modal space. After 5 s, the human operator held the acrylic block, and then picked up the block about 7.5 s. From about 12 s to 18 s, the operator moved the block while being in contact with the floor. Finally the block was inserted into the hole at about 19.5 s. After inserting the block, the operator got his finger off the block at 23 s. This motion was recorded to the motion data memory. Fig. 4-16 shows errors of responses between master and slave system. These results show that the responses of master and slave systems were almost the same because the ideal bilateral control was implemented.

Experimental Results of Motion Reproduction

Fig. 4-17 shows the experimental results of motion reproduction in case (1). Fig. 4-18 shows the errors between motion recording and motion reproducing. In this case, we succeeded the recorded task because the target object was the same. On the other hand, Figs. 4-19 and 4-20 show the experimental result of motion reproduction in case (2). In this case, the recorded task could not be reproduced because

Table 4.4: Experimental parameters for verification of adaptive motion-loading system for environmental difference.

Parameter	Description	Value
T_{s}	Sampling time	200 μs
L	length between center of the rotary motor to the end-effector	0.16 m
L_{base}	length between rotary motors of two device units	0.41 m
K_{fn}	Force coefficient of linear motor	40.0 N/A
M_{n}	Mass of linear motor	0.3 kg
$g_{\mathrm{pd,l}}$	Cut-off frequency of pseudo-derivation of linear motor	600 rad/s
$g_{\mathrm{dis,l}}$	Cut-off frequency of disturbance observer of linear motor	600 rad/s
K_{tn}	Torque coefficient of rotary motor	1.18 Nm/A
I_{n}	Inertia around rotary motor	0.00288 kgm^2
$g_{\mathrm{pd,r}}$	Cut-off frequency of pseudo-derivation of rotary motor	250 rad/s
$g_{\mathrm{dis,r}}$	Cut-off frequency of disturbance observer of rotary motor	250 rad/s
$K_{\mathrm{p,move}}$	Position gain for move-x and move-y axes	3600
$K_{\mathrm{d,move}}$	Velocity gain for move-x and move-y axes	120
$K_{\mathrm{f,move}}$	Force gain for move-x and move-y axes	5
$K_{\mathrm{p,rot}}$	Position gain for rotation axis	1600
$K_{\mathrm{d,rot}}$	Velocity gain for rotation axis	80
$K_{\mathrm{f,rot}}$	Force gain for rotation axis	2
$K_{\mathrm{p,grsp}}$	Position gain for grasp axis	3600
$K_{\mathrm{d,grsp}}$	Velocity gain for grasp axis	120
$K_{\mathrm{f,grsp}}$	Force gain for grasp axis	5
$K_{\mathrm{p,lift}}$	Position gain for lifting and z-diff axes	3600
$K_{\mathrm{d,lift}}$	Velocity gain for lifting and z-diff axes	120
$K_{\mathrm{f,lift}}$	Force gain for lifting axis	0.8
g_{wob}	Cut-off frequency of work space observer	500 rad/s
m_{obj1}	Weight of acrylic block	0.45 kg
l_{obj1}	Side length of acrylic block	0.055 m
m_{obj2}	Weight of cork block	0.05 kg
l_{obj2}	Side length of cork block	0.055 m
l_{hole}	Side length of hole	0.055 m

a target object was different. It is figured out that the force error of each axis was larger than Fig. 4-18. In particular, the contact force applied to the floor during tracing motion was different because the weight of lifting axis was different. Then, both force and trajectory of the recorded motion could not be carried out in the move-x and move-y axes. Finally, the force response after 19.5 s is too large. It means that the task to insert the block into the hole was failed and the end-effector push the block against the floor. As a result, the cork block could not be inserted into the hole because contacting force and tracing force was not reproduced during tracing motion.

Figs. 4-21 and 4-22 show the experimental result of motion reproduction in case (3). In this case, we succeeded the recorded task because the target object was the same. Fig. 4-23 (a) shows the compensation force of the lifting axis which was calculated during time period of “phase 1.” Fig. 4-23 (b) shows the estimated friction difference of the move-x and move-y axes which was calculated during time period of “phase 2.” These calculation periods were defined by the author from the responses of the recorded motion which is shown in Fig. 4-15. The period of “phase 1” is determined 8.0 s–11.5 s by position response of the lifting axis. The reason is that the block was completely taken off the floor and the response was stable. The period of “phase 2” is determined 13.2 s–14.1 s by position response of the lifting axis and force responses of move-x and move-y axes. The reason why this period was selected is that the block contacted with the floor and the searching motion started and force response was stable. In the future application, it hopes that the system recognizes the motion and defines calculation period automatically. It is shown that the recorded task was reproduced using the same block even if the force compensation was implemented. On the other hand, Figs. 4-24 and 4-25 show the experimental result of motion reproduction in case (4). In this case, we succeeded the recorded task even if the target object was different. As shown in Fig. 4-26 (a), the weight difference was calculated in “phase 1,” and applied force to the floor was compensated after that. Then as shown in Fig. 4-26 (b), the friction different of the horizontal direction was calculated in “phase 2,” and applied force of these axes were compensated after that. It is shown by Figs 4-20 and 4-25 that the applied force error during tracing motion was decreased by proposed method. In particular, the force error of the lifting axis during about 19.5 s–23 s is small. It means the task of inserting the block is achieved. As a result, the cork block could be inserted into the hole because the tracing motion was carried out successfully. By these experimental results, the validity of the proposed method is confirmed.

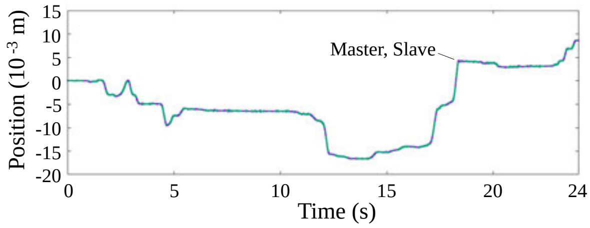

(a) Position responses of x axis.

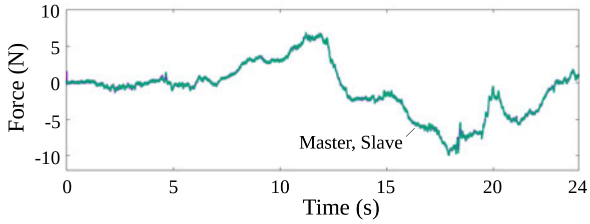

(b) Force responses of x axis.

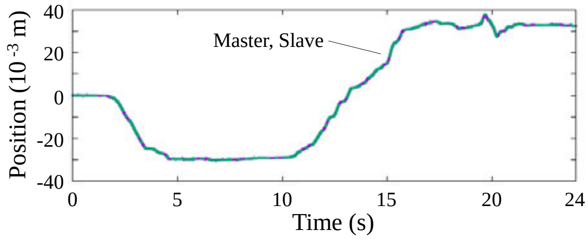

(c) Position responses of y axis.

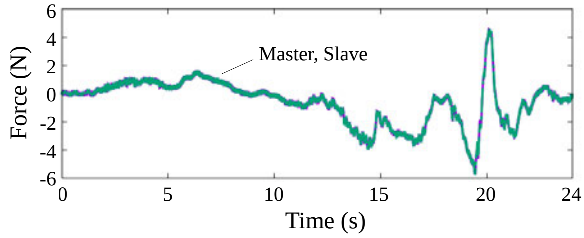

(d) Force responses of y axis.

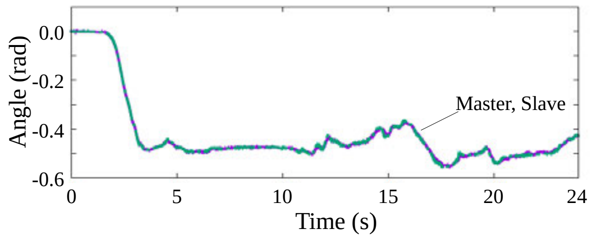

(e) Angle responses of rotation axis.

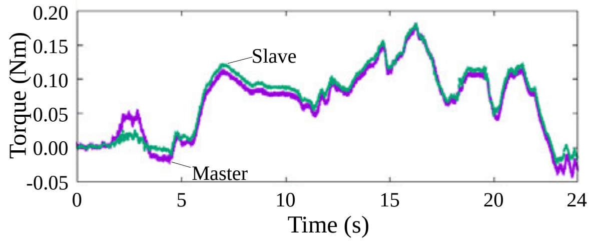

(f) Torque responses of rotation axis

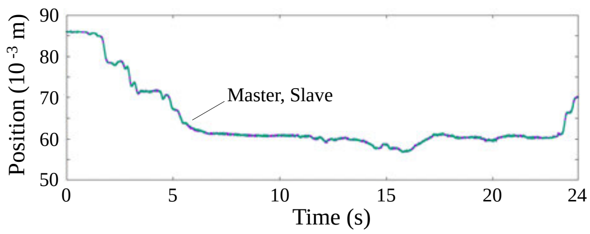

(g) Position responses of grasp axis.

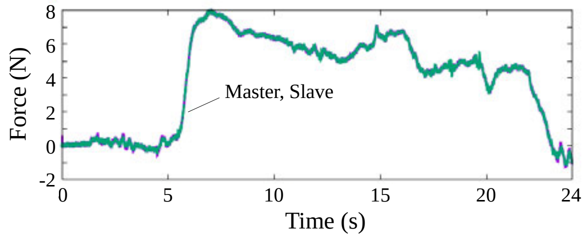

(h) Force responses of grasp axis.

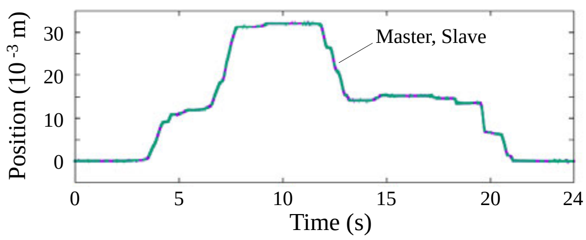

(i) Position responses of lifting axis.

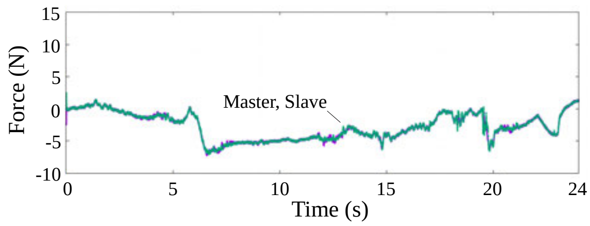

(j) Force responses of lifting axis.

Fig. 4-15: Experimental results of motion recording for verification of adaptive motion-loading system for environmental difference.

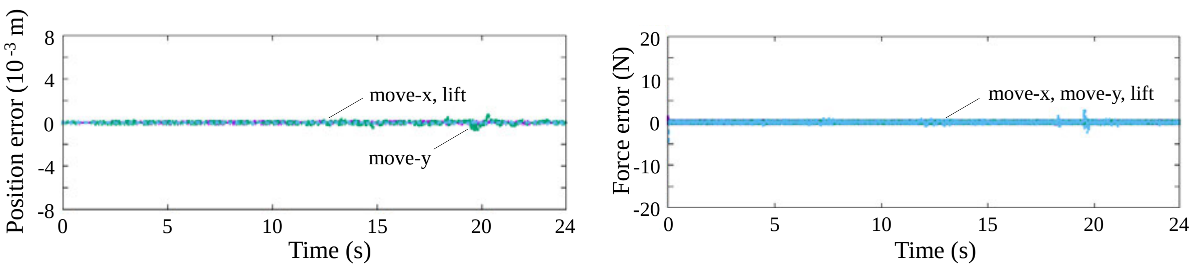

(a) Position error. (b) Force error.

Fig. 4-16: Errors of motion recording for verification of adaptive motion-loading system for environmental difference.

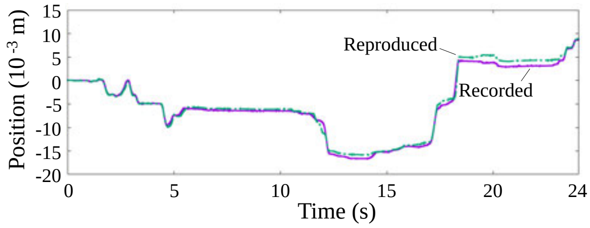

(a) Position responses of x axis.

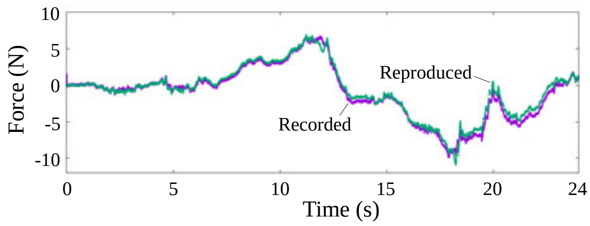

(b) Force responses of x axis.

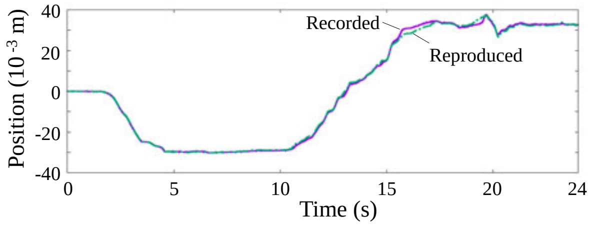

(c) Position responses of y axis.

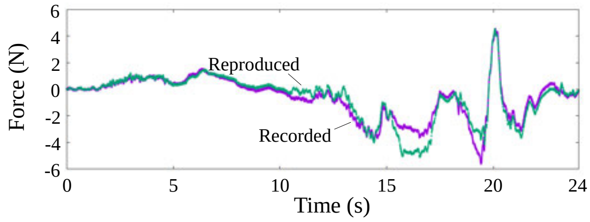

(d) Force responses of y axis.

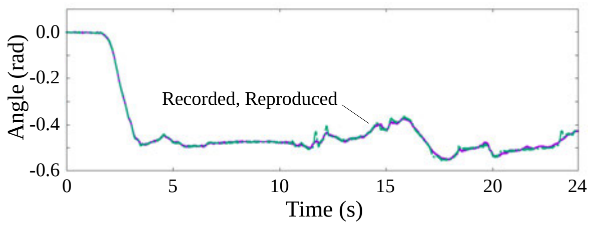

(e) Angle responses of rotation axis.

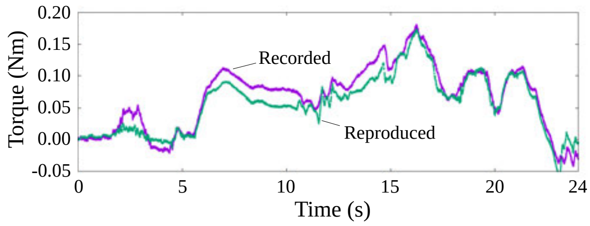

(f) Torque responses of rotation axis

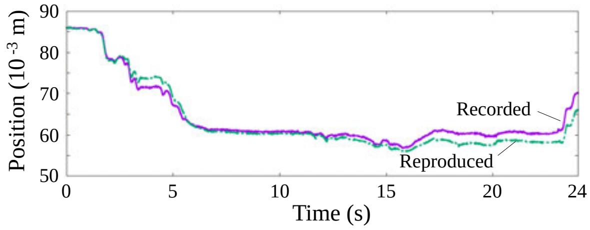

(g) Position responses of grasp axis.

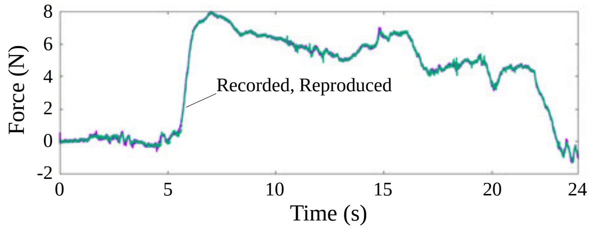

(h) Force responses of grasp axis.

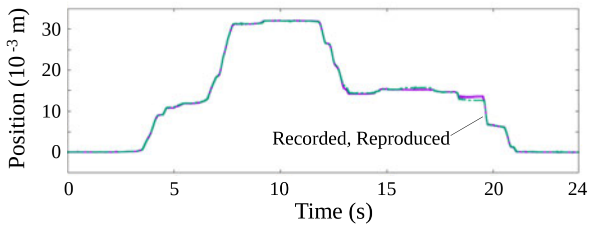

(i) Position responses of lifting axis.

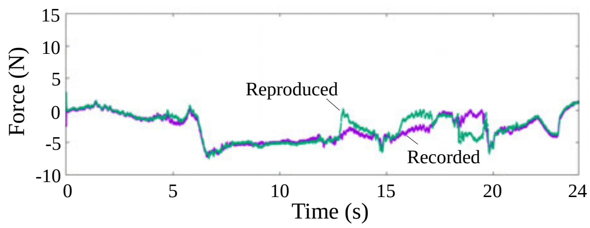

(j) Force responses of lifting axis.

Fig. 4-17: Experimental results of motion reproduction in case 1 for verification of adaptive motion-loading system for environmental difference.

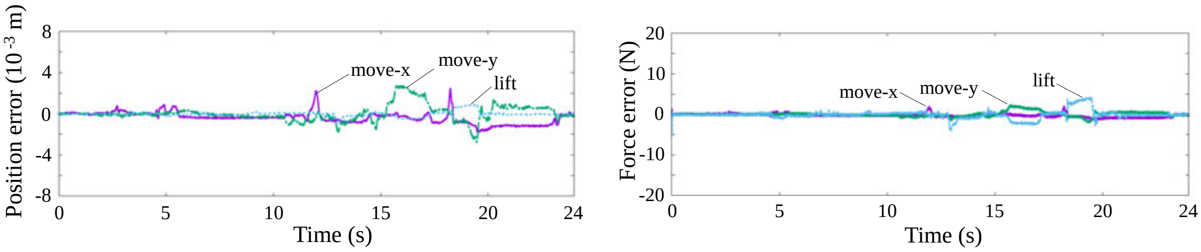

(a) Position error.

(b) Force error.

Fig. 4-18: Errors of motion reproduction in case 1 for verification of adaptive motion-loading system for environmental difference.

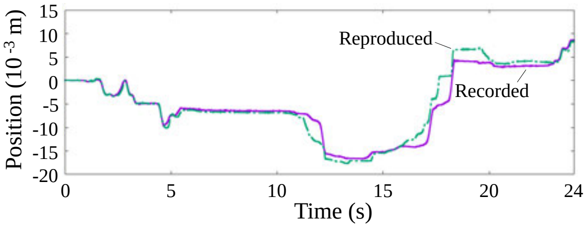

(a) Position responses of x axis.

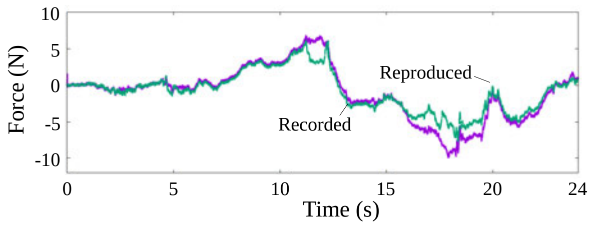

(b) Force responses of x axis.

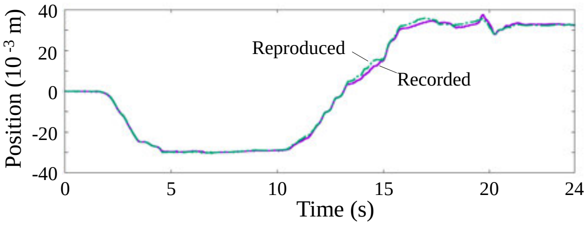

(c) Position responses of y axis.

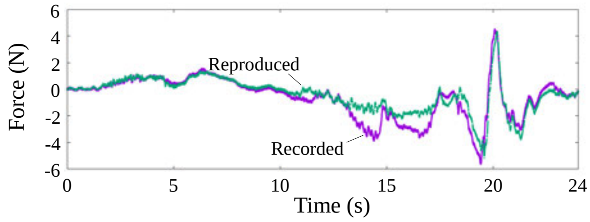

(d) Force responses of y axis.

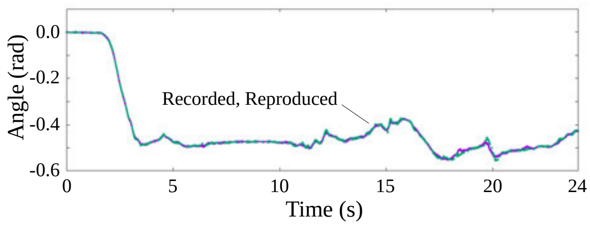

(e) Angle responses of rotation axis.

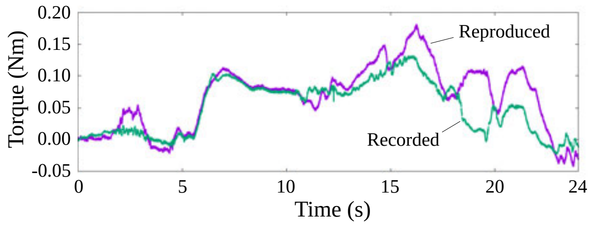

(f) Torque responses of rotation axis

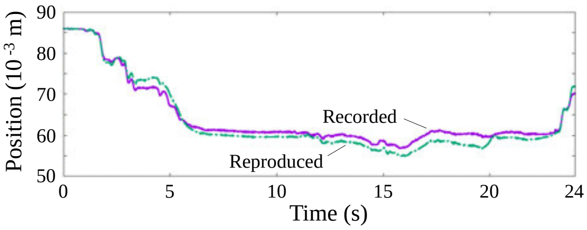

(g) Position responses of grasp axis.

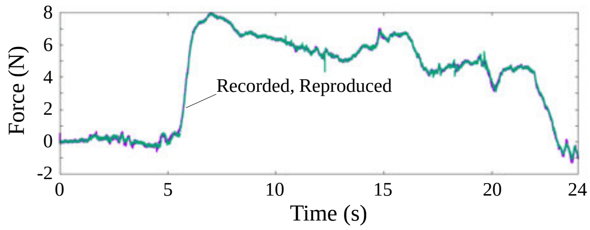

(h) Force responses of grasp axis.

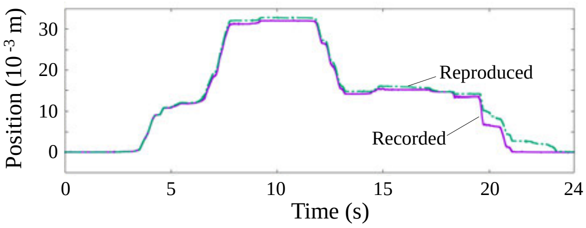

(i) Position responses of lifting axis.

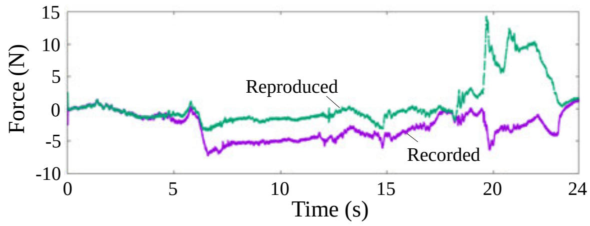

(j) Force responses of lifting axis.

Fig. 4-19: Experimental results of motion reproduction in case 2 for verification of adaptive motion-loading system for environmental difference.

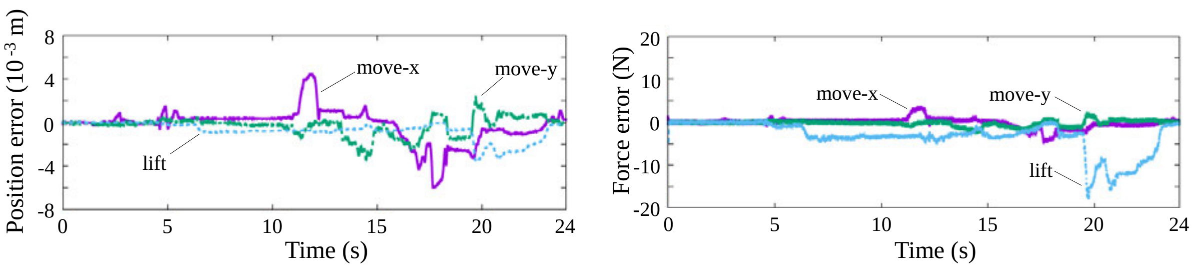

(a) Position error. (b) Force error.

Fig. 4-20: Errors of motion reproduction in case 2 for verification of adaptive motion-loading system for environmental difference.

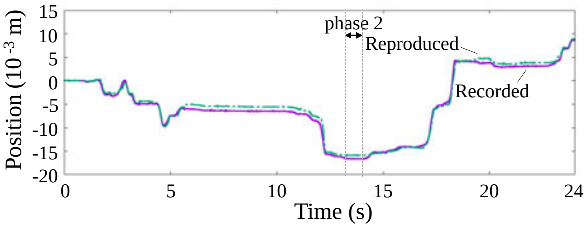

(a) Position responses of x axis.

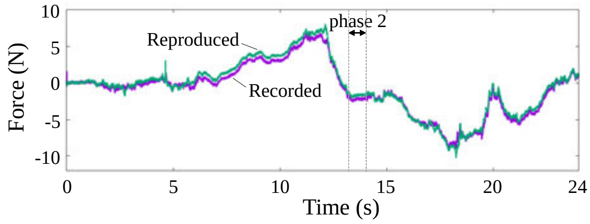

(b) Force responses of x axis.

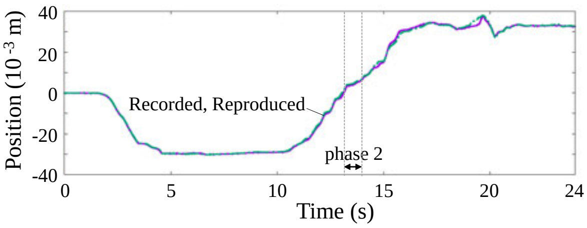

(c) Position responses of y axis.

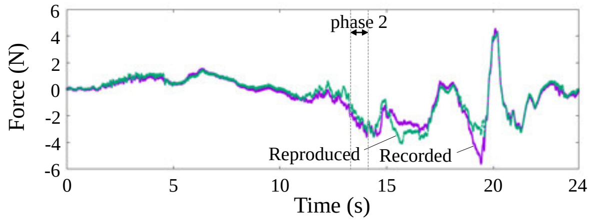

(d) Force responses of y axis.

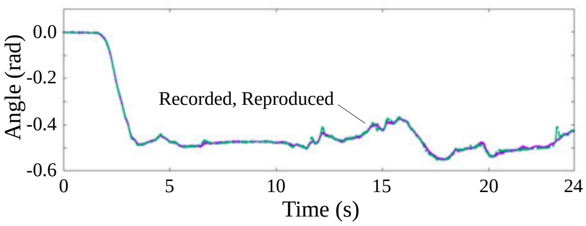

(e) Angle responses of rotation axis.

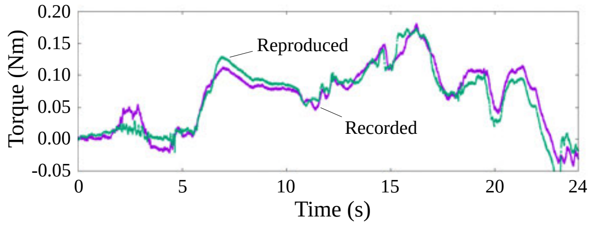

(f) Torque responses of rotation axis

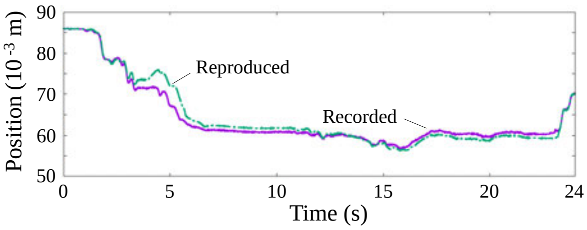

(g) Position responses of grasp axis.

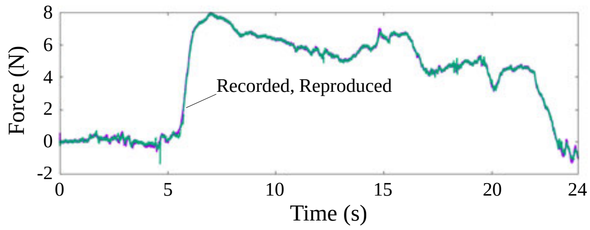

(h) Force responses of grasp axis.

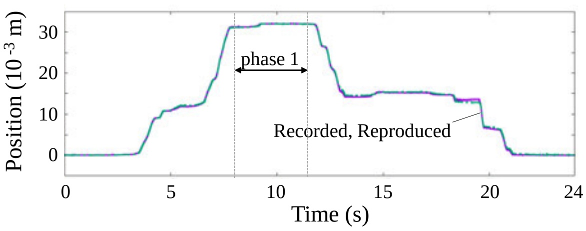

(i) Position responses of lifting axis.

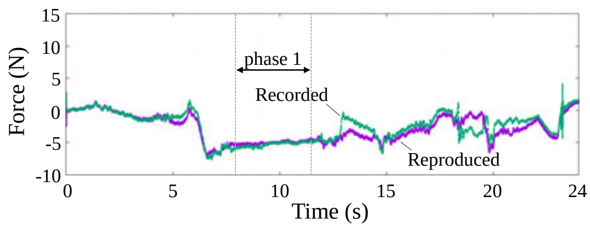

(j) Force responses of lifting axis.

Fig. 4-21: Experimental results of motion reproduction in case 3 for verification of adaptive motion-loading system for environmental difference.

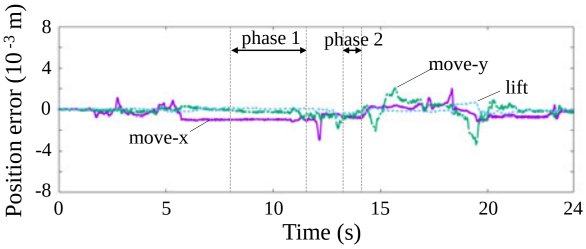

(a) Position error.

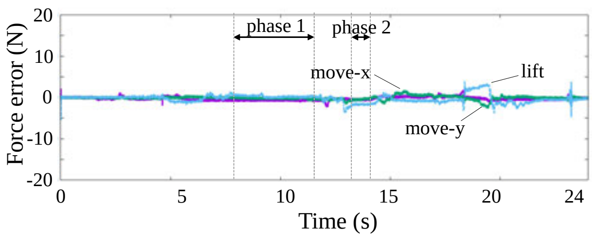

(b) Force error.

Fig. 4-22: Errors of motion reproduction in case 3 for verification of adaptive motion-loading system for environmental difference.

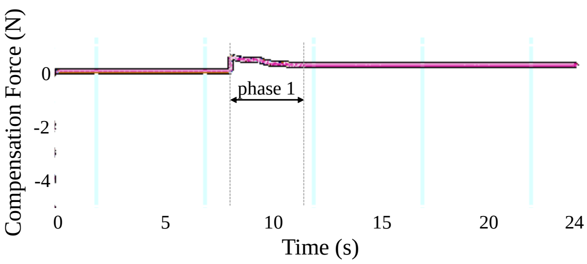

(a) Compensation force of lifting axis.

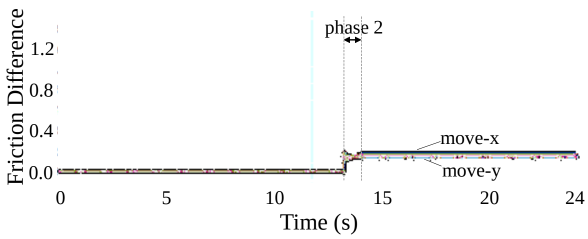

(b) Estimated friction difference.

Fig. 4-23: Compensation value in case 3 for verification of adaptive motion-loading system for environmental difference.

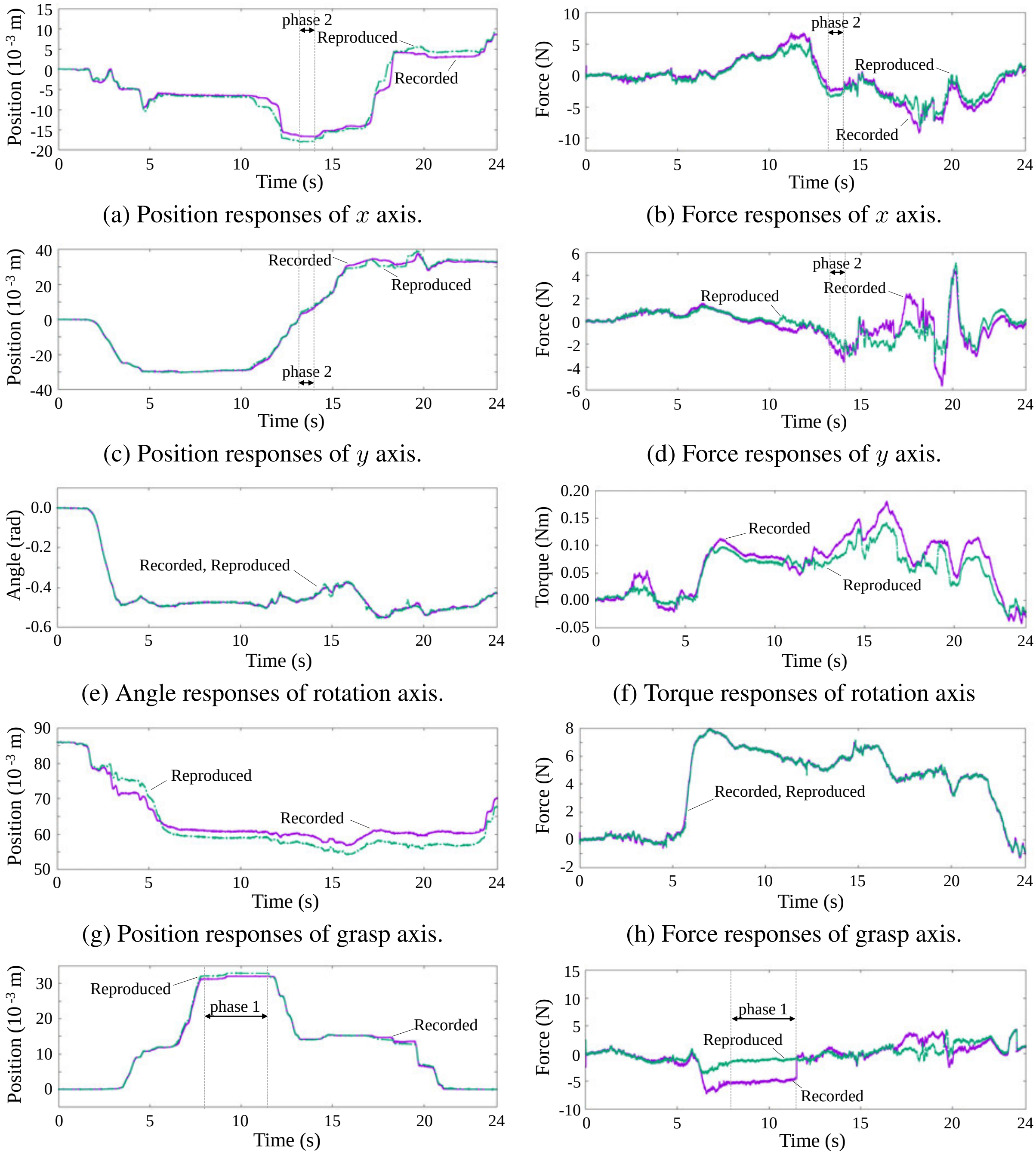

(a) Position responses of x axis.

(b) Force responses of x axis.

(c) Position responses of y axis.

(d) Force responses of y axis.

(e) Angle responses of rotation axis.

(f) Torque responses of rotation axis

(g) Position responses of grasp axis.

(h) Force responses of grasp axis.

(i) Position responses of lifting axis.

(j) Force responses of lifting axis.

Fig. 4-24: Experimental results of motion reproduction in case 4 for verification of adaptive motion-loading system for environmental difference.

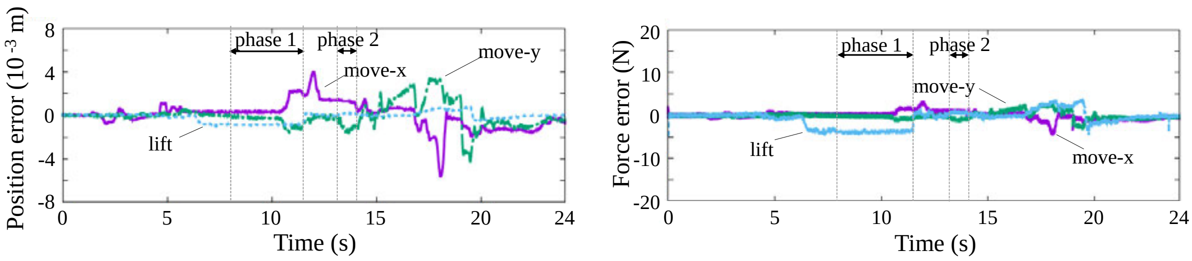

(a) Position error. (b) Force error.

Fig. 4-25: Errors of motion reproduction in case 4 for verification of adaptive motion-loading system for environmental difference.

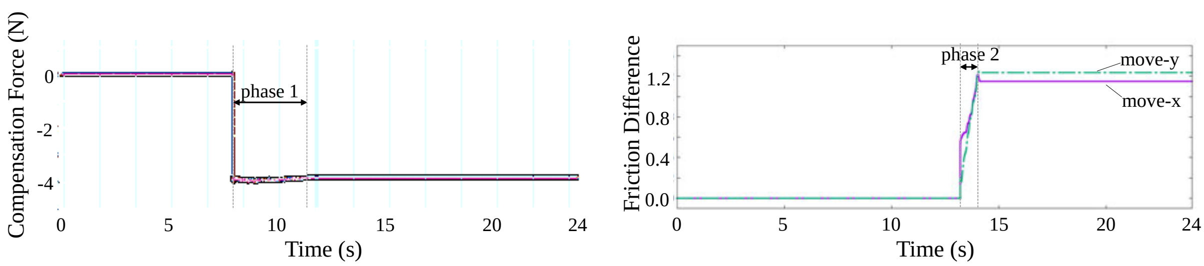

(a) Compensation force of lifting axis. (b) Estimated friction difference.

Fig. 4-26: Compensation value in case 4 for verification of adaptive motion-loading system for environmental difference.

4.4 Summary

In this chapter, the adaptation methods, when target environments between motion recording and reproducing are different, were proposed. For the future applications of the motion-copying system, it is important to reproduce recorded motions even if the environmental condition is different. In particular, 2 types of difference were dealt with in this research.

In section 4.2, the method for the position difference of the environment was proposed. In the proposed system, human motion was regarded as the acceleration information. The recorded motion does not depend on the initial position, because the acceleration information expresses the amount of change. In the case that the environmental position is nearer, the equivalent acceleration about the movement of end-effector's position is used as the applied force. On the contrary, when the environmental position is farther, the equivalent acceleration about the applied force is used as the movement of the end-effector.

The basic motion-loading system, which is position/force hybrid system, is effective method when the environmental condition is almost the same. On the other hand, the proposed method is effective method when the only environmental location is different and it is located the same direction as motion direction. Of course, the proposed method can be used when the environmental condition is almost the same. However, the basic method is more stable than acceleration-based method when the other conditions such as mass, friction, and so on are different. Hence, the proposed method should be used only when the environment location is different and it is located in the same direction of the motion direction.

In section 4.3, the method for the difference of the target environment was proposed under the application of "peg-in-hole." In the proposal, we assumed that the applied force to the external environment can be separated to the force on the basis of the difference of a target object and the common force which does not depend on it. The compensation force was applied to achieve the same force against the floor during searching motion. By the proposal, the tracing motion was successfully carried out because the applied force was modified. The effect from the difference of the target environment was omitted, and the task of the recorded motion was successfully reproduced.

In this section, the simplified method is used as a first step of the research. In the future, it is desired to use better method to estimate the compensation force. In addition, the time period during calculation is defined by the author in advance. In the future, it is expected that the system recognizes the feature of the motion, and the system decides when the compensation value is calculated and when the compensation value is added to the command.

In each section, the validities of the proposed methods was shown by the experimental results. By these methods, it is expected to reproduce the motion by the motion which is same task but for different environment.

Chapter 5

Motion Reproduction with Adaptation to Different Target Object based on Coupling of Motion Components

5.1 Background and Overview of This Chapter

For the future applications of the motion-copying system, the methods for each purpose need to be combined in order to achieve required motion reproduction. In addition, it is expected to search motion elements from the database [79, 80, 113] during motion reproduction and change the motion depending on the situation. In this chapter, the motion reproduction with the different target object is achieved by selecting and coupling the motion elements under the application of "peg-in-hole."

The goal of the application is the same as the section 4.3, but the approach is the different. The concept diagram is shown in Fig. 5-1. By selecting and changing the motion elements according to the target environment during motion reproduction, the goal of the task is achieved. Here, the proposed methods described in chapters 2–4 are implemented in each motion modal axis at the same time as culmination of this thesis.

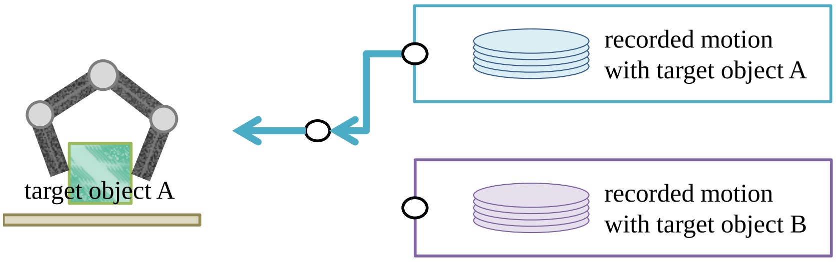

Fig. 5-1: Concept of the motion reproduction with selecting motion elements.

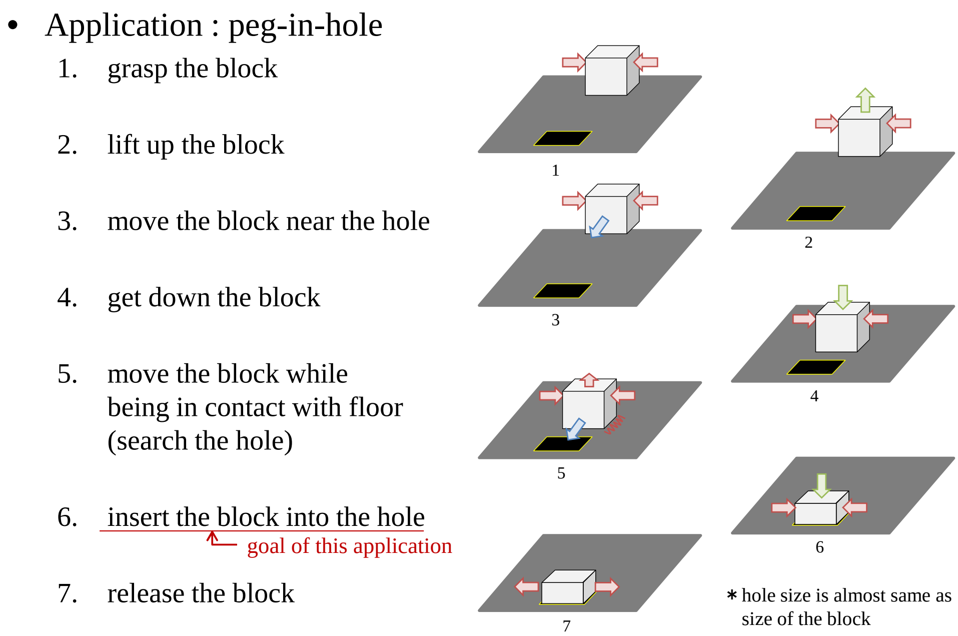

Fig. 5-2: Motion procedure of the application.

5.2 Adaptive Motion Reproduction for Different Target Object based on Selection of Motion Component

In this section, the motion reproduction when target environmental material is changed is achieved by combining method described in chapters 2–4. The application of this chapter is "peg-in-hole" which is the same application of section 4.2. The procedure of the application is shown in Fig. 5-2. In this section, the proposed method is implemented in the system described in section 2.4.

5.2.1 Control Design

In order to achieve "peg-in-hole" task even if a target block is different, the motion elements for each environment are selected and coupling. Because the roles of the axes are different, the different methods are implemented in each axis. We should consider the following two points to design the system of this application;

- which reproduction method should be selected for each axis;
- which coupling method should be selected for each axis.

First, the reproduction method is selected. The basic motion-loading system, which is position/force hybrid system, is effective method when the environmental condition is almost the same. On the other hand, the proposed acceleration-based method described in section 4.2 is effective method when the only environmental location is different and it is located the same direction as motion direction. However, the basic method is more stable than acceleration-based method when the other conditions such as mass, friction, and so on are different. In this application, the location of the target environment and the hole is almost the same in x-y surface. Hence, the position and force information is used as the motion information in move-x and move-y axes. Then, the position and force information is used as the motion information in rotation axis, because the environmental condition about rotation axis is almost the same. The target environment is located the same direction of grasp axis. Hence, the reproduction method using acceleration information is selected as the reproduction method in grasp axis. The basic motion-loading system is selected to reproduce 1st motion of lifting axis, and reproduction method of 2nd motion is based on acceleration information. It is because that height of grasp point of the block is different. As a results, distance between target environment and the floor is different. It means that the environmental location is different and floor is located the same direction. Therefore, the acceleration based method is selected to reproduce 2nd motion in lifting axis.

Then, the coupling method is selected. The proposed coupling methods depend on the reproduction method of latter motion. When the latter reproduction method is the basic motion-loading system, the interpolation method described in section 3.2 should be used. Therefore, the method of interpolation of position and force information is implemented in move-x, move-y and rotation axes. On the other hand, the method that cancels the equivalent velocity described in section 3.3 should be used when the latter reproduction method is the proposed acceleration-based method.

Table 5.1 shows the summary of implemented methods in each axis.

Table 5.1: Control method in each axis.

axis	1st motion	2nd motion	coupling method
move-x	Position & Force	Position & Force	Interpolation
move-y	Position & Force	Position & Force	Interpolation
rotation	Position & Force	Position & Force	Interpolation
grasp	Acceleration	Acceleration	equivalent velocity
lifting	Position & Force	Acceleration	equivalent velocity

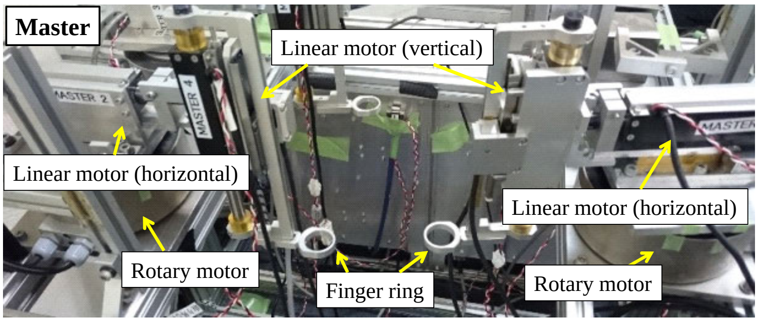

(a) Master system.

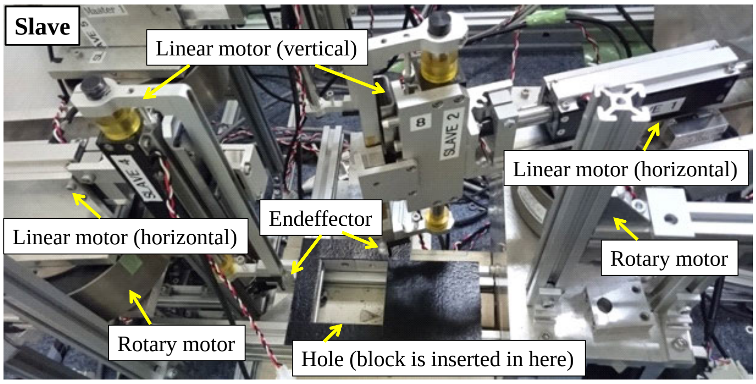

(b) Slave system.

Fig. 5-3: Experimental systems for adaptive motion reproduction based on selection of motion components.

5.2.2 Experiments

In this sub-section, the validity of the proposed methods are verified by experiments. The model of the experimental system is described in the section 2.4.

Experimental Setup

Fig. 5-3 shows the experimental system used in the experiments. This system is constructed by the master and slave systems, and each system is composed of two-device units. The device unit is


(a) Acrylic block.

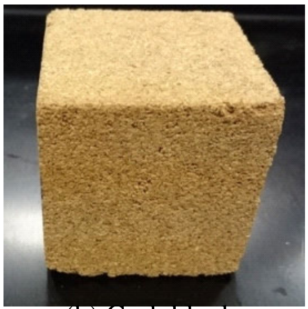
(b) Cork block.

Fig. 5-4: Target environments for adaptive motion reproduction based on selection of motion components.

constructed by three motors; a rotary motor (horizontal) and two linear motors (horizontal and vertical). In the motion-recording step, both of the master and slave systems were used. A human operator operates the master system, and the end effector in the slave system brought the block and inserted the block into the hole. In particular, motion procedure is i) grasping a block; ii) picking up a block; iii) moving the block near the hole; iv) getting down the block; v) moving while being in contact with the external environment (search the hole); vi) inserting the block into a hole. On the contrary, only the slave system was used in the motion-reproducing step. The recorded motion was reproduced by the slave system. Then, the device picked up the block and inserted the block into the hole as if it is recorded motion. The goal of this application is that the block exists in the hole after the motion reproduction.

The target object is shown in Fig. 5-4. In the motion-recording step, 2 motions are carried out. The recorded motion 1 is a motion that the acrylic block was used as the target object. Then the recorded motion 2 is a motion that the cork block was used as the target object. Size of the hole and the block are almost the same, but they are not completely the same In this experiment, 6 pattern of motion reproduction, which is shown in Table 5.2, were carried out. When 1st motion and 2nd motion is the same, the coupling time was not inserted between 1st and 2nd motions. When they are different motion, the coupling time was inserted between motions. The coupling time is set 1 s. The position response was measured by the position encoder or the rotary encoder, and the force response was estimated by reaction force observer (RFOB) [39] without force sensors. The control program was written in C language under RTAI 3.7. The parameters used in these experiments are shown in Table 5.3.

Table 5.2: Cases of motion reproduction for adaptive motion reproduction based on selection of motion components.

case No.	1st motion	2nd motion	target environment
1	Recorded motion 1	Recorded motion 1	Acrylic block
2	Recorded motion 1	Recorded motion 1	Cork block
3	Recorded motion 1	Recorded motion 2	Cork block
4	Recorded motion 2	Recorded motion 2	Cork block
5	Recorded motion 2	Recorded motion 2	Acrylic block
6	Recorded motion 2	Recorded motion 1	Acrylic block

Table 5.3: Experimental parameters for adaptive motion reproduction based on selection of motion components.

Parameter	Description	Value
$T_{\rm s}$	Sampling time	200 μs
L	length between center of the rotary motor to the end-effector	0.16 m
$L_{\rm base}$	length between rotary motors of two device units	0.41 m
$K_{\rm fn}$	Force coefficient of linear motor	40.0 N/A
$M_{\rm n}$	Mass of linear motor	0.3 kg
$g_{\rm pd,l}$	Cut-off frequency of pseudo-derivation of linear motor	600 rad/s
$g_{\rm dis,l}$	Cut-off frequency of disturbance observer of linear motor	600 rad/s
$K_{\rm tn}$	Torque coefficient of rotary motor	1.18 Nm/A
$I_{\rm n}$	Inertia around rotary motor	0.00288 kgm^2
$g_{\rm pd,r}$	Cut-off frequency of pseudo-derivation of rotary motor	250 rad/s
$g_{\rm dis,r}$	Cut-off frequency of disturbance observer of rotary motor	250 rad/s
$K_{\rm p,move}$	Position gain for move-x and move-y axes	3600
$K_{\rm d,move}$	Velocity gain for move-x and move-y axes	120
$K_{\rm f,move}$	Force gain for move-x and move-y axes	5
$K_{\rm p,rot}$	Position gain for rotation axis	1600
$K_{\rm d,rot}$	Velocity gain for rotation axis	80
$K_{\rm f,rot}$	Force gain for rotation axis	2
$K_{\rm p,grsp}$	Position gain for grasp axis	3600
$K_{\rm d,grsp}$	Velocity gain for grasp axis	120
$K_{\rm f,grsp}$	Force gain for grasp axis	5
$K_{\rm p,lift}$	Position gain for lifting and z-diff axes	3600
$K_{\rm d,lift}$	Velocity gain for lifting and z-diff axes	120
$K_{\rm f,lift}$	Force gain for lifting axis	0.8
$g_{\rm wob}$	Cut-off frequency of work space observer	500 rad/s
$m_{\rm obj1}$	Weight of acrylic block	0.45 kg
$l_{\rm obj1}$	Side length of acrylic block	0.055 m
$m_{\rm obj2}$	Weight of cork block	0.05 kg
$l_{\rm obj2}$	Side length of cork block	0.055 m
$l_{\rm hole}$	Side length of hole	0.055 m

Experimental Results of Motion Recording

Figs. 5-5 and 5-6 show the experimental results of the motion recording. The responses of the master and slave systems are depicted in the figure. The left figures show the position responses and the right figures show the force responses. The responses of the motion-modal space are shown, because the bilateral controllers are implemented in the motion-modal space. In Fig. 5-5, the human operator held the acrylic block after about 5 s, and then picked up the block about 7 s, and held the block during about 7 s to 10.5 s. From about 12 s to 18 s, the operator moved the block while being in contact with the floor. Finally, the block was inserted into the hole at about 19 s. After inserting the block, the operator got his finger off of the block at 20.5 s. The boundary of motion elements of motion 1 is defined 9 s, which time is about center of the holding motion. In Fig. 5-6, the human operator held the cork block after 4.5 s, and then picked up the block about 5.5 s, and held the block during about 5.5 s to 9 s. From about 10.5 s to 16 s, the operator moved the block while being in contact with the floor. Finally, the block was inserted into the hole at about 17 s. After inserting the block, the operator got his finger off of the block at 19 s. The boundary of motion elements of motion 2 is defined 8 s, which time is about center of the holding motion. In the future application, it hopes that the system recognizes the motion and determines boundary of motion elements automatically. But it was defined by the author in this research. These 2 motions were recorded to the motion data memory.

Experimental Results of Motion Reproduction

Fig. 5-7 shows the experimental results of motion reproduction in case (1). In this case, the target object is same as motion 1, hence the motion is not necessary to be changed and the recorded task is successfully achieved.

Fig. 5-8 shows the experimental results of motion reproduction in case (2). In this case, the recorded task could not be reproduced because a target object was different. It is figured out that the force error of each axis was large. In particular, the contact force applied to the floor during tracing motion was different because the weight of lifting axis was different. Then, both force and trajectory of the recorded motion could not be carried out in the move-x and move-y axes. The force response of lifting axis about 19 s was larger than motion recording. It means that the task to insert the block into the hole was failed and the end-effector pushed the block against the floor. As a result, the cork block could not be inserted into the hole because contacting force and tracing force was not reproduced during tracing motion.

On the other hand, Fig. 5-9 shows the experimental result of motion reproduction in case (3). In this case, we succeeded the recorded task even if the target object was different. The target environment was recognized during holding phase, and the system changed the motion from motion 1 to motion 2. Here, it was assumed that the target blocks used in the experiments were 2 kinds, and the simply method was used to recognition. After coupling time, the used motion data were correspond with that for the actual target object. The responses of the move-x, move-y, and rotation axes correspond with the recorded motion by using the basic motion-copying system and coupling method of the interpolation. The response of the grasp axis corresponds with the recorded motion by using the acceleration-based motion-copying system and coupling method of cancelling equivalent velocity. The position error of lifting axis was caused by the height difference of grasp point of two motions. Dotted line shows the position that the target block contacted with the floor. By using the acceleration-based motion-copying system, the motion reproduction not depending on the position was achieved. As a result, the cork block could be inserted into the hole because the tracing motion was carried out successfully.

Fig. 5-10 shows the experimental results of motion reproduction in case (4). In this case, the target object is same as motion 2, hence the motion is not necessary to be changed and the recorded task is successfully achieved.

Fig. 5-11 shows the experimental result of motion reproduction in case (5). In this case, the recorded task could not be reproduced because a target object was different. It is figured out that the force error of each axis was large. In particular, the contact force applied to the floor during tracing motion was different because the weight of lifting axis was different. Then, both force and trajectory of the recorded motion could not be carried out in the move-x and move-y axes. The force response of lifting axis about 17 s was larger than motion recording. It means that the task to insert the block into the hole was failed and the end-effector pushed the block against the floor. As a result, the cork block could not be inserted into the hole because contacting force and tracing force was not reproduced during tracing motion.

On the other hand, Fig. 5-12 shows the experimental result of motion reproduction in case (6). In this case, we succeeded the recorded task even if the target object was different. The target environment was recognized during holding phase, and the system changed the motion from motion 2 to motion 1. Here, it was assumed that the target blocks used in the experiments were 2 kinds, and the simply method was used to recognition. After coupling time the used motion data were correspond with that for the actual target object. The responses of the move-x, move-y, and rotation axes correspond with the recorded motion by using the basic motion-copying system and coupling method of the interpolation.

Table 5.4: Summary of experimental results for adaptive motion reproduction based on selection of motion components.

case No.	1st motion	2nd motion	target environment	result
1	Recorded motion 1	Recorded motion 1	Acrylic block	success
2	Recorded motion 1	Recorded motion 1	Cork block	fail
3	Recorded motion 1	Recorded motion 2	Cork block	success
4	Recorded motion 2	Recorded motion 2	Cork block	success
5	Recorded motion 2	Recorded motion 2	Acrylic block	fail
6	Recorded motion 2	Recorded motion 1	Acrylic block	success

The response of the grasp axis corresponds with the recorded motion by using the acceleration-based motion-copying system and coupling method of cancelling equivalent velocity. The position error of lifting axis was caused by the height difference of grasp point of two motions. Dotted line shows the position that the target block contacted with the floor. By using the acceleration-based motion-copying system, the motion reproduction not depending on the position was achieved. As a result, the cork block could be inserted into the hole because the tracing motion was carried out successfully.

Table 5.4 show the summary of the experiments. By selecting and changing the motion elements according to the target environment during motion reproduction, the goal of the task was achieved. By these experimental results, the validity of the proposed method is confirmed.

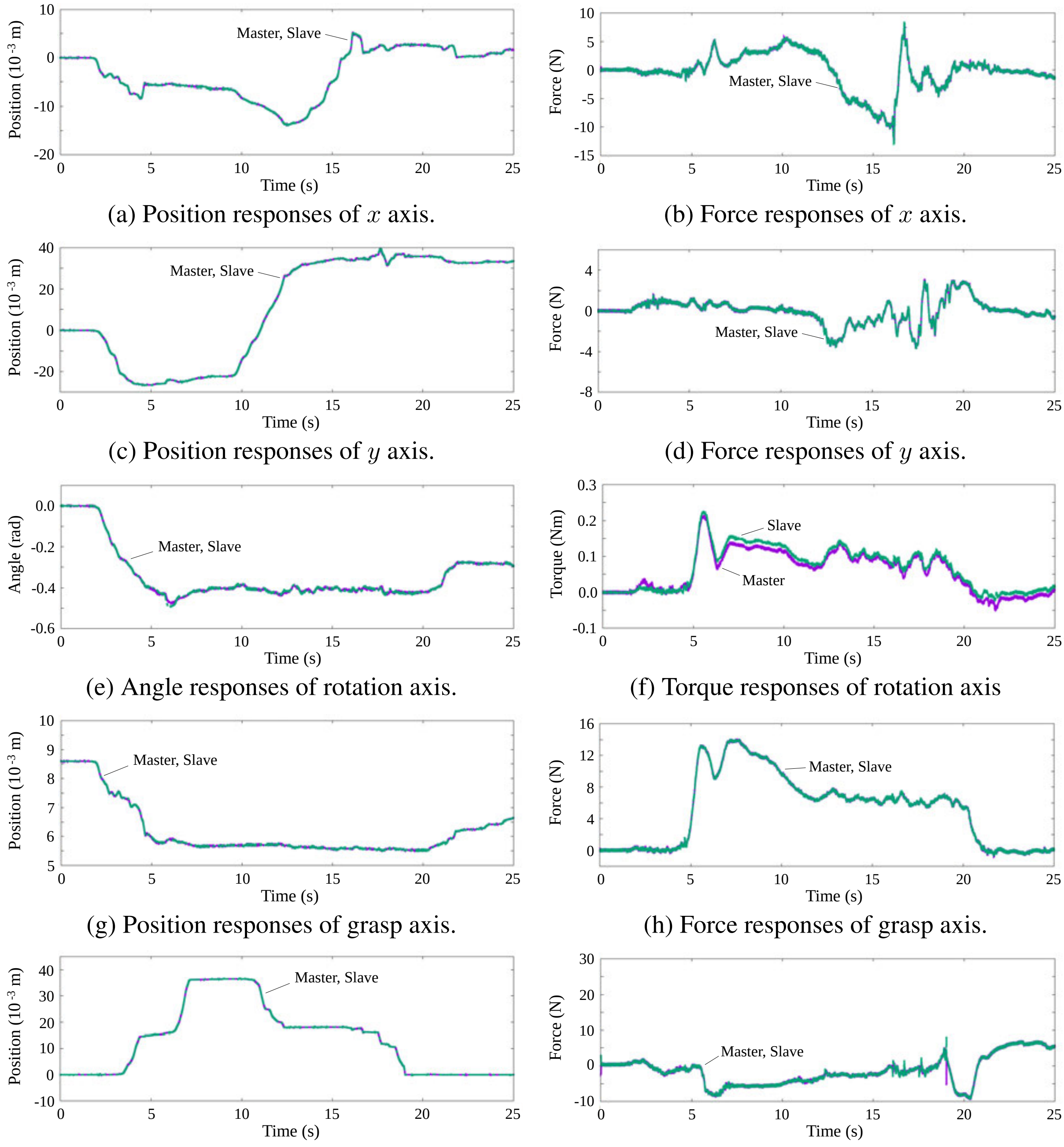

(a) Position responses of x axis.

(b) Force responses of x axis.

(c) Position responses of y axis.

(d) Force responses of y axis.

(e) Angle responses of rotation axis.

(f) Torque responses of rotation axis

(g) Position responses of grasp axis.

(h) Force responses of grasp axis.

(i) Position responses of lifting axis.

(j) Force responses of lifting axis.

Fig. 5-5: Experimental results of motion recording of motion 1 (with acrylic block) for adaptive motion reproduction based on selection of motion components.

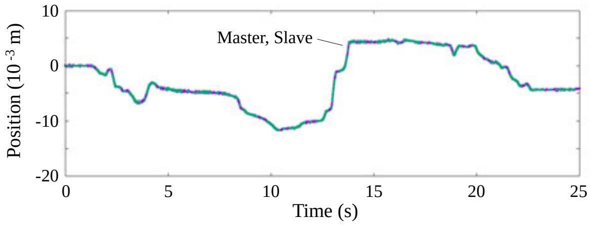

(a) Position responses of x axis.

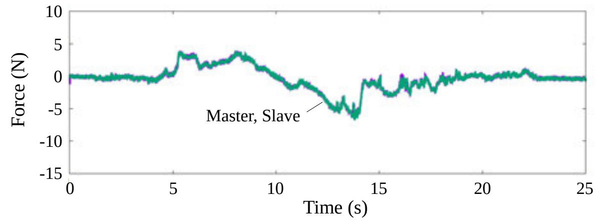

(b) Force responses of x axis.

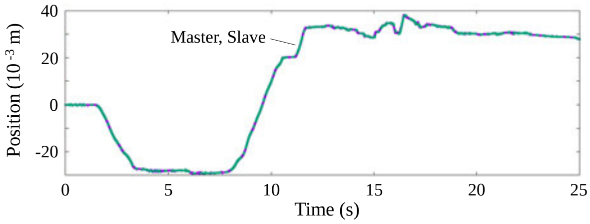

(c) Position responses of y axis.

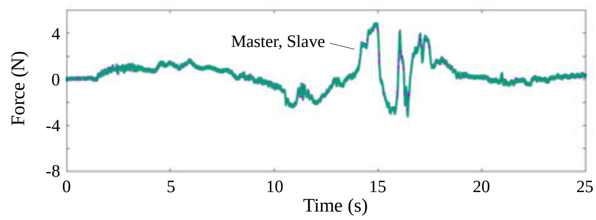

(d) Force responses of y axis.

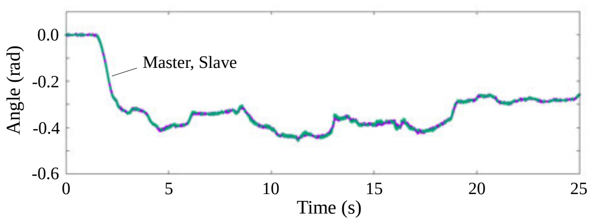

(e) Angle responses of rotation axis.

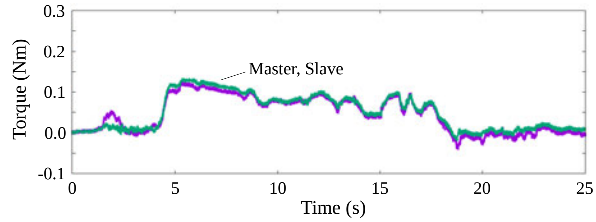

(f) Torque responses of rotation axis

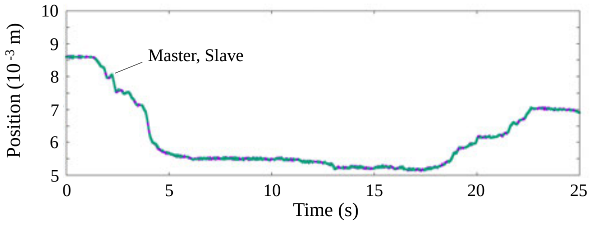

(g) Position responses of grasp axis.

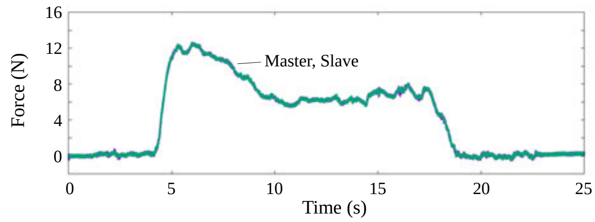

(h) Force responses of grasp axis.

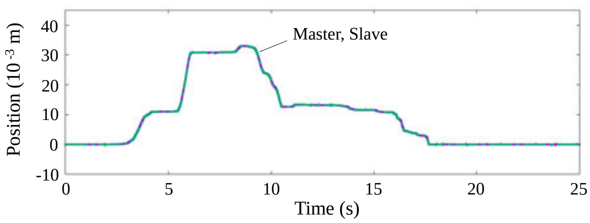

(i) Position responses of lifting axis.

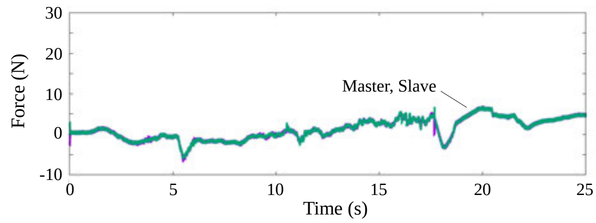

(j) Force responses of lifting axis.

Fig. 5-6: Experimental results of motion recording of motion 2 (with cork block) for adaptive motion reproduction based on selection of motion components.

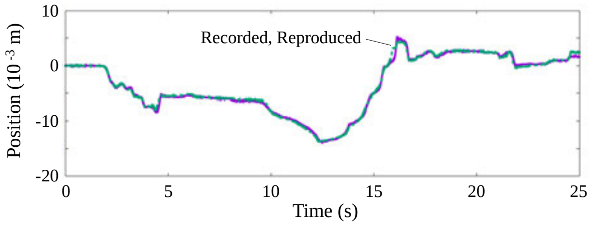

(a) Position responses of x axis.

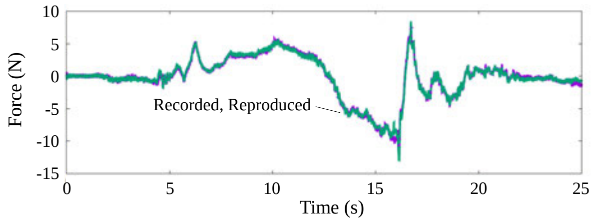

(b) Force responses of x axis.

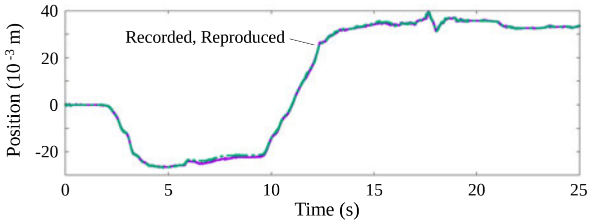

(c) Position responses of y axis.

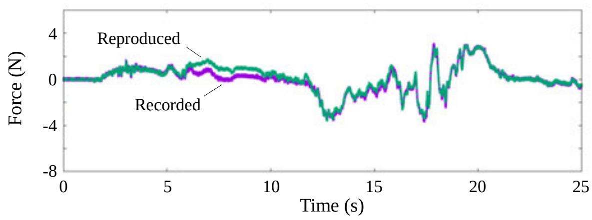

(d) Force responses of y axis.

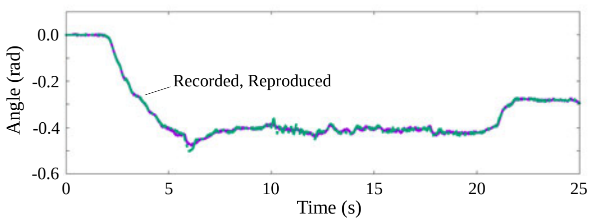

(e) Angle responses of rotation axis.

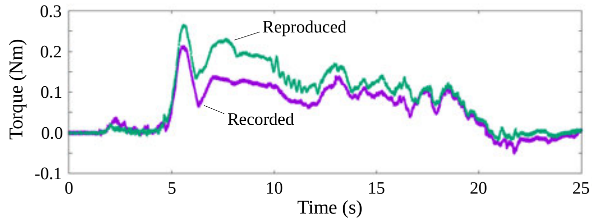

(f) Torque responses of rotation axis

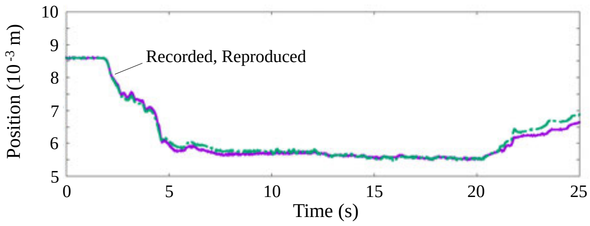

(g) Position responses of grasp axis.

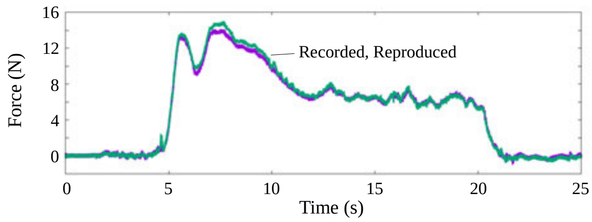

(h) Force responses of grasp axis.

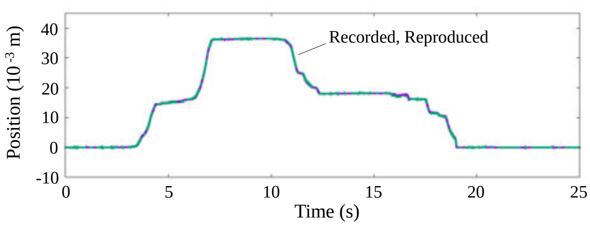

(i) Position responses of lifting axis.

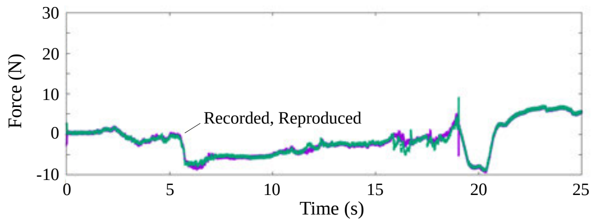

(j) Force responses of lifting axis.

Fig. 5-7: Experimental results of motion reproduction in case 1 for adaptive motion reproduction based on selection of motion components.

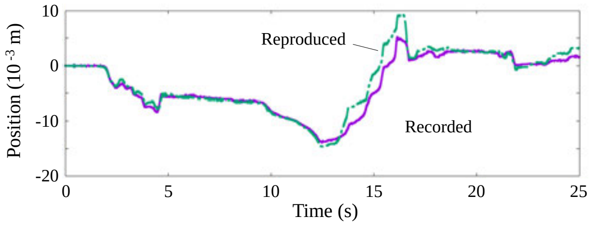

(a) Position responses of x axis.

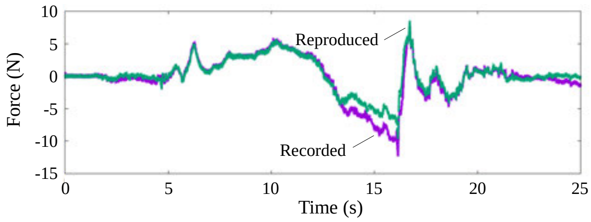

(b) Force responses of x axis.

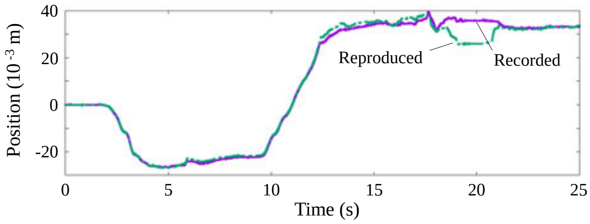

(c) Position responses of y axis.

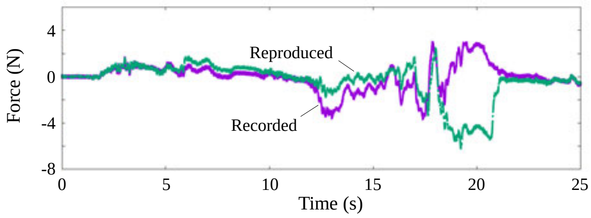

(d) Force responses of y axis.

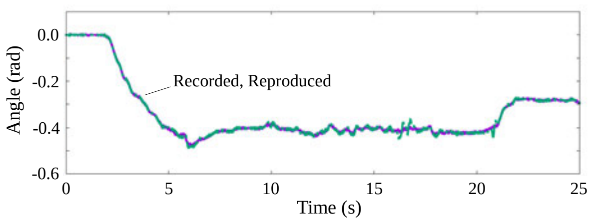

(e) Angle responses of rotation axis.

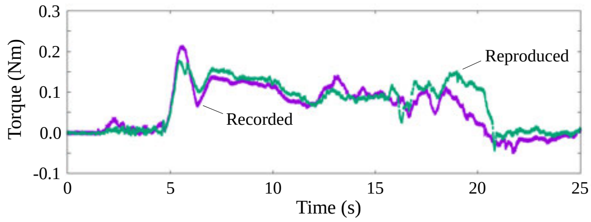

(f) Torque responses of rotation axis

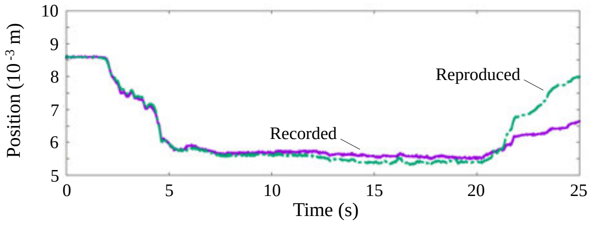

(g) Position responses of grasp axis.

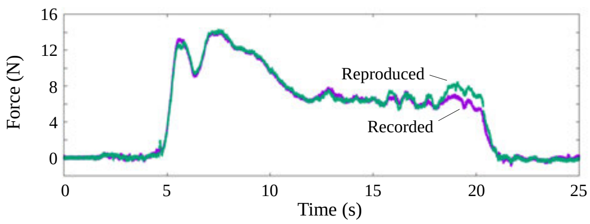

(h) Force responses of grasp axis.

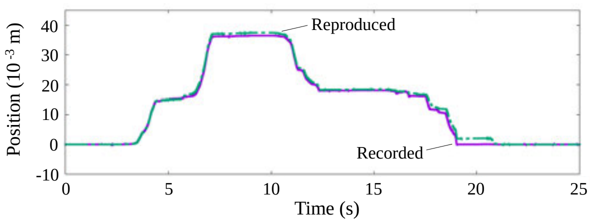

(i) Position responses of lifting axis.

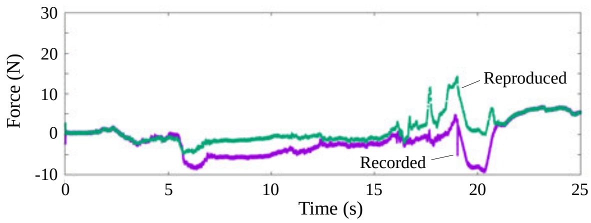

(j) Force responses of lifting axis.

Fig. 5-8: Experimental results of motion reproduction in case 2 for adaptive motion reproduction based on selection of motion components.

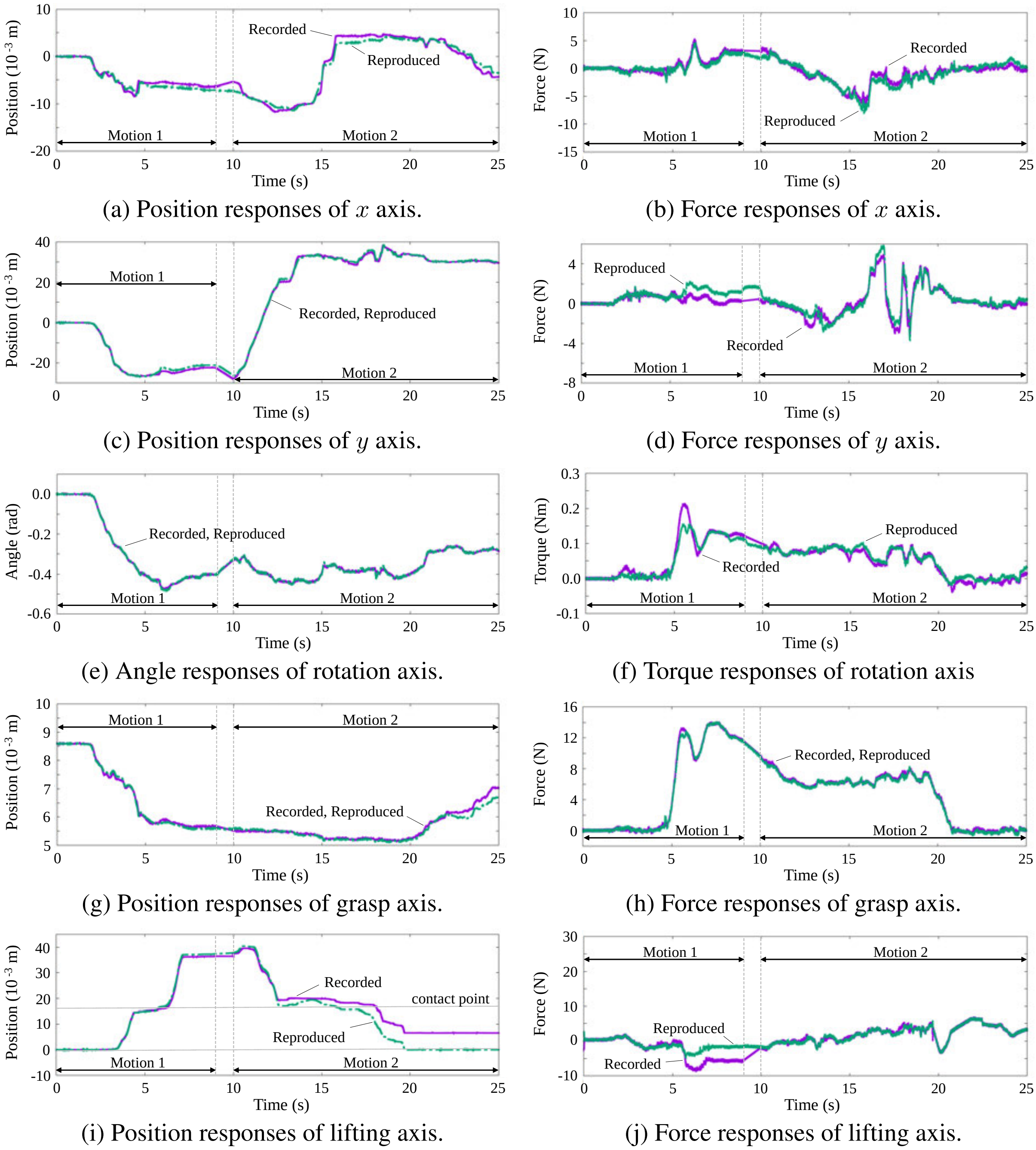

(a) Position responses of x axis.

(b) Force responses of x axis.

(c) Position responses of y axis.

(d) Force responses of y axis.

(e) Angle responses of rotation axis.

(f) Torque responses of rotation axis

(g) Position responses of grasp axis.

(h) Force responses of grasp axis.

(i) Position responses of lifting axis.

(j) Force responses of lifting axis.

Fig. 5-9: Experimental results of motion reproduction in case 3 for adaptive motion reproduction based on selection of motion components.

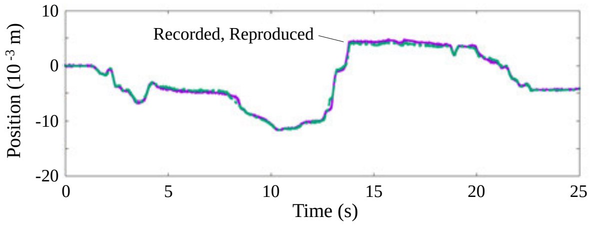

(a) Position responses of x axis.

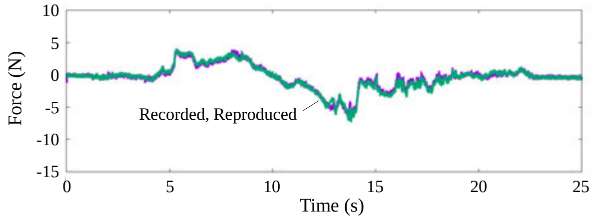

(b) Force responses of x axis.

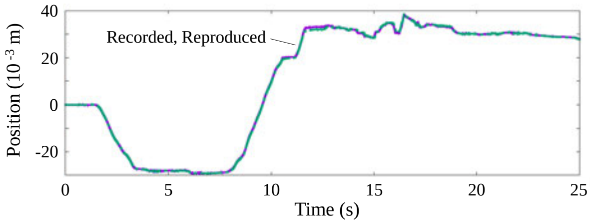

(c) Position responses of y axis.

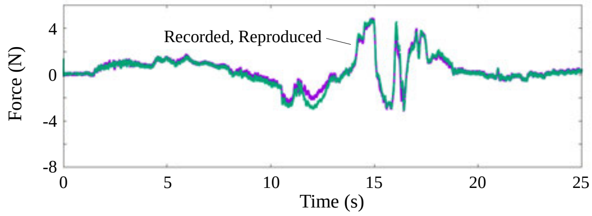

(d) Force responses of y axis.

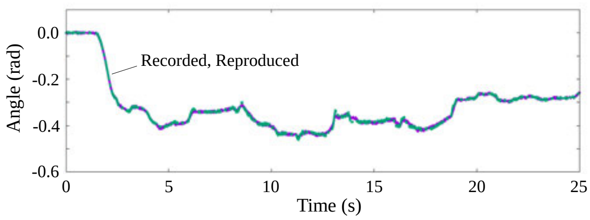

(e) Angle responses of rotation axis.

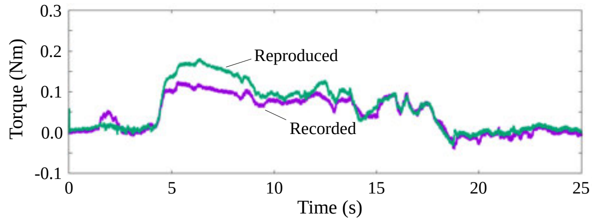

(f) Torque responses of rotation axis

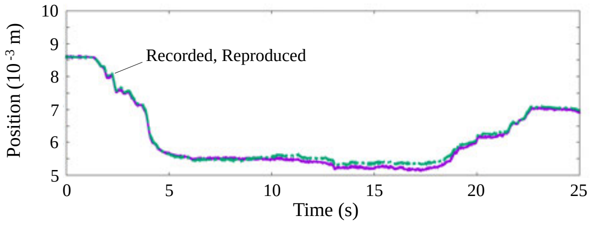

(g) Position responses of grasp axis.

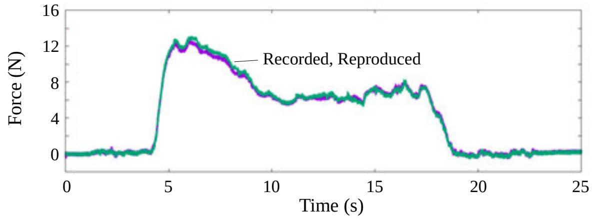

(h) Force responses of grasp axis.

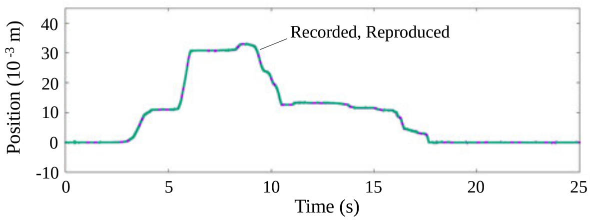

(i) Position responses of lifting axis.

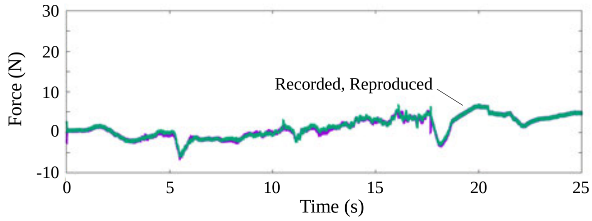

(j) Force responses of lifting axis.

Fig. 5-10: Experimental results of motion reproduction in case 4 for adaptive motion reproduction based on selection of motion components.

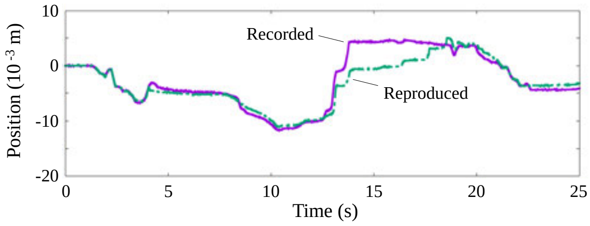

(a) Position responses of x axis.

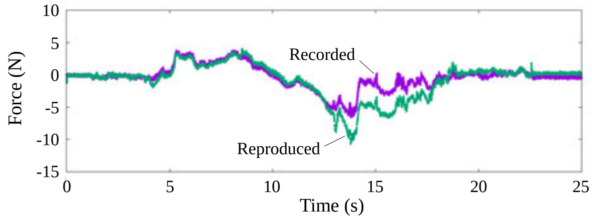

(b) Force responses of x axis.

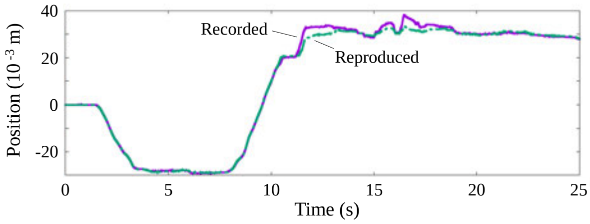

(c) Position responses of y axis.

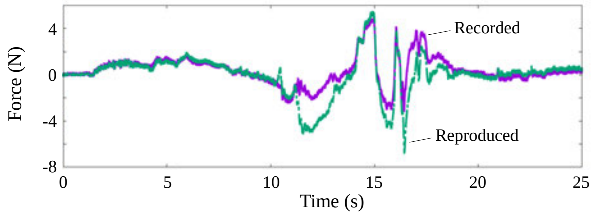

(d) Force responses of y axis.

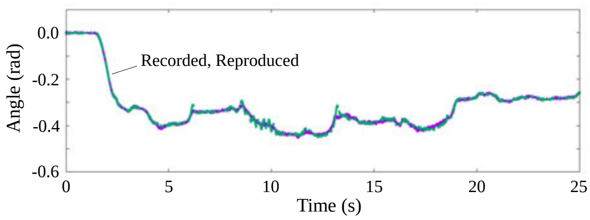

(e) Angle responses of rotation axis.

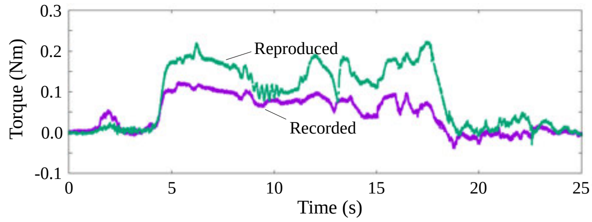

(f) Torque responses of rotation axis

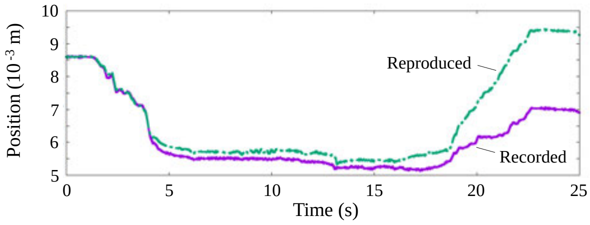

(g) Position responses of grasp axis.

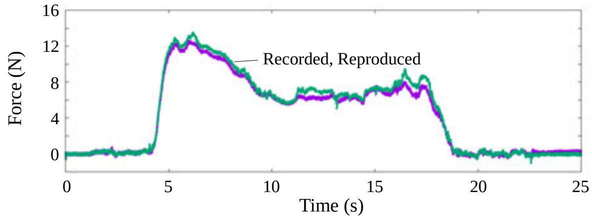

(h) Force responses of grasp axis.

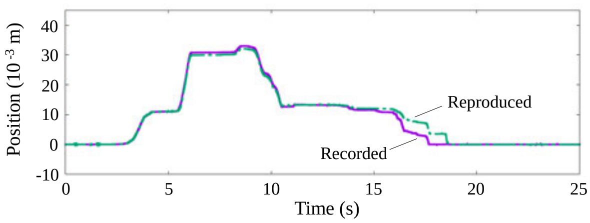

(i) Position responses of lifting axis.

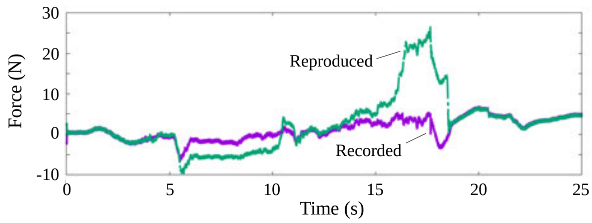

(j) Force responses of lifting axis.

Fig. 5-11: Experimental results of motion reproduction in case 5 for adaptive motion reproduction based on selection of motion components.

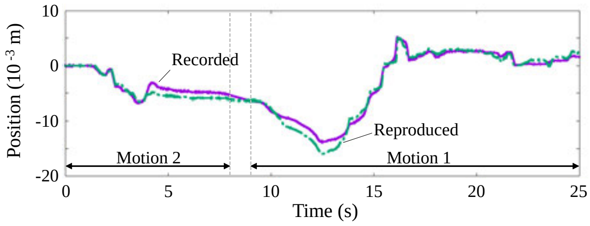

(a) Position responses of x axis.

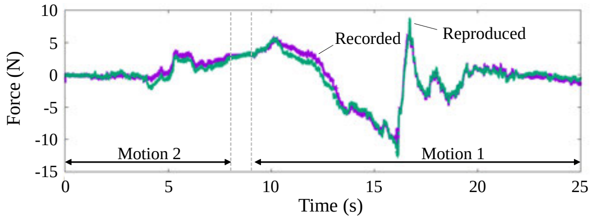

(b) Force responses of x axis.

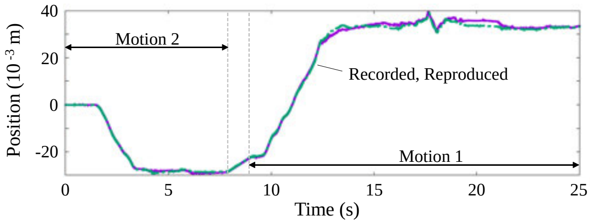

(c) Position responses of y axis.

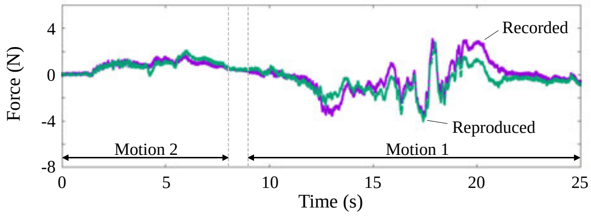

(d) Force responses of y axis.

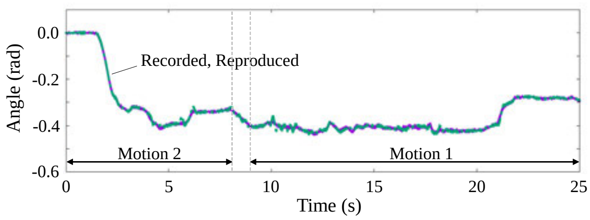

(e) Angle responses of rotation axis.

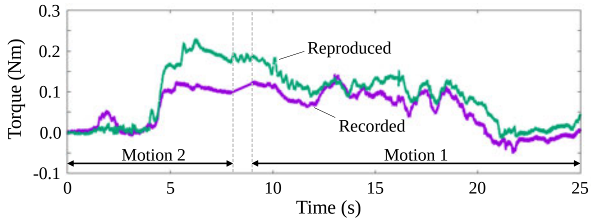

(f) Torque responses of rotation axis

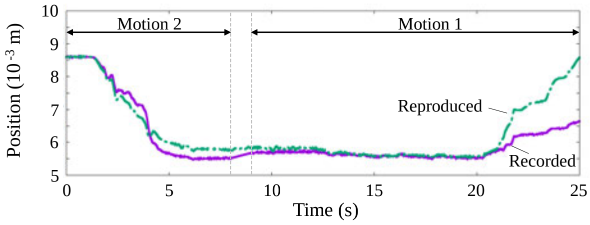

(g) Position responses of grasp axis.

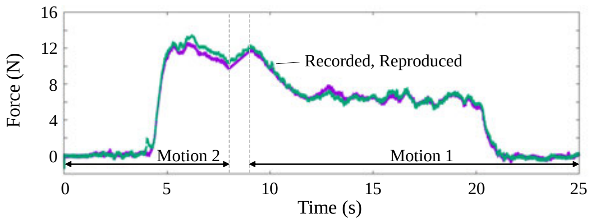

(h) Force responses of grasp axis.

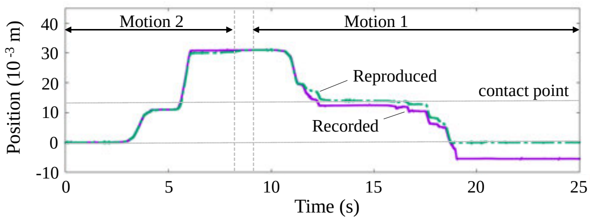

(i) Position responses of lifting axis.

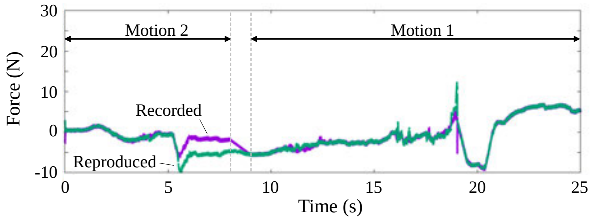

(j) Force responses of lifting axis.

Fig. 5-12: Experimental results of motion reproduction in case 6 for adaptive motion reproduction based on selection of motion components.

5.3 Summary

In this chapter, motion reproduction with the different target object was achieved by coupling the motion elements. The application of this chapter was "peg-in-hole," which is the same application as section 4.3. By selecting and changing the motion elements according to the target environment during motion reproduction, the goal of the task was achieved. In order to connect two motions, the control design for each motion axis which has different feature was shown. In this chapter, it was confirmed that the proposed methods of chapters 2–4 were able to be implemented in each axis at the same time. The validity of the proposed method was shown by the experimental results.

In this chapter, it was assumed that the target object in the motion reproduction was the same as the target object which was used in the motion recording phase. Therefore, the recorded motion could be used directly. At the general application, the target object is not always the same as them of the recorded motions. In this case, it is expected that the nearest motion is selected and the adaptation method like as the method described in section 4.3 is applied to the second motion at the same time.

Finally, the expected flow of the motion reproduction is discussed. Fig. 5-13 shows the expected flow of the motion reproduction. First, the system calculates error between the reproducing motion information and the actual reproduced response. Then, the system decides which motion element is suitable to be reproduced, and if necessary the system changes the motion element. In order to change motion element, reproduction method is selected according to the feature of the axis, and the coupling method is selected according to the data format of the reproduction method. If the motion element is a suitable one but error still occurs, the system applies the adaptive method against environmental difference. In this way, the required task will be achieved. In the section 5.2, the simple case of the left side of Fig. 5-13 was carried out. However, it is expected in future to improve each process elements such as judging the motion result, recognizing the motion, searching and deciding the motion elements, applying adaptive method, and so on.

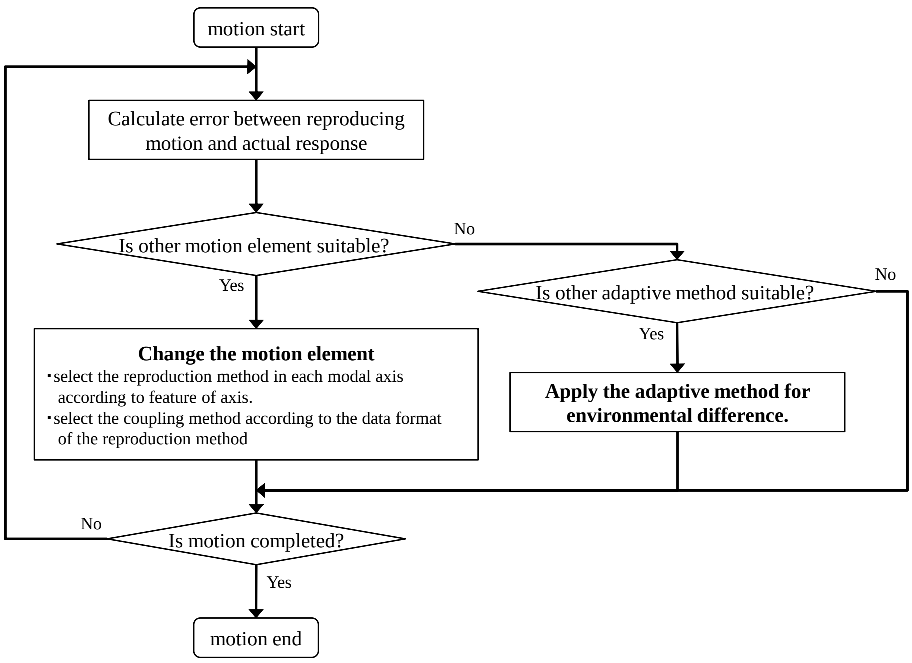

Fig. 5-13: Expected motion reproduction flow.

Chapter 6

Conclusions

The purpose of this research was to expand the adaptability of the motion-copying system. In this thesis, the author researched based on the following three points of view in order to apply the motion-copying system to various applications in future,

- motion recording and reproduction in multi-DOF system;
- integrated reproduction of motion components;
- adaptation for difference of environment.

In chapter 2, the control spaces to deal with the information of the motion were discussed. In order to apply the motion-copying system to multi-DOF applications, the motion data should be dealt with in common coordinate. The work space is one of the common coordinates which does not depend on the structures of the devices. In other words, the information in the actuator space is abstracted by transforming to the work space. Therefore, the motion-copying system was implemented in the work space first. Then, the human modal space and the motion modal space were introduced to specialize motion data for applications. The control spaces should be selected according to the application, and it was expressed as "specialization" in this thesis. The human modal space was introduced to treat human motion on the basis of the human model. It was assumed that an exoskeleton haptic device is used in motion recording and an endoskeleton haptic device is used in motion reproduction. On the other hand, the motion modal space was introduced to separate motion elements from human motion. By this transformation, the adequate control methods can be implemented in each motion element. By the proposed methods, the recorded motion can be reproduced even if the structures of the devices are different.

In chapter 3, the integrated reproduction of motion components were proposed. The purpose of chapter 3 was that one motion was reproduced from some motion components by connecting them time series. In chapter, 2 connecting methods were proposed. These methods depend on the format of motion data. One of the methods can be applied to the case when the motion information is on the basis of position and force information. In this method, position and force information of two motions ware interpolated to maintain continuousness. The other method can be applied to the case when the motion information is on the basis of acceleration information. In this method, equivalent velocities of the two motions were connected by adding acceleration between two motions. By these methods, it is expected to reproduce many motions by combining motion components.

In chapter 4, the methods to reproduce recorded task even if the environmental conditions are different between the motion recording and the motion reproducing. In this chapter, two types of the difference of the environmental condition were discussed. One of them was difference of the environmental location. The other one was difference of the target environmental material, which included weight and friction differences. First, the motion reproduction method when target environmental size is different was proposed. By using acceleration information as the motion information, the reproduction which is not according to base point was achieved. Then, the motion reproduction method when the target environmental material is different was proposed. By omitting the effect from the difference of the target environment, the common force which does not depend on the target object was achieved. By these methods, it is expected to reproduce the motion by the motion which is same task but for different environment.

Finally in chapter 5, the proposed methods were implemented in each motion modal axis at the same time. In other words, this chapter was culmination of this thesis. The motion reproduction with the different target object under the application of "peg-in-hole" was achieved by coupling the motion elements. Here, the recorded task was achieved by selecting and changing the motion elements according to the target environment during motion reproduction. The design method how to select the reproduction method according to the characteristics of the motion axis and how to select the coupling method according to the reproduction method is described. In addition, we discussed the expected motion reproduction flow.

The validities of the each proposed method were verified by each experimental result. The motion-copying system becomes more useful by the research described in this thesis, and it is expected to be applied to preserve the expert motions in the industrial processing and so on. Furthermore, the haptic recording will be able to be utilized in our lives such as the audio recording and the visual recording.

Future Work of Motion-Copying System

In this section, the challenges for the future application of the motion-copying system are described. We discussed here on the basis of three view points; i) to improve the reproduction performance; ii) to use motion data as media contents; iii) to know what human motion is. In other words, they are the view points of control engineering, computer science, and ergonomics.

In order to improve the reproduction performance, we introduce several research fields. First, the reproduction method adapting to the environmental difference is required. Almost of the proposed methods in this thesis is included in this research field. However, the many cases that the motion-copying system cannot reproduce the recorded motion still exist. In particular, there are some researches to focus the external environmental difference, but there are few researches to focus the difference of the device own. In order to use the multi-degree-of-freedom system which is a different device from motion recording phase, the influence from the uncertainty of the device's structure will be the problem. For example, null space should be used to maintain the condition which does not affect the motion. In addition, it is required to integrate other information such as visual information. As described in section 2, human motion is a relative motion of the target environment. Therefore, the relative coordinate between the device and the external environment is necessary. It is little difficult to adapt external environment for the current motion-copying system, because it uses only information from the devices. In the future, it is hoped that the motion-copying system and vision based system are integrated and the system recognize the relation between the device and the external environment. Then, the reproduction control system is composed on the basis of the relative relation.

Then, we discuss how to construct and use the motion data. The one of the main purposes of the motion-copying system is to use the motion data like as audio and visual information. In order to use the motion data as media information, it is necessary to define the format of the data, to compress the data, and so on. For example, the current motion data of the motion-copying system is too large. In order to transmit, reserve, and reproduce the multi-degree-of-freedom motion data, it will be necessary to achieve the precise motion reproduction from smaller data. Meanwhile, there are some methods which use the information other than position and force information. Hence, we should consider which kind of information to be recorded, and we should define the data format according to it.

Finally, the research field to know the human motion should be combined the motion-copying system. In particular, in order to apply the motion-copying system under the different environmental condition,

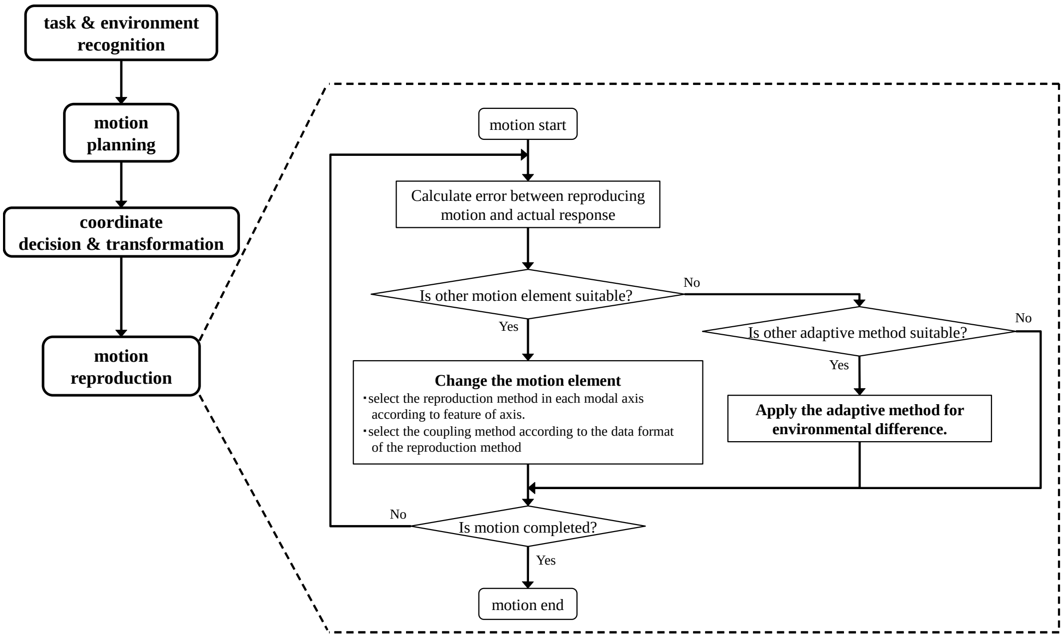

Fig. 6-1: Whole system of the task reproduction.

the goal of the motion and adequate reproduction method depend on the characteristic of the motion. For example in this thesis, time period to calculate the compensation value was decided by the author. However, it is expected that the system recognizes the characteristic of the motion, and the system decides when the compensation value should be calculated and when the compensation value should be added to the command. Meanwhile, how to associate the task with the motion elements is one of the important future works. It is expected to acquire the principal motion component of the "task," and to maintain the principal motion component in order to reproduce the "task" of the motion. In the motion-copying system, one of the most difficult problems is to define the control aim of the reproduction. There are many control methods to achieve the control aim, but it is difficult to turn out what the control aim is for the reproducing task. Therefore, it is necessary to analyze and recognize the characteristics of the human motion.

In this thesis, the methods about motion reproduction were described. However, it is not sufficient to achieve the task of the motion. The motion reproduction is the one part of the system of task reproduction. The whole system of the task reproduction is shown in Fig. 6-1. The system is composed of several layers. First, the system recognizes the task of the motion and the external environment which is the relation between the device and the target environment. Here, the study fields of the motion recognition or signature analysis of the motion are necessary. In addition, it is necessary to combine the other information such as visual servoing in order to know the relation between the system and external environment. Then, the system should carry out the motion planning to achieve the task of the motion under the condition of the device and the external environment. Here, the control aim of the reproducing motion is defined. After that, the system should select the coordinate to control the motion, and the system should transform the motion data according to the coordinate. Finally, the motion reproduction is carried out. The control aim is achieved by applying the reproduction methods. As mentioned above, several study fields should be integrated as one system in order to reproduce the intended task of the motion.

References

[1] K. Kosugea, T. Fukuda, and H. Asada : "Acquisition of Human Skills for Robotic System," *Proceedings of the 1991 IEEE International Symposium on Intelligent Control*, pp. 469–474, August, 1991.

[2] R. Watanabe and M. Hashimoto : "Automatic Description System of the Motion Procedure and Trajectories of Hands and Eye-gaze for Analysis of Assembly Work," *Journal of the Japan Society for Precision Engineering*, Vol. 82, No. 5, pp. 473–480, May, 2016. (in Japanese)

[3] X. Liang, H. Kato, N, Hashimoto, and K. Okawa : "High Efficiency Skill Training for Manual Welding Using Virtual Reality," *Journal of the Japan Society for Precision Engineering*, Vol. 80, No. 10, pp. 933–938, October, 2014. (in Japanese)

[4] H. Onda, H.Hirukawa, and K. Takase : "Assembly Motion Teaching System Using Position/Force Simulator - Extracting a Sequence of Contact State Transition," *Proceedings of IEEE/RSJ International Conference on Intelligent Robots and Systems 95*, pp. 9–16, August, 1995.

[5] H. Onda, H.Hirukawa, F. Tomita, T. Suehiro, and K. Takase : "Assembly Motion Teaching System Using Position/Force Simulator - Generating Control Program," *Proceedings of the 1997 IEEE/RSJ International Conference on Intelligent Robots and Systems, 1997. IROS '97*, pp. 1–8, September, 1997.

[6] V.B. Zoadan and J.K. Hodgins : "Motion Capture-Driven Simulations that Hit and React," *Proceedings of the 2002 ACM SIGGRAPH/Eurographics Symposium on Computer Animation*, pp. 89–96, July, 2002.

[7] L. Sigal, A.O. Balan, and M.J. Black : "HumanEva: Synchronized Video and Motion Capture Dataset and Baseline Algorithm for Evaluation of Articulated Human Motion," *International Journal of Computer Vision*, Vol. 87 No. 1–2, pp. 4–27, March, 2010.

[8] J. Rosado, F. Silva, V. Santos, and Z. Lu : 'Reproduction of Human Arm Movements Using Kinect-Based Motion Capture Data," *Proceedings of 2003 IEEE International Conference on Robotics and Biomimetics*, pp. 885–890, December, 2013.

[9] Y. Endo, M. Tada, and M. Mochimaru : "Reconstruction of Digital Hand Models for Individuals by Using Motion Capture System," *Journal of the Japan Society for Precision Engineering*, Vol. 79, No. 9, pp. 860–867, September, 2013. (in Japanese)

[10] Y. Kuniyoshi, M. Inaba, and H. Inoue : "Learning by Watching: Extracting Reusable Task Knowledge from Visual Observation of Human Performance," *IEEE Transactions on Robotics and Automation*, Vol. 10, No. 6, pp. 799–822, December, 1994.

[11] K. Ogawa, J. Takamatsu, H. Kimura, and K Ikeuchi : "Extraction of Essential Interactions Through Multiple Observations of Human Demonstrations," *IEEE Transactions on Industrial Electronics*, Vol. 50, No. 4, pp. 667–675, August, 2003.

[12] M. Skubic and R.A. Volz : "Acquiring Robust, Force-Based Assembly Skills from Human Demonstration," *IEEE Transactions on Robotics and Automation*, Vol. 16, No. 6, pp. 772–781, December, 2000.

[13] P. Kormushev, S. Calinon, and D.G. Caldwell : "Imitation Learning of Positional and Force Skills Demonstrated via Kinesthetic Teaching and Haptic Input," *Advanced Robotics*, Vol. 25, No. 5, pp. 581–603, April, 2011.

[14] A.E. Saddik : "The Potential of Haptics Technologies," *IEEE Instrumentation & Measurement Magazine*, Vol. 10, No. 1, pp. 10–17, February, 2007.

[15] A. Yamamoto, S. Nagasawa, H. Yamamoto, and T. Higuchi : "Electrostatic Tactile Display with Thin Film Slider and Its Application to Tactile Telepresentation Systems," *IEEE Transactions on Visualization and Computer Graphics*, Vol. 12, No. 2, pp. 168–177, March–April, 2006.

[16] K. Suwanratchatamanee. M. Matsumoto, and S. Hashimoto : "Robotic Tactile Sensor System and Applications," *IEEE Transactions on Industrial Electronics*, Vol. 57, No. 3, pp. 1074–1087, March, 2010.

[17] Y. Yokokohji, R.L. Hollis, T. Kanade, K, Henmi, and T. Yoshikawa : "Toward Machine Mediated Training of Motor Skills. Skill Transfer from Human to Human via Virtual Environment," *Proceedings of 5th IEEE International Workshop on Robot and Human Communication*, pp. 32–37, November, 1996.

[18] K. Henmi and T. Yoshikawa : "Virtual Lesson and Its Application to Virtual Calligraphy System," *Proceedings of the 1998 IEEE International Conference on Robotics and Automation*, pp. 1275–1280, May, 1998.

[19] R. Kikuuwe and T. Yoshikawa : "Haptic Display Device with Fingertip Presser for Motion/Force Teaching to Human," *Proceedings of 2001 ICRA. IEEE International Conference on Robotics and Automation*, pp. 868–873, May, 2001.

[20] S. Saga, N, Kawakami, and S. Tachi : "Haptic Teaching using Opposite Force Presentation," *Proceedings of 2005 World Haptics Conference*, p. 1, March, 2005.

[21] S. Saga, K. Vlack, H. Kajimoto, and S. Tachi : "Haptic Video," *Proceedings of the ACM SIGGRAPH 2005 Emerging technologies*, No. 7, p. 1, August, 2005.

[22] D. A. Lawrence : "Stability and Transparency in Bilateral Teleoperation," *IEEE Transactions on Robotics and Automation*, Vol. 9, No. 5, pp. 624–637, October, 1993.

[23] K. Hashtrudi-Zaad and S. E. Salcudean : "On the Use of Local Force Feedback for Transparent Teleoperation," *Proceedings of the 1999 IEEE International Conference on Robotics and Automation*, Vol. 3, pp. 1863–1869, May, 1999.

[24] Y. Yokokohji : "Control Theory of Master-Slave System," *Journal of the Robotics Society of Japan*, Vol. 11, No. 6, pp. 794–802, September, 1993. (in Japanese)

[25] T. Imaida and K. Senda : "Performance Improvement of the PD-based Bilateral Teleoperators with Time Delay by Introducing Relative D-control," *Advanced Robotics*, Vol. 29, No. 6, pp. 385–400, March, 2015.

[26] K. Furuta, K. Kosuge, Y. Shiote, and H. Hatano : "Master-slave Manipulator Based on Virtual Internal Model Following Control Concept," *Proceedings of the 1987 IEEE International Conference on Robotics and Automation*, pp. 567–572, March, 1987.

[27] S. Tachi and T. Sakaki : "Impedance Controlled Master Slave Manipulation System Part I: Basic Concept and Application to the System with a Time Delay," *Journal of the Robotics Society of Japan*, Vol. 8, No. 3, pp. 241–252, June, 1990. (in Japanese)

[28] A. Sabanovic : "SMC Framework in Motion Control Systems," *International Journal of Adaptive Control and Signal Processing*, Vol. 21, No. 8-9, pp. 731–744, October–November, 2007.

[29] S. Khan, A. Sabanovic, and A. O. Nergiz : "Scaled Bilateral Teleoperation Using Discrete-Time Sliding-Mode Controller," *IEEE Transactions on Industrial Electronics*, Vol. 56, No. 9, pp. 3609–3618, September, 2009.

[30] A. Sabanovic, M. Elitas, and K. Ohnishi : "Sliding Modes in Constrained Systems Control," *IEEE Transactions on Industrial Electronics*, Vol. 55, No. 9, pp. 3332–3339, September, 2008.

[31] L. Bate, C.D. Cook, and Z. Li : "Reducing Wave-Based Teleoperator Reflections for Unknown Environments," *IEEE Transactions on Industrial Electronics*, Vol. 58, No. 2, pp. 392–397, February, 2011.

[32] A.F. Villaverde, A.B. Blas, J. Carrasco, and A.B. Torrico : "Reset Control for Passive Bilateral Teleoperation," *IEEE Transactions on Industrial Electronics*, Vol. 58, No. 7, pp. 3037–3045, July, 2011.

[33] S. Katsura, W. Iida, and K. Ohnishi : "Medical Mechatronics - An Application to Haptic Forceps," *IFAC Annual Reviews in Control*, Vol. 29, No. 2, pp. 237–245, November, 2005.

[34] W. Iida and K. Ohnishi : "Reproducibility and Operationality in Bilateral Teleoperation," *Proceedings of the 8th IEEE International Workshop on Advanced Motion Control, AMC 2004*, pp. 217–222, March, 2004.

[35] K. Ohnishi, M. Shibata, and T. Murakami : "Motion Control for Advanced Mechatronics," *IEEE/ASME Transactions on Mechatronics*, Vol. 1, No. 1, pp. 56–67, March, 1996.

[36] K. Ohnishi : "Robust Motion Control by Disturbance Observer", *Journal of the Robotics Society of Japan*, Vol. 11, No. 4, pp. 486–493, May, 1993. (in Japanese)

[37] W.S. Huang, C.W. Liu, P.L. Hsu, and S.S. Yeh : "Precision Control and Compensation of Servomotors and Machine Tools via the Disturbance Observer," *IEEE Transactions on Industrial Electronics*, Vol. 57, No. 1, pp. 420–429, January, 2010.

[38] S. Katsura, K. Irie, and K. Ohishi : "Wideband Force Control by Position-Acceleration Integrated Disturbance Observer," *IEEE Transactions on Industrial Electronics*, Vol. 55, No. 4, pp. 1699–1706, April, 2008.

[39] T. Murakami, F. Yu, and K. Ohnishi : "Torque Sensorless Control in Multidegree-of-Freedom Manipulator," *IEEE Transactions on Industrial Electronics*, Vol. 40, No. 2, pp. 259–265, April, 1993.

[40] T. Murakami, R. Nakamura, F. Yu, and K. Ohnishi : "Force Sensorless Compliant Control Based on Reaction Force Estimation Observer in Multi-Degrees-of-Freedom Robot", *Journal of the Robotics Society of Japan*, Vol. 11, No. 5, pp. 765–768, July, 1993.

[41] M. Mizuochi, T. Tsuji, and K. Ohnishi : "Multirate Sampling Method for Acceleration Control System," *IEEE Transactions on Industrial Electronics*, Vol. 54, No. 3, pp. 1462–1471, June, 2005.

[42] S. Katsura, Y. Matsumoto, and K. Ohnishi : "Analysis and Experimental Validation of Force Bandwidth for Force Control," *IEEE Transactions on Industrial Electronics*, Vol. 53, No. 3, pp. 922–928, June, 2006.

[43] S. Katsura, Y. Matsumoto, and K. Ohnishi : "Modeling of Force Sensing and Validation of Disturbance Observer for Force Control," *IEEE Transactions on Industrial Electronics*, Vol. 54, No. 1, pp. 530–538, February, 2007.

[44] C. Mitsantisuk. S. Katsura, and K. Ohishi : "Force Control of Human-Robot Interaction Using Twin Direct-Drive Motor System Based on Modal Space Design," *IEEE Transactions on Industrial Electronics*, Vol. 57, No. 4, pp. 1383–1392, April, 2010.

[45] T. Miyagi and S. Katsura : "Design of Friction Compensation Filter in Frequency Domain by Spectral Envelope for Sensor-less Force Control," *Journal of the Japan Society for Precision Engineering*, Vol. 80, No. 8, pp. 792–798, August, 2014. (in Japanese)

[46] K. Natori and K. Ohnishi : "A Design Method of Communication Disturbance Observer for Time-Delay Compensation, Taking the Dynamic Property of Network Disturbance Into Account," *IEEE Transactions on Industrial Electronics*, Vol. 55, No. 5, pp. 2152–2168, May, 2008.

[47] K. Natori, T. Tsuji, K. Ohnishi, A. Hace, and K Jezernik : "Time-Delay Compensation by Communication Disturbance Observer for Bilateral Teleoperation Under Time-Varying Delay," *IEEE Transactions on Industrial Electronics*, Vol. 57, No. 3, pp. 1050–1062, March, 2010.

[48] D. Yashiro and K. Ohnishi : "Performance Analysis of Bilateral Control System With Communication Bandwidth Constraint," *IEEE Transactions on Industrial Electronics*, Vol. 58, No. 2, pp. 436–443, February, 2011.

[49] T. Shimono, S. Katsura, S. Susa, T. Takei, and K. Ohnishi : "Transmission of Force Sensation by Micro-Macro Bilateral Control with Respect to Standardized Modal Space," *Proceedings of the 4th IEEE International Conference on Mechatronics, ICM 2007*, pp. 1–6, May, 2007.

[50] S. Sakaino, T. Sato, and K. Ohnishi : "Oblique Coordinate Control for Advanced Motion Control - Applied to Micro-Macro Bilateral Control -," *IEEE International Conference on Mechatronics, ICM 2009*, pp. 1–6, April, 2009.

[51] M. Sitti, B. Aruk, H. Shintani and H. Hashimoto : "Development of a Scaled Teleoperation System for Nano Scale Interaction and Manipulation," *Proceedings of the 2001 IEEE International Conference on Robotics and Automation, ICRA 2001*, Vol. 1, pp. 860–867, May, 2001.

[52] K. Ohnishi, T. Shimono, and K. Natori : "Haptics for Medical Applications," *Artificial Life and Robotics*, Vol. 13, No. 2, pp. 383–389, March, 2009.

[53] H. Tanaka, K. Ohnishi, H. Nishi, T. Kawai, Y. Morisawa, S. Ozawa, and T. Furukawa : "Implementation of Bilateral Control System Based on Acceleration Control Using FPGA for Multi-DOF Haptic Endoscopic Surgery Robot," *IEEE Transactions on Industrial Electronics*, Vol. 56, No. 3, pp. 618–627, March, 2009.

[54] W. Yamanouchi, S. Katsura, and K. Ohishi : "Bilateral Force Feedback Control with Different Configurations based on Dimensional Scaling for Realization of Mobile-Hapto," *IEEJ Transactions on Industry Applications*, Vol. 131-D, No. 2, pp. 180–186, February, 2011. (in Japanese)

[55] W. Yamanouchi and S. Katsura : "Tele-Operation of a Mobile Haptic System Using Dynamical Modal Transformation," *IEEJ Transactions on Industry Applications*, Vol. 132-D, No. 3, pp. 315–321, March, 2012. (in Japanese)

[56] S. Katsura, Y. Matsumoto, and K. Ohnishi : "Realization of "Law of Action and Reaction" by Multilateral Control," *IEEE Transactions on Industrial Electronics*, Vol. 52, No. 5, pp. 1196–1205, October, 2005.

[57] S. Katsura, T. Suzuyama, and K. Ohishi : "A Realization of Multilateral Force Feedback Control for Cooperative Motion," *IEEE Transactions on Industrial Electronics*, Vol. 54, No. 6, pp. 3298–3306, December, 2007.

[58] S. Katsura : "Multilateral Force Feedback Control," *Journal of the Robotics Society of Japan*, Vol. 27, No. 4, pp. 28–31, May, 2009. (in Japanese)

[59] C. Mitsantisuk, S. Katsura, and K. Ohishi : "Kalman-Filter-Based Sensor Integration of Variable Power Assist Control Based on Human Stiffness Estimation," *IEEE Transactions on Industrial Electronics*, Vol. 56, No. 10, pp. 3897–3905, October, 2009.

[60] Y. Can-Jun, N. Bin, and C. Ying : "Adaptive Neuro-Fuzzy Control Based Development of a Wearable Exoskeleton Leg for Human Walkingmentation," *Proceedings of IEEE/ASME International Conference on Advanced Intelligent Mechatronics*, pp. 467–472, July, 2005.

[61] W. Yamanouchi and S. Katsura : "Variable Time-Space Compliance Control for Human Support," *Proceedings of the 36th Annual Conference of the IEEE Industrial Electronics Society, IECON'10-PHOENIX*, pp. 2093–2098, November, 2010.

[62] Y. Yang, L. Wang, J. Tong, and L. Zhang : "Arm Rehabilitation Robot Impedance Control and Experimentation," *Proceedings of the 2006 IEEE international Conference on Robotics and Biomimetics, ROBIO'06*, pp. 914–918, December, 2006.

[63] T. Shimono, S. Katsura, and K. Ohnishi : "Abstraction and Reproduction of Force Sensation From Real Environment by Bilateral Control," *IEEE Transactions on Industrial Electronics*, Vol. 54, No. 2, pp. 907–918, April, 2007.

[64] Y. Yokokura and S. Katsura : "Representation of Haptic Environment by Using Spatial Laplace Operator," *Proceedings of the 8th France-Japan and 6th Europe-Asia Congress on Mechatronics, MECATRONICS'10-YOKOHAMA*, pp. 355–360, November, 2010.

[65] Y. Yokokura, S. Katsura, K. Ohishi : "Stability Analysis and Experimental Validation of a Motion-Copying System," *IEEE Transactions on Industrial Electronics*, Vol. 56, No. 10, pp. 3906–3913, October, 2009.

[66] Y. Yokokura and S. Katsura : "Adaptive Motion-Copying System Based on Real-World Haptics," *Proceedings of the 36th Annual Conference of the IEEE Industrial Electronics Society, IECON'10-PHOENIX*, pp. 1228–1233, November, 2010.

[67] S. Yajima and S. Katsura : "Multi-DOF Motion Reproduction Using Motion-Copying System With Velocity Constraint," *IEEE Transactions on Industrial Electronics*, Vol. 61, No. 7, pp. 3765–3775, October, 2013.

[68] R. Honjo and S. Katsura : "Multi-Degree-of-Freedom Motion-Copying System Considering Variation in Friction," *IEEJ Journal of Industry Applications*, Vol. 4, No. 3, pp. 262–267, May, 2015.

[69] T. Nozaki, T Mizoguchi, and K. Ohnishi : "Motion-Copying System with Variable-Impedance based on Scaled Bilateral Control in One Degree of Freedom Robot," *IEEJ Journal of Industry Applications*, Vol. 3, No. 1, pp. 1–9, January, 2014.

[70] E. Sariyildiz and K. Ohnishi : "Stability and Robustness of Disturbance Observer based Motion Control Systems," *IEEE Transactions on Industrial Electronics*, Vol. 62, No. 1, pp. 414–422, January, 2015.

[71] Y. Yokokura, S. Katsura, and K. Ohishi : "Motion Copying System Based on Real-World Haptics in Variable Speed," *Proceedings of the 13th Power Electronics and Motion Control Conference, EPE-PEMC 2008*, pp. 1604–1609, September, 2008.

[72] Y. Kobayashi and S. Katsura : "Processed Control of Haptic Information on Environmental Surface by Haptic Scanner," *ICROS-SICE International Joint Conference 2009, ICCAS-SICE 2009-FUKUOKA*, pp. 223–228, August, 2009.

[73] K. Igarashi and S. Katsura : "Motion-Data Processing and Reproduction Based on Motion-Copying System," *IEEJ Journal of Industry Applications*, Vol. 4, No. 5, pp. 543–549, September, 2015.

[74] Y. Yokokura, S. Katsura, and K. Ohishi : "A Realization of Motion Copying System Based on Multilateral Control," *IEEJ Transactions on Industry Applications*, Vol. 128-D, No. 9, pp. 1140–1146, September, 2008. (in Japanese)

[75] T. Ishii and S. Katsura : "Construction of Haptic Transmission Network for Haptic Broadcasting by Articulated Multilateral Control," *IEEJ Transactions on Industry Applications*, Vol. 131-D, No. 3, pp. 343–349, March, 2011. (in Japanese)

[76] H. Tanaka and K. Ohnishi : "Haptic Data Compression/Decompression Using DCT for Motion Copy System," *IEEE International Conference on Mechatronics, ICM 2009*, pp. 1–6, April, 2009.

[77] H. Tanaka and K. Ohnishi : "Lossy Compression of Haptic Data by Using DCT," *IEEJ Transactions on Industry Applications*, Vol. 130-D, No. 8, pp. 945–952, August, 2010. (in Japanese)

[78] Y. Kasahara, K. Ohnishi, K. Nagase, and S. Katsura : "Reduction of Motion Data by Using Motion Assembly System for Haptic Database," *IEEJ Transactions on Industry Applications*, Vol. 130-D, No. 9, pp. 1043–1050, September, 2010. (in Japanese)

[79] Y. Yokokura and S. Katsura : "Construction of Motion Database Based on Real-World Haptics," *IEEJ Transactions on Industry Applications*, Vol. 131-D, No. 3, pp. 319–326, March, 2011. (in Japanese)

[80] Y. Ohnishi and S. Katsura : "Modeling of Multi-Degree-of-Freedom Motions for Motion Database," *IEEJ Transactions on Industry Applications*, Vol. 132-D, No. 7, pp. 747–754, July, 2012. (in Japanese)

[81] N. Tsunashima, Y. Yokokura, and S. Katsura : "Saving and Reproduction of Human Motion Data by Using Haptic Devices with Different Configurations," *IEEJ Transactions on Industry Applications*, Vol. 131-D, No. 3, pp. 267–274, March, 2011. (in Japanese)

[82] N. Tsunashima and S. Katsura : "Reproduction of Human Motion Using Different Structual Haptic System," *Proceedings of the 27th Annual Conference of the Robotics Society of Japan, RSJ 2009, Yokohama*, pp. 1–4, September, 2009. (in Japanese)

[83] N. Tsunashima and S. Katsura : "Integrated Reproduction of Human Motion Components by Motion Copying System," *IEEJ Transactions on Industry Applications*, Vol. 130-D, No. 4, pp. 436–442, April, 2010. (in Japanese)

[84] N. Tsunashima and S. Katsura : "Continuous Integration of Motion Components Using Motion Copying System," *Proceedings of ICROS-SICE International Joint Conference 2009, ICCAS-SICE 2009-FUKUOKA*, pp. 1563–1568, August, 2009.

[85] N. Tsunashima and S. Katsura : "Spatiotemporal Coupler: Storage and Reproduction of Human Finger Motions," *IEEE Transactions on Industrial Electronics*, Vol. 59, No. 2, pp. 1074–1085, February, 2012

[86] N. Tsunashima and S. Katsura : "Reproduction of Integrated Motions Based on Haptic Recording," *Proceedings of the 2010 Annual Meeting of the Institute of Electrical Engineers of Japan*, Vol. 4, pp. 283–284, March, 2010. (in Japanese)

[87] T. Sato, S. Sakaino, and K. Ohnishi : "Motion Reproduction System with Haptic Information for Different Environment Location," *Proceedings of the 35th Annual Conference of the IEEE Industrial Electronics Society, IECON'09*, pp. 1651–1656, November, 2009.

[88] T. Nozaki, T. Mizoguchi, and K. Ohnishi : "Motion-copying System with Variable Impedance based on Scaled Bilateral Control in One-degree-of-freedom Robot," *IEEJ Journal of Industry Applications*, Vol. 3, No. 1, pp. 1–9, January, 2014.

[89] Y. Yokokura, S. Katsura, and K. Ohishi : "Stability Analysis and Experimental Validation of a Motion-Copying System," *IEEE Transactions on Industrial Electronics*, Vol. 56, No. 10, pp. 3906–3913, July, 2009.

[90] Y. Nagatsu and S. Katsura : "Design Strategies for Motion Reproduction Based on Environmental Disturbance Compensation," *IEEE Transactions on Industrial Electronics*, Vol. 62, No. 9, pp. 5786–5798, September, 2015.

[91] N. Tsunashima and S. Katsura : "Reproduction of Real-World Human Motion by Motion Copying System Based on Acceleration Information," *2009 Annual Conference of I.E.E of Japan. Industry Application Society, JIASC'09-Mie*, pp. 331–336, August, 2009. (in Japanese)

[92] N. Tsunashima, Y. Yokokura, and S. Katsura : "Reproduction of Linear Motion with Adaptation for Change in Environmental Position," *IEEJ Transactions on Industry Applications*, Vol. 132-D, No. 5, pp. 526–533, March, 2011. (in Japanese)

[93] N. Tsunashima and S. Katsura : "Reproduction of Human Motion Using Motion-Copying System Based on Coordinate Modification," *Proceedings of the 36th Annual Conference of the IEEE Industrial Electronics Society, IEEE IECON 2010-PHOENIX*, pp. 1609–1614, November, 2010.

[94] N. Tsunashima and S. Katsura : "Reproduction of Contact Motion Using Motion-Copying System Based on Spatiotemporal Disturbance Compensation," *2010 Annual Conference of I.E.E of Japan. Industry Application Society, JIASC10-Tokyo*, pp. 455–460, August, 2010. (in Japanese)

[95] N. Tsunashima and S. Katsura : "Adjustable Motion Reproduction for Transferring Different Objects Using Hybrid Position/Force Control," *Journal of the Japan Society for Precision Engineering*, 2017. (accepted) (in Japanese)

[96] A. Vakanski, I. Mantegh, A.Irish, and F.I. Sharifi : "Trajectory Learning for Robot Programming by Demonstration Using Hidden Markov Model and Dynamic Time Warping," *IEEE Transactions on Systems, Man, and Cybernetics, Part B (Cybernetics)*, Vol. 42, No. 4, pp. 1039–1052, August, 2012.

[97] S. Wu and Y.F. Li : "Motion Trajectory Reproduction from Generalized Signature Description," *The Journal of the Pattern Recognition Society*, Vol. 43, No. 1, pp. 204–221, January, 2010.

[98] S. Katsura and K. Ohnishi : "Quarry of Modal Information from Environment for Advanced Motion Control," *IEEJ Transactions on Industry Applications*, Vol. 126-D, No. 4, pp. 372–378, April, 2006.

[99] S. Katsura and K. Ohishi : "Modal System Design of Multirobot Systems by Interaction Mode Control," *IEEE Transactions on Industrial Electronics*, Vol. 54, No. 3, pp. 1537–1546, June, 2007.

[100] V. Bundhoo and E.J. Park : "Design of an Artificial Muscle Actuated Finger towards Biomimetic Prosthetic Hands," *Proceedings of the 12th International Conference on Advanced Robotics, ICAR'05*, pp. 368–375, July, 2005.

[101] T. Tsuji, K. Ohnishi, and A. Sabanovic : "A Controller Design Method Based on Functionality," *IEEE Transactions on Industrial Electronics*, Vol. 54, No. 6, pp. 3335–3343, December, 2007.

[102] S. Hyodo and K. Ohnishi : "A Method for Motion Abstraction Based on Haptic Information Directionality and an Application to Haptic Motion Display System," *IEEE Transactions on Industrial Electronics*, Vol. 56, No. 5, pp. 1356–1363, May, 2009.

[103] T. Murakami and K. Ohnishi : "A study of Stability and Workspace Decoupling Control Based on Robust Control in Multi-degrees-of-freedom Robot," *IEEJ Transactions on Industry Applications*, Vol. 113, No. 5, pp. 639–646, May, 1993.

[104] T. Shibata and T. Murakami : "Null Space Motion Control by PID Control Considering Passivity in Redundant Manipulator," *IEEE Transactions on Industrial Informatics*, Vol. 4, No. 4, pp. 261–270, November, 2008.

[105] P.K.W. Abeygunawardhana and T. Murakami : "Vibration Suppression of Two-Wheel Mobile Manipulator Using Resonance-Ratio-Control-Based Null-Space Control," *IEEE Transactions on Industrial Electronics*, Vol. 57, No. 12, pp. 4137–4146, December, 2010.

[106] T. Inamura, I. Toshima, and Y. Nakamura : "Acquisition and Embodiment of Motion Elements in Closed Mimesis Loop," *Proceedings. ICRA '02. IEEE International Conference on Robotics and Automation, 2002*, pp. 1539–1544, May, 2002.

[107] M. Do, P. Azad, T. Asfour, and R. Dillmann : "Imitation of Human Motion on a Humanoid Robot Using Non-Linear Optimization," *Proceedings of 8th IEEE-RAS International Conference on Humanoid Robots, 2008. Humanoids 2008*, pp. 545–552, December, 2008.

[108] M. Muhlig, M. Gienger, and J.J. Steil : "Interactive imitation learning of object movement skills," *Autonomous Robotics*, Vol. 32, No. 2, pp. 97–114, February, 2012.

[109] K. Ohishi, M. Miyazaki, and M. Fujita : "Hybrid Control of Force and Position without Force Sensor," *Proceedings of the 1992 International Conference on Industrial Electronics, Control, Instrumentation, and Automation, 1992. Power Electronics and Motion Control*, pp. 671–675, November, 1992.

[110] M.H. Raibert and J.J. Craig : "Hybrid Position/Force Control of Manipulators," *Journal of Dynamic Systems, Measurement, and Control*, Vol.103, No. 2, pp. 126–133, June, 1981.

[111] A. Feuer, G.C. Goodwin, and M. Salgado : "Potential Benefits of Hybrid Control for Linear Time Invariant Plants," *Proceedings of the 1997 American Control Conference*, pp. 2791–2794, June, 1997.

[112] S. Yajima, E. Saito, and S. Katsura : "Controller Design for Reproduction of Grasping/Manipulation Motion of Grasping Object with Different Diameters," *IEEJ Journal of Industry Applications*, Vol. 2, No. 1, pp. 7–13, January, 2013.

[113] M. Muller, T. Roder, and M. Clausen : "Efficient Content-Based Retrieval of Motion Capture Data," *Proceedings of ACM SIGGRAPH 2005*, pp. 677–685, July, 2005.

List of Achievements

Journals (As a first author)

[1] Noboru Tsunashima and Seiichiro Katsura, "Integrated Reproduction of Human Motion Components by Motion Copying System," *IEE Japan Transactions on Industry Applications*, Vol. 130-D, No. 4, pp. 436–442, April, 2010. (in Japanese)

[2] Noboru Tsunashima, Yuki Yokokura, and Seiichiro Katsura, "Saving and Reproduction of Human Motion Data by Using Haptic Devices with Different Configurations," *IEE Japan Transactions on Industry Applications*, Vol. 131-D, No. 3, pp. 267–274, March, 2011. (in Japanese)

[3] Noboru Tsunashima and Seiichiro Katsura, "Spatiotemporal Coupler: Storage and Reproduction of Human Finger Motions," *IEEE Transactions on Industrial Electronics*, Vol. 59, No. 2, pp. 1074–1085, February, 2012

[4] Noboru Tsunashima and Seiichiro Katsura, "Reproduction of Linear Motion with Adaptation for Change in Environmental Position," *IEE Japan Transactions on Industry Applications*, Vol. 132-D, No. 5, pp. 526–533, May, 2012. (in Japanese)

[5] Noboru Tsunashima and Seiichiro Katsura, "Adjustable motion reproduction for transferring different objects using hybrid position/force control," *Journal of the Japan Society for Precision Engineering*, 2017. (accepted) (in Japanese)

International Conference (As a first author)

[1] Noboru Tsunashima and Seiichiro Katsura, "Continuous Integration of Motion Components Using Motion Copying System," *ICROS-SICE International Joint Conference 2009, ICCAS-SICE 2009-FUKUOKA*, pp. 1563–1568, August 18–21, 2009.

[2] Noboru Tsunashima and Seiichiro Katsura, "Bilateral Control Based on Human Model for Haptic Communication," *The 11th International Workshop on Advanced Motion Control, AMC 2010-Nagaoka*, pp.319–324, March 21–24, 2010.

[3] Noboru Tsunashima and Seiichiro Katsura, "Reproduction of Human Motion Using Motion Copying System Based on Coordinate Modification," *The 36th Annual Conference of the IEEE Industrial Electronics Society, IEEE IECON 2010-PHOENIX*, pp. 1603–1608, November 7–10, 2010.

[4] Noboru Tsunashima and Seiichiro Katsura, "An Analysis of the Motion-Copying System," *The 8th edition of France-Japan and 6th Europe-Asia Congress on Mechatronics, MECHATRONICS2010-YOKOHAMA*, pp. 447–452, November 22–24, 2010.

[5] Noboru Tsunashima, Hidetaka Morimitsu and Seiichiro Katsura, "Reproduction of 2-DOF Motion Adapting to Environmental Angle Change," *The 13th International Workshop on Advanced Motion Control, AMC 2014-Yokohama*, pp. 729–734, March 14–16, 2014.

International Conferences (As a Co-author)

[1] Hiroaki Kuwahara, Kohei Ohnishi, Noboru Tsunashima, and Seiichiro Katsura, "Design Method for Motion Reproduction System Including Time Scaling Based on Robot Dynamics," *International Conference on Industrial Technology, IEEE-ICIT 2010*, pp. 483–488, March 15–17, 2010.

[2] Seiichiro Katsura, Noboru Tsunashima, Wataru Yamanouchi, and Yuki Yokokura, "Preservation and Reproduction of Real-World Haptic Information," *IEEJ International Power Electronics Conference, IPEC-SAPPORO 2010*, pp. 2216–2221, June 21–24, 2010.

Domestic Conference (As a first author)

[1] Noboru Tsunashima and Seiichiro Katsura, "Integrated Reproduction of Human's Motion Components by Motion Copying System," *IEEJ, The papers of Technical Meeting on Industrial Instrumentation and Control, IIC09*, Vol. 3, pp. 121–126, March 9–10, 2009. (in Japanese)

[2] Noboru Tsunashima and Seiichiro Katsura, "Integrated Reproduction of Motion Components Using Motion Copying System," *Proceedings of the 2009 Annual Meeting of the Institute of Electrical Engineers of Japan*, Vol. 4, pp. 392–393, March 17–19, 2009. (in Japanese)

[3] Noboru Tsunashima and Seiichiro Katsura, "Reproduction of Real-World Human Motion by Motion Copying System Based on Acceleration Information," *2009 Annual Conference of I.E.E of Japan. Industry Application Society, JIASC09, Mie*, pp. 331–336, August 31–September 2, 2009. (in Japanese)

[4] Noboru Tsunashima and Seiichiro Katsura, "Reproduction of Human Motion Using Different Structual Haptic System," *The 27th Annual Conference of the Robotics Society of Japan, RSJ 2009, Yokohama*, pp. 1–4, September 15–17, 2009. (in Japanese)

[5] Noboru Tsunashima, Yuki Yokokura, and Seiichiro Katsura, "Saving and Reproduction of Human Motion Using Haptic Devices with Different Configurations," *IEEJ, The papers of Technical Meeting on Industrial Instrumentation and Control, IIC10*, pp. 33–38, March 8–9, 2009. (in Japanese)

[6] Noboru Tsunashima and Seiichiro Katsura, "Reproduction of Integrated Motions Based on Haptic Recording," *Proceedings of the 2010 Annual Meeting of the Institute of Electrical Engineers of Japan*, Vol. 4, pp. 283–284, March 17–19, 2010. (in Japanese)

[7] Noboru Tsunashima and Seiichiro Katsura, "Reproduction of Contact Motion Using Motion Copying System Based on Spatiotemporal Disturbance Compensation," *2010 Annual Conference of I.E.E of Japan. Industry Application Society, JIASC10, Tokyo*, pp. 455–460, August 24–26, 2010. (in Japanese)

Domestic Conference (As a co-author)

[1] Yuki Nagatsu, Noboru Tsunashima, and Seiichiro Katsura, "AA," *Proceedings of the 2010 Annual Meeting of the Institute of Electrical Engineers of Japan*, Vol. 4, pp. 304–305, March 3–5, 2013. (in Japanese)

Awards

[1] August 21st, 2009
"ICCAS-SICE 2009 Annual Conference Award Finalists of International Award"
The Society of Instrument and Control Engineers (SICE)

[2] January 6th, 2010
"平成 22 年 電気学会 産業計測制御技術委員会 優秀論文発表賞"
The Institute of Electrical Engineers of Japan (IEE Japan)

[3] February 24th, 2010
"2009 年度計測自動制御学会学術奨励賞技術奨励賞"
The Society of Instrument and Control Engineers (SICE)

Patent Applications

[1] Seiichiro Katsura, Yuki Yokokura, Noboru Tsunashima, and Tatsuhito Watanabe
"相関性評価方法、相関性評価装置、動作再現装置"
Serial Number: 2010-040421
Application Date: February 25th, 2010
Applicants: Keio University.